

**CHIRAL DISCRIMINATION OF SELENIUM-CONTAINING COMPOUNDS  
THROUGH MULTINUCLEAR NMR SPECTROSCOPY IN THE  
PRESENCE OF A CHIRAL DIRHODIUM COMPLEX**

DISSERTATION

Dem Fachbereich Chemie  
der Universität Hannover  
Zur Erlangung des Grades

Doktor der Naturwissenschaften

— Dr. rer. nat. —

genehmigte Dissertation

von

**Muhammad Shahid Malik M.Sc., M. Phil.**

geboren am 05.02.1970 in Lahore / Pakistan

October 2002

Referee : Prof. Dr. Helmut Duddeck

Co-Referee : Prof. Dr. Hartmut Meyer

Promotion Day: 7<sup>th</sup> November 2002

## ZUSAMMENFASSUNG

### Chirale Erkennung Selenhaltiger Verbindungen durch Multikernmagnetische Resonanzspektroskopie in Gegenwart eines Chiralen Dirhodium-Komplexes

Ausgangspunkt der Arbeit ist der Befund, dass Enantiomerentrennung chiraler Verbindungen mit solchen funktionellen Gruppen, die schwache Basen darstellen, durch NMR-Spektroskopie in Gegenwart eines chiralen Dirhodiumkomplexes mit vier Mosher-säure-Resten, nämlich  $\text{Rh}_2[(R)\text{-}(+)\text{-MTPA}]_4$ , (**Rh-Rh**), möglich ist ("Dirhodium-Methode"). Die meisten konventionellen Methoden, wie z. B. chromatographische Trennung oder Lanthaniden-Verschiebungsreagenzien versagen bei diesem Verbindungstyp.

Die vorliegende Dissertation ist in drei Abschnitte unterteilt:

Der erste Teil behandelt die chirale Unterscheidung einer Reihe selenhaltiger Verbindungen mit **Rh-Rh** als NMR-Auxiliar. Dabei handelt es sich um Phosphinselenide ( $\text{P}=\text{Se}$ ) sowie um Phenylselenenylalkane ( $\text{C}_6\text{H}_5\text{-Se-R}$ ). Zunächst wurden die  $^1\text{H}$ -,  $^{13}\text{C}$ -,  $^{31}\text{P}$ - und  $^{77}\text{Se}$ -NMR-Signale aller freier Liganden auf der Basis ein- und zweidimensionaler NMR-Techniken (COSY, HMQC, HMBC etc.) zugeordnet. Danach wurden die Liganden mit einer äquimolaren Menge des chiralen Auxiliars **Rh-Rh** versetzt. Dadurch spalten sich viele Signale auf Grund der Bildung diastereomerer Addukte zwischen den Liganden und dem Komplex **Rh-Rh** auf. Dies liefert zwei neue Parameter: (a) Es kommt zu Komplexierungsverschiebungen ( $\Delta\delta$ ), d. h. Signalverschiebungen im Vergleich zu denen im freien Ligand, was Informationen über die Komplexierungsstelle im Liganden liefert; hier: das Selenatom. (b) Es ergeben sich Signaldispersionen  $\Delta\nu$ , Signalaufspaltungen wegen der oben erwähnten Existenz diastereomerer Addukte, was chirale Erkennung, also die Bestimmung der Enantiomerenverhältnisse der Liganden ermöglicht.

Im zweiten Teil werden die Stöchiometrie sowie die Thermodynamik der Adduktbildung mit Hilfe von Tieftemperatur-NMR-Messungen untersucht. Zum ersten Mal im "Dirhodium-Projekt" überhaupt war es bei Selenliganden möglich, die verschiedenen Selenid-**Rh-Rh**-Adduktspezies auszufrieren und die zugrunde liegenden Austauschmechanismen direkt zu untersuchen. Dadurch wurde es möglich, thermodynamische Parameter sowie die bevorzugte Stöchiometrie als 2:1-Addukte (zwei Selenid- und ein **Rh-Rh**-Molekül)

abzuschätzen. Desweiteren konnte diese Stöchiometrie durch unabhängige NMR-Messungen nach der Job-Methode bestätigt werden.

Die beiden achiralen diastereomeren, axial- bzw. equatorial-substituierten 1-Phenylselenenyl-4-*tert.*-butylcyclohexane wurden als Modellverbindungen ausgewählt, an Hand deren NMR-Untersuchung zwei verschiedene Ligandaustausch-Mechanismen, "Switch" und "Replacement", identifiziert werden konnten, deren Auftreten vom molaren Verhältnis der beiden Adduktcomponenten abhängig ist. "Switch"-Gleichgewichte treten bei molaren Verhältnissen 1:1 auf (Rhodium-Überschuss); an diesen Gleichgewichten sind 1:1- und 2:1-Addukte sowie noch freie **Rh-Rh**-Komplexmoleküle beteiligt, die aus Gründen der sprachlichen Konsistenz auch "0:1-Addukte" genannt werden können. Anders bei den "Replacement"-Gleichgewichten, die bei einem Ligandenüberschuss (molares Verhältnis > 2:1) existieren. Hier gibt es nur 2:1-Addukte sowie überschüssige Ligandenmoleküle. Die Energiebarrieren sind für beide Prozesse ca. 54-55 kJ/mol, aber Unterschiede auf Grund des sterischen Raumbedarfs können durch die Tieftemperatur-<sup>1</sup>H-NMR-Spektroskopie erkannt werden. Analoge Experimente mit 2-Phenylselenenylbutan, das einen viel kleineren Alkylrest aufweist, zeigen, dass hier der "Switch" leichter abläuft, also eine geringere Barriere aufweist. Alle sterischen Effekte bei diesen Gleichgewichten werden diskutiert und interpretiert.

Im dritten Teil wird ein Syntheserversuch beschrieben, bei dem ein chirales Selenochroman dargestellt werden sollte. Ziel dieses Teilprojekts war es, ein neues cyclisches chirales Derivatisierungsreagenz zu erhalten, das über eine Carboxylfunktion mit Alkohol- oder Amins substraten leicht zu diastereomeren Estern bzw. Amiden umgesetzt werden kann. Hierbei ist es ratsam, ein sterisch anspruchsvolles und konformativ starres Molekülgerüst aufzubauen, so dass das Benzoselenochroman-System angestrebt wurde. Allerdings erwies sich die letzte Stufe (Carbonsäure) also sehr schwierig, so dass dieses Teilprojekt zu Gunsten der in den vorherigen Abschnitten beschriebenen Untersuchungen abgebrochen wurde, die für uns eine höhere Priorität hatten. Das als Zwischenstufe auftretende chirale Phenylderivat wurde erfolgreich durch die "Dirhodium-Methode" untersucht.

**Schlagerworte:** NMR, Dirhodium-Komplex, Chirale Erkennung.

## ABSTRACT

### Chiral Discrimination of Selenium-Containing Compounds Through Multinuclear Magnetic Resonance Spectroscopy in the Presence of a Chiral Dirhodium Complex

It has been proven that for a variety of functionalities in chiral molecules the dirhodium complex with four Mosher acid (MTPA) residues,  $\text{Rh}_2[(R)\text{-}(+)\text{-MTPA}]_4$ , (**Rh-Rh**), is an excellent chiral solvating agent for recognition if the functionalities investigated are soft bases by NMR spectroscopy, i. e., for molecules where conventional methods (chromatographic separation, lanthanide shift reagents in NMR) may easily fail ("Dirhodium Method").

The dissertation is mainly divided into three parts:

The first part deals with the chiral discrimination of a variety of selenium-containing compounds in the presence of **Rh-Rh**, namely phosphine selenides (P=Se derivatives) and phenylselenenylalkanes ( $\text{C}_6\text{H}_5\text{-Se-R}$ ). First, the  $^1\text{H}$ ,  $^{13}\text{C}$ ,  $^{31}\text{P}$  and  $^{77}\text{Se}$  NMR signals of all free ligands were assigned on the basis of one- and two-dimensional NMR experiments (COSY, HMQC, HMBC etc.). Then, these ligands were subjected to the chiral auxiliary **Rh-Rh** in a 1 : 1 molar ratio. Thereby, many signals split due to the creation of diastereomeric adducts between the ligand and the **Rh-Rh** complex molecules. This provides two new parameters: (a) complexation shifts ( $\Delta\delta$ ), i.e., signal shifts due to adduct formation providing information about the position of the binding site in the ligand (here: the selenium atom); and (b) signal dispersions ( $\Delta\nu$ ; signal duplications due to the above mentioned existence of diastereomeric complexes) allowing chiral recognition, i.e., the determination of enantiomeric excess of the ligand.

In the second part of the work, the stoichiometry and thermodynamics of the adduct formation is studied with the help of low-temperature NMR spectra. For the first time in the "Dirhodium Project", it was possible to freeze out the different species of the selenide-**Rh-Rh**-adducts and to observe the underlying equilibria directly. Thereby, thermodynamic parameters and the stoichiometry of the complexes could be estimated.

First, the preferred 2:1-stoichiometry of selenide-**Rh-Rh**-adducts was derived from NMR titration experiments and independently by applying the Job Method procedure.

The two achiral diastereomeric axially- and equatorially-substituted 1-phenylselenenyl-4-*tert.*-butylcyclohexanes were selected as model compounds, and two different ligand exchange mechanisms, "switch" and "replacement", can be identified depending on the molar composition of the mixture. "Switch" equilibria occur in 1 : 1 molar ratios (rhodium sites excess), and here fast exchange processes between 1 : 1- and 2 : 1- adducts involving free **Rh-Rh** complex (called "0 : 1-adducts") exist in solution. On the other hand, "replacement" equilibria are present under conditions of ligand excess (molar ratio > 2:1). Here, only 2 : 1-adducts exist along with free ligand molecules. Exchange barriers of ca 54-55 kJ/mol can be estimated but differences due to the steric position of the selenium could be identified from the low-temperature <sup>1</sup>H NMR spectra. Repeating these experiments with 2-phenylselenenylbutane with its much lesser steric demand of the alkyl group revealed that here the "switch" is easier, i.e., the barrier lower. All steric effects are discussed and interpreted.

In the third part; the attempted synthesis of a chiral selenochroman is described. The aim of this project was to design a new cyclic selenium-containing chiral derivatizing agent (CDA) with a carboxyl group ready for the formation of diastereomeric derivatives of an alcohol or amine substrate (esters and amides, respectively). Here, it is advisable to have a sterically demanding and conformationally rigid molecular skeleton, and therefore, the benzoselenochroman system was selected. However, the synthesis of the final carboxylic acid appeared to be quite difficult so that this project was cancelled in favor of those studies described in the previous sections which appeared to us more important. The respective intermediate phenyl derivative was successfully subjected to the "Dirhodium Method".

**Key words:** NMR, Dirhodium-Complex, Chiral Recognition

## Acknowledgments

Countless thanks to Almighty Allah, who guides in Darkness and helps in difficulties. All respect for our Holy prophet (Peace Be Upon Him) who enable us to recognize our creator.

My deep, sincere indebtedness and high tribute to my inspiring supervisor **Prof. Dr. Helmut Duddeck** for his friendly guidance, support and constant care throughout the course of the present work. I have been fortunate to learn a great deal of chemistry from him.

I would like to thank the German Academic Exchange Service (DAAD) for granting the scholarship and providing me the opportunity to complete my research work.

Many thanks to Prof. Gábor Tóth, Dr. Andreás Simon and Tamás Gáti (University of Technology and Economics, Budapest, Hungary) for providing NMR spectrometer time to run all low-temperature NMR spectra and for fruitful discussions. Without their invaluable co-operation it was difficult to complete this work.

Thanks to Dr. Zbigniew Rozwadowski for involving into the selenium project and to help me in completing the project.

No words can pay my debts to Mrs. Annette Kandil for every help she has provided with a smiling face when and where needed.

My special thanks to the "spectroscopic family", particularly Mrs. Dagmar Körtje, Mrs. Monika Rettstadt, Mr. Rainer Nöthel, Mr. Joachim Küster, Mrs. Christine Bartetzko and Dr. Edgar Hofer for recording spectra sometime on first priority.

Thanks are due to Dipl.-Chem. Damian Magiera for his continuous help which make my work easy in the lab.

I wish to record my sincere appreciation to all my friends specially Maria Viad Pascual for their advises, support and to provide friendly atmosphere to make my stay in Germany enjoyable.

I hardly find any words to express my gratitude to my paramount parents which are and will always be an eternal source of inspiration. My every breath is indebted to their kindness and love.

**Muhammad Shahid Malik**

Hannover, 2002



**DEDICATED**

*To*

MY PARENTS

*AND*

THOS WHOSE ENCOURAGEMENT BRIGHTENED

*MY*

CAREER



## CONTENTS

<b>1</b>	<b>INTRODUCTION</b> .....	1
1.1	<b>History</b> .....	1
1.2	<b>Biological Importance</b> .....	1
1.3	<b><sup>77</sup>Se NMR Spectroscopy</b> .....	2
1.4	<b>Determination of Enantiomeric Purity</b> .....	2
1.5	<b>Chiral Recognition</b> .....	4
1.6	<b>Chiral Recognition By NMR Spectroscopy</b> .....	5
	1.6.1 <i>Chiral Derivatizing Agents (CDAs)</i> .....	5
	1.6.2 <i>Chiral Solvating Agents (CSA)</i> .....	6
	1.6.3 <i>Chiral Lanthanide Shift Reagents (CLSR)</i> .....	9
	1.6.4 <i>Dirhodium Carboxylates</i> .....	11
<b>2</b>	<b>CHIRAL RECOGNITION ON SELENIUM-CONTAINING COMPOUNDS</b> .....	14
2.1	<b>Definition of NMR-Spectroscopic Parameters in Rh-Rh Experiments</b> .....	15
2.2	<b>Phosphine Selenides (20 - 24)</b> .....	15
	2.2.1 <i>Signal Assignments and NMR Parameters of the Free Phosphine Selenides 20 - 24</i> .....	16
	2.2.2. <i>Adduct Formation Shifts (Dd) in the Presence of Rh-Rh</i> .....	20
	2.2.3. <i>Signal Dispersion Effects (Dn) and Chiral Recognition</i> .....	22
2.3.	<b>Phenylselenenylmenthane and –Menthene Derivatives (25 – 28)</b> .....	30
	2.3.1 <i>Signal Assignments of the Free Phenylselenenylmenthanes and -Menthene 25 - 28</i> .....	30
	2.3.2 <i>Complexation Shifts (Dd) in the Presence of Rh-Rh</i> .....	33
	2.3.3 <i>Diastereomeric Dispersion Effect (Dn) – Determination of Absolute Configuration?</i> .....	35
	2.3.4 <i>Conclusions</i> .....	35

2.4.	<b>Phenylselenenylcyclohexane Derivatives and Other Secondary Selenides (29 – 37)</b> .....	43
2.4.1.	<i>Signal Assignments and Conformational Analysis in 29 - 37</i> .....	43
2.4.2.	<i>Adduct Formation Shifts (Dd) and Diastereomeric Dispersion (Dn) – Chiral Recognition</i> .....	45
3	<b>ADDUCT FORMATION – STOICHIOMETRY</b> .....	53
3.1	<b>Stoichiometry of the adducts</b> .....	53
3.1.1.	<i>NMR Titration Experiments</i> .....	56
3.1.2.	<i>Job’s Method</i> .....	59
3.2	<b>Adduct Formation and Thermodynamics Investigated by Variable-Temperature NMR Spectroscopy</b> .....	65
3.2.1.	<i>A Primary Selenide</i> .....	66
3.2.2.	<i>Secondary Selenides</i> .....	71
3.2.2.1.	“Switch” Equilibria.....	71
3.2.2.2.	“Replacement” Equilibria.....	77
3.2.2.3.	Activation Barriers.....	80
3.2.3	<i>Characterisation of Phenylselenenylcyclohexanes and -Menthanes and Their Rh<sub>2</sub>(MTPA)<sub>4</sub>-Adducts by <sup>77</sup>Se NMR Spectroscopy</i> .....	81
4	<b>SELENOCHROMANS</b> .....	88
4.1	<b>Synthesis of Selenochromans</b> .....	88
4.2	<b>Chiral Discrimination by the Dirhodium Complex Rh–Rh</b> .....	89
5	<b>EXPERIMENTAL SECTION</b> .....	92
5.1.	<b>General Methods</b> .....	92
5.1.1.	<i>Infrared Spectroscopy (IR)</i> .....	92
5.1.2.	<i>Mass Spectroscopy (MS)</i> .....	92
5.1.3.	<i>Melting Points (m.p.)</i> .....	92
5.1.4.	<i>Solvents</i> .....	92
5.1.5.	<i>Chromatographic Techniques</i> .....	92
5.1.6.	<i>Specific Rotation</i> .....	93
5.1.7.	<i>Molecular Geometry Calculations</i> .....	93

<b>5.2</b>	<b>Nuclear Magnetic Resonance Spectroscopy (NMR) Parameters</b> .....	93
<b>5.3</b>	<b>NMR Samples Preparation</b> .....	95
5.3.1.	<i>Samples Preparation for Job Plots</i> .....	95
5.3.2.	<i>Stock Solution for Job Plot</i> .....	95
<b>5.4.</b>	<b>Synthetic Procedures</b> .....	96
5.4.1.	<i>Synthesis of Dirhodium Carbonate Sodium Salt</i> <i>[Na<sub>4</sub>Rh<sub>2</sub>(CO<sub>3</sub>)<sub>4</sub>]</i> .....	96
5.4.2.	<i>Tetrakis-[(R)-(+)-<b>a</b>-methoxy-<b>a</b>-trifluoromethylphenyl-acetate)-</i> <i>dirhodium(II)]</i> .....	96
5.4.3.	<i>Synthesis of Phosphine Selenides</i> .....	96
5.4.4.	<i>Synthesis of Phenylselenenylalkanes Derivatives</i> .....	97
5.4.4.1.	General Method for the Synthesis of Selenides From Respective Alcohols .....	97
5.4.4.2.	General Method for the Synthesis of Bis-Selenides From Respective Ketones By Using (PhSe) <sub>3</sub> B: .....	98
5.4.4.3.	General Method for the Synthesis of Selenides From Respective Halides .....	98
<b>5.5</b>	<b>Method for the Synthesis of Selenochroman (39)</b> .....	99
<b>5.6</b>	<b>Collection of Spectroscopic Data</b> .....	100
5.6.1.	<i>Tetrakis-[(R)-(+)-<b>a</b>-methoxy-<b>a</b>-trifluoromethylphenyl-acetate)-</i> <i>dirhodium(II)]</i> .....	100
5.6.2.	<i>O-Methyl methylphenylphosphinoselenoate (20)</i> .....	101
5.6.3.	<i>O-Isopropyl methylphenylphosphinoselenoate (21)</i> .....	102
5.6.4.	<i>N,N,-Diethyl methylphenylphosphinoselenoamidate (22)</i> .....	103
5.6.5.	<i>O-Methyl methylpentafluorophenylphosphinoselenoate (23)</i> ...	104
5.6.6.	<i>O-Isopropyl methylpentafluorophenylphosphinoselenoate</i> <i>(24)</i> .....	105
5.6.7.	<i>3-Phenylselenenylmenthane (25)</i> .....	106
5.6.8.	<i>3-Phenylselenenylneomenthane (26)</i> .....	107
5.6.9.	<i>3,3-di-Phenylselenenylmenthane (27)</i> .....	108
5.6.10.	<i>3-Phenylselenenyl-3-menthene (28)</i> .....	109
5.6.11.	<i>Phenylselenenylcyclohexane (29)</i> .....	110
5.6.12.	<i>Cis-1-Phenylselenenyl-4-tert-butylcyclohexane (30)</i> .....	111

5.6.13. <i>Trans-1-Phenylselenenyl-4-tert-butylcyclohexane (31)</i> .....	112
5.6.14. <i>Cis-1-Phenylselenenyl-3-methylcyclohexane (32)</i> .....	113
5.6.15. <i>Trans-1-Phenylselenenyl-3-methylcyclohexane(33)</i> .....	114
5.6.16. <i>1,1-di-Phenylselenenyl-2-methylcyclohexane (34)</i> .....	115
5.6.17. <i>1,1-Di-phenylselenenyl-3-methylcyclohexane (35)</i> .....	116
5.6.18. <i>2-Phenylselenenylbutane (36)</i> .....	117
5.6.19. <i>2-Phenylselenenylpropane (37)</i> .....	118
5.6.20. <i>3-Phenylselenenyl-1-phenyl-1-propene (38)</i> .....	119
5.6.21. <i>3-Phenylselenenylchroman (39)</i> .....	120
<b>6 REFERENCES</b> .....	<b>121</b>

**Abbreviations:**

1D	One- <b>d</b> imensional
2D	Two- <b>d</b> imensional
Ar	<b>A</b> ryl
ATR	<b>A</b> ttenuated <b>T</b> otal <b>R</b> eflection
BB	<b>B</b> road- <b>B</b> and
br	<b>b</b> road signal (in NMR spectrum)
CDA	<b>C</b> hiral <b>D</b> erivatizing <b>A</b> gent
CH-COSY	<b>C</b> arbon- <b>H</b> ydrogen <b>C</b> orrelation <b>S</b> pectroscopy
CLSR	<b>C</b> hiral <b>L</b> anthanide <b>S</b> hift <b>R</b> eagent
COSY	<b>C</b> orrelated <b>S</b> pectroscopy
CSA	<b>C</b> hiral <b>S</b> olvating <b>A</b> gent
d	<b>d</b> oublet
dd	<b>d</b> oublet of <b>d</b> oublets
ddd	<b>d</b> oublet of <b>d</b> oublets of <b>d</b> oublets
ddq	<b>d</b> oublet of <b>d</b> oublets of <b>q</b> uartets
DEPT	<b>D</b> istortionless <b>E</b> nhancement by <b>P</b> olarization <b>T</b> ransfer
dm	<b>d</b> oublet of <b>m</b> ultiplets
dq	<b>d</b> oublet of <b>q</b> uartets
dt	<b>d</b> oublet of <b>t</b> riplets
EA	<b>E</b> lemental <b>a</b> nalysis
e. e.	<b>e</b> nantiomeric <b>e</b> xcess = %( <i>R</i> ) - %( <i>S</i> )
eq	<b>e</b> quatorial
FAB	<b>F</b> ast <b>A</b> tom <b>B</b> ombardment
fod	6,6,7,7,8,8,8- <b>H</b> epta <b>f</b> luor-2,2- <b>d</b> imethyl-3,5- <b>o</b> ctan <b>d</b> ionato
g	<b>g</b> ram
gs	<b>g</b> radient- <b>s</b> electe <b>d</b>
HH-COSY	<b>H</b> ydrogen- <b>H</b> ydrogen <b>C</b> orrelation <b>S</b> pectroscopy
HMBC	<b>H</b> eteronuclear <b>M</b> ultiple- <b>B</b> ond <b>C</b> orrelation
HMQC	<b>H</b> eteronuclear <b>M</b> ultiple <b>Q</b> uantum <b>C</b> oherence

HOMO	<b>H</b> ighest <b>O</b> ccupied <b>M</b> olecular <b>O</b> rbital
HRMS	<b>H</b> igh <b>R</b> esolution <b>M</b> ass <b>S</b> pectrometry
HSQC	<b>H</b> eteronuclear <b>S</b> ingle <b>Q</b> uantum <b>C</b> oherence
IR	<b>I</b> nfrared(-spectrum/-spectroscopy)
L	<b>L</b> igand/Substrate
LUMO	<b>L</b> owest <b>U</b> noccupied <b>M</b> olecular <b>O</b> rbital
m	<b>m</b> ultiplet (in NMR spectrum) or <b>m</b> edium intensity (in IR-Spectrum)
<i>m</i>	<i>m</i> eta-position in Phenyl group
M	<b>M</b> olarity
Me	<b>M</b> ethyl
MeOH	Methanol
min	<b>m</b> inute(s)
MO	<b>M</b> olecular <b>O</b> rbital
MS	<b>M</b> ass <b>S</b> pectrum or <b>M</b> ass <b>S</b> pectrometry
MTPA	<i>o</i> - <b>M</b> ethoxy- <i>o</i> - <b>t</b> rifluoromethyl <b>p</b> henyl <b>a</b> ccetate
MTPA-H	<i>o</i> - <b>M</b> ethoxy- <i>o</i> - <b>t</b> rifluoromethyl <b>p</b> henyl <b>a</b> ccetic acid; <b>M</b> OSHER'S acid
n. d.	<b>n</b> ot <b>d</b> etected
NMR	<b>N</b> uclear <b>M</b> agnetic <b>R</b> esonance
NOE	<b>N</b> uclear <b>O</b> verhauser <b>E</b> nhancement
NS	<b>N</b> umber of <b>S</b> cans
<i>o</i>	<i>o</i> rtho-position in Phenyl group
<i>p</i>	<i>p</i> ara-position in Phenyl group
PE	<b>p</b> etrol <b>e</b> ther
Ph	<b>P</b> henyl
ppm	<b>p</b> arts <b>p</b> er <b>m</b> illion
q	<b>q</b> uartett
qa	<b>q</b> uasiaxial
qe	<b>q</b> uasiequatorial
<b>Rh-Rh</b>	Dirhodium complex Rh <sub>2</sub> [( <i>R</i> )-(+)-MTPA] <sub>4</sub>
RT	<b>R</b> oom temperature



s	<b>s</b> inglet (in NMR spectrum) or <b>s</b> trong intensity (in IR spectrum)
S/N	<b>S</b> ignal to <b>N</b> oise ratio
t	<b>t</b> riplet
TMS	<b>T</b> etra <b>m</b> ethyl <b>s</b> ilane
UV	<b>U</b> ltrav <b>i</b> olet
w	<b>w</b> eak intensity

**Symbols**

$[\alpha]_l^J$	Specific Rotation at wavelength $[\lambda]$
$B_0$	Magnetic field of NMR spectrometers
$d$	Chemical Shift in NMR
$\Delta\delta$	Complexation Shifts (difference between chemical shifts of free ligand and complex with <b>Rh-Rh</b> ) [ppm]
$\Delta\nu$	Dispersion (signal duplication due to the existence of diastereomeric complex) [Hz]
${}^nJ$	spin-spin couplings constant over n bond [Hz]
$l$	wavelength
$m$	mass
$n$	frequency
T	Tesla

# 1 INTRODUCTION AND BACKGROUND

The first synthetic organoselenium compound, diethyl selenide, was prepared by Löwig in 1836.<sup>1</sup> The highly malodorous nature of selenium compounds, difficulties in purification, and the instability of many of the derivatives hampered the early developments. Organoselenium chemistry intensified during the 1970s when the discovery of several useful new reactions and a variety of novel structures with unusual properties began to attract a more general interest in the discipline.

## 1.1 History

In 1817 the Swedish chemist Jöns Jacob Berzelius discovered a new element during the processing of copper pyrites for sulphuric acid production. He realized that its properties were somewhere between those of sulphur and tellurium and called it selenium after Selene, the ancient Greek goddess of the Moon. Although selenium is a rare element it is widely occurring in some rocks and coal, but it is unevenly distributed. Its relative abundance on earth is about  $9 \times 10^{-6}$  % which is close to those of antimony, argon, cadmium, iodine and silver.

## 1.2 Biological Importance

Selenium compounds are notorious for being toxic<sup>2</sup> and of particularly unpleasant smell. Their toxicity is believed to originate in the ability of selenium to replace sulphur in proteins.<sup>3</sup> Organoselenium compounds seem to be less toxic than salts which are readily soluble in water. On the other hand, selenium is an essential trace element<sup>2</sup> and some selenium-containing proteins, e.g., glutathione peroxidase, have been observed.<sup>2,4</sup> In several places of the world, selenium deficiency syndromes (e.g., Keshan disease) have been observed.<sup>5</sup> Medical treatments of heart diseases and of intoxications by arsenic, cadmium and mercury as well as cancer therapies and the stimulation of the immune system widely use selenium-containing substances.<sup>2,6</sup>

### 1.3 $^{77}\text{Se}$ NMR Spectroscopy

While the earliest reports reach back to the 1950s,<sup>7,8</sup> the first systematic investigation in the field of  $^{77}\text{Se}$  NMR spectroscopy seems to have been published by Birchall *et al.* (1965) on inorganic selenium compounds<sup>9</sup> and by Lardon (1970) on organic selenium compounds.<sup>10</sup> Later the interest in this nucleus increased steadily when it was noticed that its favorable nuclear properties make it rather easily accessible under routine pulse Fourier transform recording conditions.

In the beginning the interest was focused on exploring the general NMR characteristics of  $^{77}\text{Se}$ . Later, however, more and more reports were published dealing with studies of chemical reactions, stereochemistry, molecular dynamics and last but not least, biochemical applications of various compounds. Needless to say that  $^{77}\text{Se}$  NMR spectroscopy is also an important tool for the investigation of inorganic selenium compounds. In addition,  $^{77}\text{Se}$  NMR has gained increasing usage in studies of metal complexes with organic or inorganic selenium-containing ligands.

### 1.4 Determination of Enantiomeric Purity

Chiral organoselenium compounds have gained increasing importance in asymmetric synthesis during the last decade.

It has taken time and consideration to find means of achieving accurate, reliable and easy methods of measuring enantiomeric purity. Along with these measures the pharmaceutical industry has introduced the requirement of marketing the chiral drugs as pure enantiomers. From the marketed commercial drugs more than 50% are chiral and less than half of these are in an enantiomerically pure form. Among the synthetic chiral drugs only 10% are available in an enantiopure form.

In the early 1960s, chiroptical methods were used to assess the enantiomeric purity of a chiral molecule which often required the measurement of optical rotation of the sample with a polarimeter. This involved the measurement not only under defined conditions of

temperature, solvent and concentration but also at a given wavelength of the incident plane-polarized light. The value so obtained needed to be compared with the value obtained for an enantiomerically pure sample of the same compound measured under identical conditions. This value is commonly known as “optical purity”.

The optical purity can be defined as the specific rotation,  $[\alpha]$ , of a substance divided by the specific rotation,  $[A]$ , of the pure enantiomers.

$$\text{optical purity} = [\alpha] / [A]$$

If the measurements of optical purity are carried out under strictly controlled conditions along with appropriate calibrations, then this value may be equated with “enantiomeric excess”. The enantiomeric excess is a measure of the excess of one enantiomer over the other.

$$\text{enantiomeric excess} = e.e. = (F^+ - F^-) / (F^+ + F^-) = 2F^+ - 1$$

Where  $F^+$  and  $F^-$  are the mole fraction of the enantiomers,  $F^+$  is taken as that of the predominant isomer for convenience.

The determination of enantiomeric excess by measurement of the ratios of enantiomers without physical separation of the diastereomers or enantiomers, in principle, needs the measurement of two associated parameters. One of these should correspond to a structure-dependent intensive property and must give distinguishable values for the two stereoisomers. The other should be a structure-independent extensive parameter, which must provide a measure of the relative quantities of the two stereoisomers. NMR chemical shifts and interacted intensities appear to be two convenient parameters.

## 1.5 Chiral Recognition

In modern organic chemistry, asymmetric synthesis is one of the most important fields. Therefore, it is necessary to have efficient methods for chiral recognition, i.e., for the determination of enantiomeric ratios.

It has always been and still is a realized factor that in principle a chiral environment might perturb the properties of the enantiomeric molecules unequally, and thereby alter the stereochemical course of reactions. This principle has been comprised in many forms in practical applications of selectively preparing, separating and determining the absolute configuration and enantiomeric purity of optical isomers. However, this appreciation has never been authentically comprehended as it commonly gives a vague understanding of the mechanism of chiral recognition. Chiral recognition, the ability of one chiral molecule to somehow “recognize” the chirality of another, is a term used for its convenience rather than soundness of its significance. In fact, the observer does the recognition, not the molecules.

Most often chiral recognition has been studied in the liquid phase. The diastereomeric interaction in solution can be detected by number of methods.<sup>11</sup> Physical properties such as boiling points, density and dipole moment difference between the individual diastereomers and their mixtures, have little practical applications and contribute scarcely, if at all, to the understanding of these interactions. However, the knowledge of these intrinsic properties is a prerequisite for designing new and more effective methods of chiral recognition. The determination of enantiomeric compositions by the measurement of optical rotation appears to be very simple; yet in practice to obtain correct values extra care must be taken. There are several major potential sources of error in this method, e.g., the presence of a chiral impurity, magnitude of the optical rotation and experimental conditions such as polarity of the solvent, temperature and pH of the medium etc. Therefore, it is necessary to use independent methods of analysis when assaying enantiomeric purity. The plausible classifications of these methods, based on the review of literatures are nuclear magnetic resonance, chromatographic, kinetic, enzymatic and other methods.

## 1.6 Chiral Recognition By NMR Spectroscopy

In an achiral medium enantiomers cannot be differentiated as the resonances of enantiomeric nuclei are isochronous. However, resonances of diastereomers are anisochronous, so they may be distinguished. Therefore, for the determination of enantiomeric purity using NMR, a chiral auxiliary is required to convert the mixture of enantiomers into a diastereomeric mixture. The non-equivalent chemical shifts of diastereomers generally give a resolution of the appropriate signals and then the diastereomeric composition can be measured directly from integration which gives the enantiomeric composition of the original mixture.

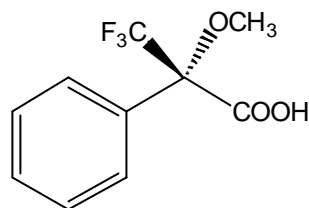
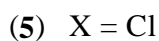
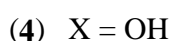
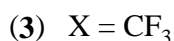
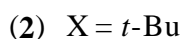
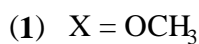
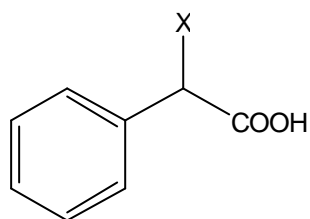
The auxiliaries used in NMR methods are: chiral derivatizing agents (CDA), chiral solvating agents (CSA) and chiral lanthanid shift reagents (CLSR).

### 1.6.1 Chiral Derivatizing Agents (CDAs)

In the chiral derivatizing technique an enantiomeric mixture is converted into a pair of diastereomers with an appropriate chiral derivatizing agent (CDA), and then the enantiotopic atoms or groups in the original sample are observed as diastereotopic atom or groups by internal comparison.

The application and limitations of a series of  $\alpha$ -substituted phenylacetic acids (**1-5**) as CDAs for NMR analysis have been studied. An extremely useful CDA,  $\alpha$ -methoxy- $\alpha$ -trifluoromethylphenylacetic acid [(**6**), Mosher acid, MTPA], was developed on the basis of these studies.<sup>12</sup>

There is a number of disadvantages of the CDA use, the basic one being the necessity of an additional reaction before the NMR analysis. Secondly, large excesses of the CDA are used to assure complete reaction of both enantiomers.<sup>13</sup>

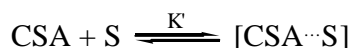
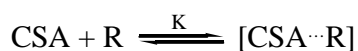


### 1.6.2 Chiral Solvating Agents (CSA)

Chiral solvating agents (CSA) create different spatial environments for enantiomeric nuclei; as a result chiral enantiomeric solutes reveal different NMR spectra when dissolved in an enantiopure chiral solvent. This fact was proposed by Mislow and Raban<sup>14</sup> and experimentally demonstrated by Pirkle.<sup>15</sup>

Typical chiral solvating agents are amines, alcohols, acids, sulfoxides or cyclic compounds such as cyclodextrins, crown ethers, or peptides.

The interaction of enantiomeric (*R*, *S*) ligands, with chiral solvating agents CSA, gives the complexes [R··CSA] and [S··CSA]. These diastereomeric association complexes can have different properties.<sup>16</sup>



Exchange between chiral and achiral solvates is rapid on the NMR time scale and the observed resonance signals derived from each enantiomers  $\delta_R(\text{obs})$  represent the population-weighted averages of the chemical shifts for the discrete chiral and achiral



solvates  $\delta_R$ ,  $\delta_S$ , and  $\delta_{\text{ach}}$  respectively. Given that  $\phi_R$  and  $\phi_S$  are the fractional populations of achiral solvates, so that  $K_R = (1 - \phi_R) \phi_R$ , then

$$\delta_R(\text{obs}) = \phi_R \delta_{\text{ach}} + (1 - \phi_R) \delta_R$$

$$\delta_S(\text{obs}) = \phi_S \delta_{\text{ach}} + (1 - \phi_S) \delta_S$$

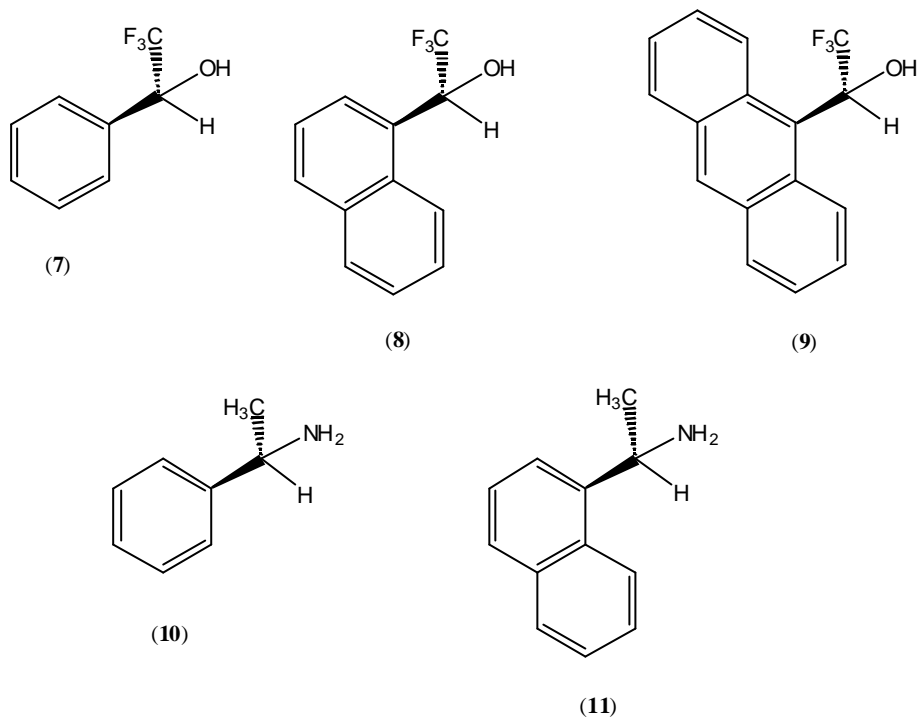
hence

$$\Delta\delta = \phi_R (\delta_{\text{ach}} + K_R \delta_R) - \phi_S (\delta_{\text{ach}} + K_R \delta_S)$$

The ligand-ligand associations are assumed to be relatively unimportant and can be neglected since the diastereomeric association complexes are typically more stable and CSA is used in excess. The magnitude of nonequivalence may be affected by some other variables. Solvent effects are generally dramatic. In non-polar solvents the association is much stronger. The non-equivalence is severely reduced on addition of a small quantity of a polar material, as it competes with the solute for CSA.

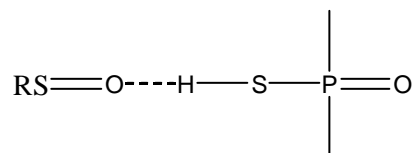
In all cases, the ligand and the chiral solvating agent have the common feature of complementary functionality that permits their interaction. Most of the CSAs rely on hydrogen bonding as the primary ligand-binding force. Generally, if the ligand is a hydrogen bond donor, the CSA of choice is a hydrogen bond acceptor. Some other interactions may also contribute primary or secondarily towards association complexes. The formation of diastereomeric charge-transfer ( $\pi$ -acid –  $\pi$ -base) complexes can also induce anisochrony. Dipole-dipole attraction in some cases may be another source of association. Release of high-energy water molecules and van der waals attractions may also contribute towards complexation. Finally, ion pairing may also be a principle contributor to binding in certain cases.

Frequently used CSAs are 2,2,2-trifluoro-1-phenylethanol [TFPE, **(7)**], 2,2,2-trifluoro-1-(1-naphthyl)ethanol [TFNE, **(8)**], 2,2,2-trifluoro-1-(9-anthryl)ethanol [TFAE, **(9)**], 1-phenylethylamine [PEA, **(10)**] and 1-(1-naphthyl)ethylamine [NEA, **(11)**].

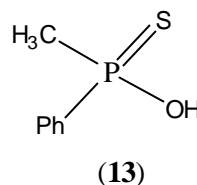
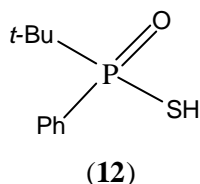


Of these CSA's, TFAE (**9**) is the most commonly used. It has been used to determine the enantiomeric purity of a very broad range of compounds including lactones, ethers, oxiziridines and sulfinate esters.<sup>17</sup> TFAE has also been used recently for observation of chirality in stereolabile chiral isomers of *N*-naphthylimines at low temperature.<sup>18</sup>

Until recently it was difficult to determine the e.e. of various sulfoxides, especially those containing longer aliphatic constituents at sulfur. Now, for this purpose, (-)-(*S*)-*t*-butylphenylphosphinothioic acid (**12**) has been reported to be advantageous.<sup>19</sup> In this method the spectral nonequivalence observed is due to the formation of hydrogen-bonded complexes between **12** and sulfoxide shown below:



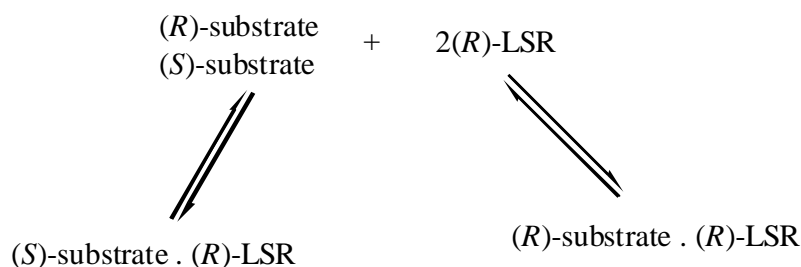
(-)-(*S*)-Methylphenylphosphinothioic acid (**13**) has been used<sup>20</sup> as a CSA for the studies on asymmetric induction in the base-induced rearrangement of *N*-(diphenylphosphinoyl)-*O*-(camphor-10-sulfonylamine).



### 1.6.3 Chiral Lanthanide Shift Reagents (CLSR)<sup>21</sup>

Since the introduction of the chiral lanthanide shift reagents (CLSR), almost all lanthanide (III) ions have been tried for their applicability. The most useful ones are Eu(III), Pr(III) and Yb(III) although for special purposes some others have been proposed. The most commonly used lanthanide ion is Eu(III) as it causes least line broadening; note that all lanthanide ions are paramagnetic. The primary purpose of using a CLSR is to separate the signals of a pair of enantiomers by inducing chemical shift non-equivalence and to observe their relative intensities.

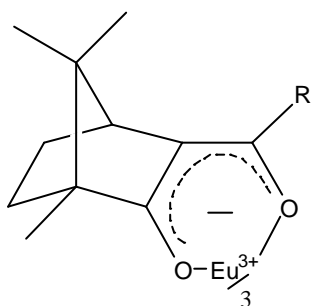
On the NMR time scale the exchange between the substrate and the CLSR is rapid under normal conditions. As a result, a time-averaged signal of complexed and uncomplexed substrate molecules is produced. Rapidly equilibrating complexes are formed by an enantiomerically pure CLSR binding to each of the two enantiomers.



These complexes can have different average chemical shifts as they are diastereomeric. There are two reasons for this difference in shifts:

- For diastereomeric complexes the equilibrium constants may be different. The complex having larger binding constant will have the greater shift.
- The geometry of the two diastereomeric complexes may also be different. Thus resulting in producing a difference in the induced shift for corresponding signals in the two complexes.

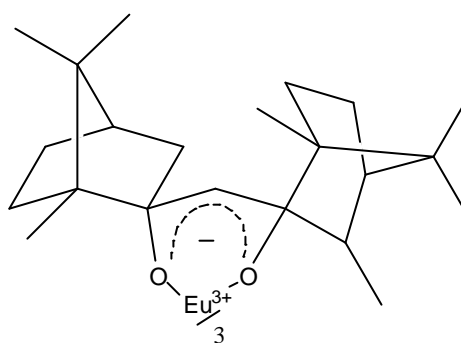
The first chiral LSR reported<sup>22</sup> was *tris*(3-*t*-butylhydroxymethylene-*d*-camphorato)-europium(III) [Eu(PVC)<sub>3</sub>] (**14**) which was used to separate the signals of the enantiomers of  $\alpha$ -phenylethyl amine and of several other amines. Some common CLSRs (**15-17**) are:



R = *t*-butyl, Eu(PVC)<sub>3</sub> (**14**)

R = C<sub>3</sub>F<sub>7</sub>, Eu(hfc)<sub>3</sub> (**15**)

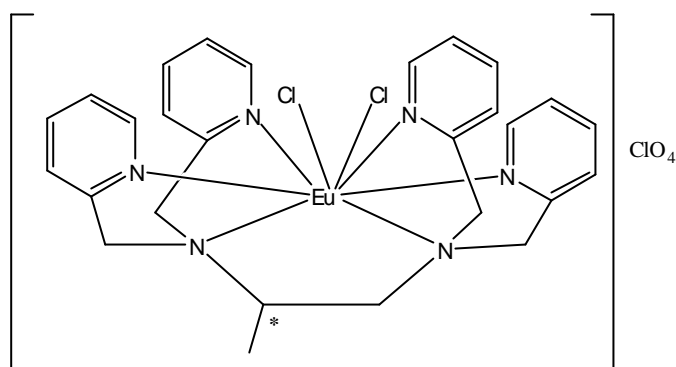
R = CF<sub>3</sub>, Eu(tfc)<sub>3</sub> (**16**)



Eu(dcm)<sub>3</sub> (**17**)

Recently, a new chiral LSR, [*N,N,N',N'*-*tetrakis*(2-pyridylmethyl)propylene-diamine]dichloroeuropium(III)chlorate<sup>23</sup> [Eu(III)Cl<sub>2</sub>{(*R*)-tppn}]ClO<sub>4</sub>, (**18**) has been reported. The most significant feature of this reagent is that it can resolve the enantiomeric signals of  $\alpha$ -amino acids under neutral conditions. This is in contrast to reported reagents which are effective only under alkaline conditions.<sup>24-27</sup>

Binuclear complexes for the analysis of chiral olefins arenas and allenes a useful NMR auxiliaries have been devised.<sup>28,29</sup>



(18)

#### 1.6.4 Dirhodium Carboxylates

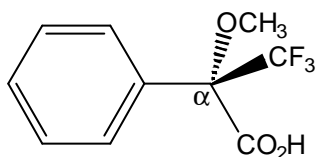
There is a prerequisite for the substrate molecule for the classical NMR methods of chiral recognition. It must contain a functional group to react with a CDA or at least a polar group that can complex with a CSA or a CLSR. Though CLSR have been most widely used for chiral recognition, yet there are many classes of compounds including olefins, aromatic hydrocarbons, ethers, nitriles, selenides etc., where these methods fail or their application is difficult and the results are quite unsatisfactory.

Recently some binuclear transition metal [Mo, Rh] complexes, especially carboxylates like Rh<sub>2</sub>(O<sub>2</sub>CCH<sub>3</sub>)<sub>4</sub>, have been introduced as additives for determination of absolute configuration by CD spectroscopy.<sup>30-32</sup> These carboxylates have the ability to bind ligand molecules at the rhodium atoms in the axial position, i.e., along the rhodium-rhodium bond direction.

Dirhodium tetra(trifluoroacetate) has proved to be suitable for the investigation of olefins.<sup>30</sup> As this complex is diamagnetic, its potential for chiral recognition by NMR spec-

troscopy can be further explored. However, in contrast to CD, NMR spectroscopy is an achiral technique so that one has to introduce chirality into the rhodium complex. Chiral dirhodium complexes can easily be prepared by exchange of the acetate groups with chiral ones or from rhodium carbonates sodium salt (prepared from dirhodium tetraacetate) and a chiral carboxylic acid.

Dirhodium tetrakis-(*R*)- $\alpha$ -methoxy- $\alpha$ -(trifluoromethyl)phenylacetate [Rh<sub>2</sub>(MTPA)<sub>4</sub>; (**6**) has been prepared and used quite successfully for chiral recognition of olefins<sup>33</sup> epoxides,<sup>34</sup> nitriles,<sup>35</sup> iodides,<sup>36</sup> methyl phenyl sulfoxides,<sup>37</sup> xanthines,<sup>38</sup> phosphorus thionates,<sup>39</sup> phosphine selenides,<sup>40</sup> and selenides.<sup>41(a-c)</sup>



(*R*)-(+)-MTPA-H (**6**)

Oxiranes are another important functional group that often does not bind to CLSRs efficiently. The chiral recognition of some oxiranes has also been studied by dirhodium-MTPA complex.<sup>34</sup>

This NMR method of chiral recognition using dirhodium-MTPA-complexes appears to be superior to the use of CLSRs. The use of this method has number of advantages.

- a) In contrast to lanthanide shift reagents, the dirhodium complex is diamagnetic so that line broadening caused by the auxiliary is not observed:
- b) The experiment is performed with a simple two-component mixture of substrate and the complex. Often, a 1:1 ratio is recommendable but examples have also been found where a smaller amount of dirhodium complex is sufficient.

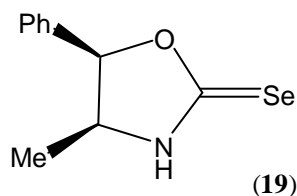
- c) The dirhodium complex is stable, non-hygroscopic and easy to prepare. A  $\text{CDCl}_3$  solution can be stored and used over a long period of time.
- d) Both the complex and the substrate can easily be recovered after the NMR experiments by simply adding methanol and chromatography separation.
- e)  $^1\text{H}$  signal shifts ( $\Delta\delta$ ) are generally much smaller than in experiments using LSR so that  $^1\text{H}$  signals can easily be identified even after a one-molar addition of complex.

The present work is part of the project to explore the chiral recognition, the thermodynamics and the stoichiometry of various selenium-containing compounds ligated to  $\text{Rh}_2(\text{MTPA})_4$ .

## 2 CHIRAL RECOGNITION USING SELENIUM-CONTAINING COMPOUNDS

NMR methods are frequently used to determine optical purity owing to their ready availability, simplicity, low cost, sufficient sensitivity<sup>42</sup> and <sup>31</sup>P NMR spectroscopy plays a significant role in this field if the functional group of the chiral substrate is polar.<sup>43, 44</sup> In addition, <sup>77</sup>Se NMR has proven its remarkable ability, which is due to the large chemical shift range of this nucleus.<sup>45</sup> Gronowitz and co-workers were the first to report that <sup>77</sup>Se NMR is the excellent tool for the chiral recognition. They found two resonances at  $\delta = 136.6$  and  $134.5$  in the <sup>77</sup>Se NMR spectrum of a mixture of diastereomeric esters produced from (*R*)-2-phenylselenenylpropanoic acid and (*R,S*)-2-octanol.<sup>46</sup>

The first chiral selenium-containing derivatizing agent, enantiomerically pure (4*S*,5*R*)-(-)-4-methyl-5-phenyloxazolidine-2-selone (**19**) designed for the determination of enantiomeric purities by <sup>77</sup>Se NMR was introduced by Dunlap *et al.* in 1990.<sup>47-49</sup>



Stereochemical recognition is even possible in chiral selenium-containing solvating reagents. Racemic  $\alpha$ -phenylselenenylalkanoic acids and enantiomerically pure amines have been examined in analogy to the Pirkle method.<sup>50</sup> The methods work excellently even with tertiary amines and amines without aromatic groups where the Pirkle method fails due to the lack of an additional intermolecular stabilization.<sup>50</sup>



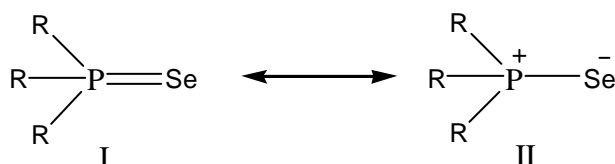
## 2.1 Definition of NMR-Spectroscopic Parameters in Rh-Rh Experiments

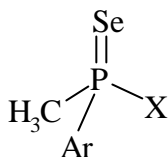
The two most important NMR spectroscopic parameters for chiral recognition of ligand molecules in the presence of our chiral dirhodium auxiliary **Rh-Rh** are the following:

- The position of a signal, i.e. its chemical shift, is changed by adduct formation. This is called adduct formation shift  $\Delta\delta$  (in ppm). Positive values refer to deshielding and negative to shielding.
- If mixtures of chiral ligand molecules **L** are added to equimolar amounts of **Rh-Rh**, diastereomeric adducts are formed and can be discriminated by their different  $^1\text{H}$  and  $^{13}\text{C}$  signals. In principle, each signal of the free ligand is split into two. The distance within such signal pairs is called diastereomeric dispersion ( $\Delta\nu$ ; in Hz). Note that  $\Delta\nu$ -values are field-dependent; in this study they are referred to 400, 500 MHz ( $^1\text{H}$ ) and 100.6 MHz ( $^{13}\text{C}$ ). Due to different quantities of the enantiomers in each sample, it is possible to identify most of the signals of each by its intensity.

## 2.2 Phosphine Selenides (20 – 24)

The  $\delta$ -values of  $^{77}\text{Se}$  in the P=Se bonds of organo-phosphine selenides are negative. This suggests a substantial contribution of the dipolar mesomeric form (II) with a negative charge at Se. The  $^{77}\text{Se}$  chemical shifts depend strongly on the nature of the substituent while this is not the case for  $^{31}\text{P}$ .<sup>45</sup>



2.2.1 Signal Assignments and NMR Parameters of the Free Phosphine Selenides **20** - **24**

	Ar	X
<b>20</b>	C <sub>6</sub> H <sub>5</sub>	OCH <sub>3</sub>
<b>21</b>	C <sub>6</sub> H <sub>5</sub>	O-CH(CH <sub>3</sub> ) <sub>2</sub>
<b>22</b>	C <sub>6</sub> H <sub>5</sub>	N(CH <sub>2</sub> -CH <sub>3</sub> ) <sub>2</sub>
<b>23</b>	C <sub>6</sub> F <sub>5</sub>	OCH <sub>3</sub>
<b>24</b>	C <sub>6</sub> F <sub>5</sub>	O-CH(CH <sub>3</sub> ) <sub>2</sub>

**Scheme 1.** Structures of the phosphine selenides investigated; all compounds are racemates.

Only for compound **20** some NMR data (in CCl<sub>4</sub>) have been published before<sup>51, 52</sup>:  $\delta(^{31}\text{P}) = 90$ ,  $\delta(^1\text{H}) = 1.91$  (d, 14 Hz, P-CH<sub>3</sub>), 3.28 (d, 14 Hz, P-OCH<sub>3</sub>). There were no NMR data for compounds **21-23** reported previously. Therefore, we started our investigation by an inspection of the <sup>1</sup>H, <sup>13</sup>C, <sup>31</sup>P and <sup>77</sup>Se nuclei in all compounds **20** - **24** used as ligands (Tables 1 and 2). The interpretation of the spectra was assisted by performing routine 1D and 2D NMR experiments such as DEPT, COSY 45<sup>0</sup>, HMQC and HMBC. Nearly all signal assignments of **20** - **24** were straightforward due to the simplicity of the NMR spectra. *Ortho*- vs. *meta*-positioned carbon atoms in the phenyl residues of **20** - **22** had to be differentiated. This was possible by inspecting the <sup>1</sup>H signals which appeared as pseudo-doublets (*ortho*) and pseudo-triplets (*meta*). The respective, directly attached carbons were identified by HMQC. It should be noted that diastereotopism of the isopropyl methyl groups in **21** and **24** is reflected in significant chemical shift differences. The two ethyl groups in **22** cannot be differentiated due to nitrogen inversion but the diastereotopic geminal protons within the N-CH<sub>2</sub> group produce a complex signal (ABX<sub>3</sub> spin system).

Replacing the phenyl group in **20** or **21** by C<sub>6</sub>F<sub>5</sub> (leading to **23** and **24**, respectively) reveals marked effects on <sup>13</sup>C, <sup>31</sup>P and <sup>77</sup>Se atoms up to three bonds away and <sup>1</sup>H atoms even four bonds away (Table 1, Scheme 2). All proton and carbon atoms of the methyl groups and the methine in **21/24** are deshielded. This can be interpreted in terms of a strong electron withdrawing effect of the C<sub>6</sub>F<sub>5</sub> group as compared to C<sub>6</sub>H<sub>5</sub><sup>53</sup>. The P=Se group, however, experiences a distinct polarization: whereas the <sup>77</sup>Se nucleus is deshielded by 134 ppm in **23** relative to **20** and in **24** relative to **21**; the phosphorus is shielded by ca 17 ppm in the C<sub>6</sub>F<sub>5</sub> analogs relative to the respective C<sub>6</sub>H<sub>5</sub> derivatives (see Table 1). Strengthening of the double bond character in the C<sub>6</sub>F<sub>5</sub> analogs is indicated by a significant increase of the absolute values of the one-bond <sup>77</sup>Se,<sup>31</sup>P coupling constants by 35.1 Hz (**20** → **23**) and 29.3 Hz (**21** → **24**); in general, <sup>1</sup>J(<sup>77</sup>Se,<sup>31</sup>P) coupling constants are negative. This polarization points to a difference in mesomeric interactions (see page 15, bottom),<sup>54</sup> an interpretation which is supported by semi empirical calculations (PM3) resulting in coplanar Ar-P=Se molecular fragments (Ar = C<sub>6</sub>H<sub>5</sub> or C<sub>6</sub>F<sub>5</sub>, respectively).

**Table 1.**  $^1\text{H}$ ,  $^3\text{P}$  and  $^{77}\text{Se}$  NMR chemical shifts (in ppm,  $\delta$  scale) of the phosphine selenides **20** - **24**;  $^3\text{P}$ ,  $^1\text{H}$  coupling constants in parentheses,  $^{19}\text{F}$ ,  $^1\text{H}$  coupling constants in square brackets,  $^{77}\text{Se}$ ,  $^3\text{P}$  coupling constants in waved brackets, all in Hz.<sup>a</sup>

	$\text{CH}_3$	<i>ortho</i> -H	<i>meta</i> -H	<i>para</i> -H	$\text{OCH}_3$	$\text{O-CH}(\text{CH}_3)_2$	$\text{O-CH}(\text{CH}_3)_2$	$\text{NCH}_2\text{-CH}_3$	$\text{NCH}_2\text{-CH}_3$	P	Se
<b>20</b>	2.21	7.94	7.51	7.55	3.55					91.8	-279
	(13.3)	ca 14			(14.7)					{788.9}	{789.3}
<b>21</b>	2.17	7.90	7.46	7.54	-	4.74	1.36, 1.08			85.1	-270
	(13.3)	(ca 14)				(13.3)	(6.3)			{778.7}	{779.1}
<b>22</b>	2.21	7.97	7.49	7.52				3.01	1.12	60.9	-250
	(12.7)	(ca 14)						(11.9) <sup>b</sup> , (7.1) <sup>c</sup>		{728.3}	{728.1}
<b>23</b>	2.42	-	-	-	3.88	-				74.1	-145
	(14.4)				(15.9)					{824.0}	{821.0}
	[2.0]				[0.8]						
<b>24</b>	2.42	-	-	-	-	5.12	1.37, 1.40			68.6	-136
	(14.4)					(13.3)	(6.3)			{808.0}	{808.0}
	[2.6]										

<sup>a</sup> In  $\text{CDCl}_3$ ; recorded at  $B_0 = 9.4$  or  $11.7$  Tesla; for details and referencing see experimental part. Generally,  $^1J(^{77}\text{Se}, ^3\text{P})$  values are negative.

<sup>b</sup>  $^2J(^1\text{H}, ^1\text{H})$ , in Hz.

<sup>c</sup>  $^3J(^1\text{H}, ^1\text{H})$ , in Hz

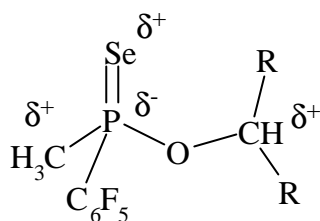
**Table 2.**  $^{13}\text{C}$  NMR chemical shifts (in ppm,  $\delta$  scale) of the phosphine selenides **20** - **24**;  $^3\text{P}$ ,  $^{13}\text{C}$  coupling constants in parentheses,  $^{19}\text{F}$ ,  $^{13}\text{C}$  coupling constants in square brackets, all in Hz.<sup>a</sup>

	$\text{CH}_3$	<i>ipso-C</i>	<i>ortho-C</i>	<i>meta-C</i>	<i>para-C</i>	$\text{OCH}_3$	$\text{O-CH}(\text{CH}_3)_2$	$\text{O-CH}(\text{CH}_3)_2$	$\text{NCH}_2\text{-CH}_3$	$\text{NCH}_2\text{-CH}_3$
<b>20</b>	25.6 (73.0)	131.6 (87.3)	133.0 (11.7)	128.3 (12.9)	132.2 (2.9)	52.1 (5.8)	-	-	-	-
<b>21</b>	27.3 (73.2)	135.5 (88.9)	130.9 (11.7)	128.2 (12.8)	131.9 (1-2)	-	71.5 (5.2)	24.1, 23.5 (4.0)	41.2 (3.3)	14.0 (5.4)
<b>22</b>	24.4 (65.9)	134.0 (90.9)	131.4 (11.3)	128.3 (12.7)	131.6 (2.9)	-	-	-	-	-
<b>23</b>	27.6 (77.4)	112.5 <sup>b</sup>	145.8 <sup>b</sup>	137.9 <sup>b</sup>	143.3 <sup>b</sup>	53.9 (5.9)	-	-	-	-
<b>24</b>	30.1 (73.6)	112.8 <sup>b</sup>	145.9 <sup>b</sup>	137.5 <sup>b</sup>	143.1 <sup>b</sup>	-	73.5 (5.6)	24.6, 23.1 (2.7), (6.5)	-	-
	[4.2]						<sup>c</sup>	[1.1]		

<sup>a</sup> In  $\text{CDCl}_3$ ; recorded at 125.7 MHz (**20**) or at 100.6 MHz (**21** - **24**); chemical shifts relative to internal TMS ( $\delta = 0$ ).

<sup>b</sup> Doublets of multiplets.

<sup>c</sup> Signal not resolved, i.e.,  $<1.0$  Hz.



**Scheme 2.** Inductive effects of the  $\text{C}_6\text{F}_5$  group in **23** and **24**, deduced from chemical shift comparisons with the respective phenyl derivatives **20** and **21**.<sup>a</sup>

- <sup>a</sup> Note that in this scheme “ $\delta^+$ ” and “ $\delta^-$ ” do not indicate the actual partial charges of the atoms themselves but rather the changes of partial charges on replacement of  $\text{C}_6\text{H}_5$  by  $\text{C}_6\text{F}_5$ . High-frequency shifts generally indicate a decrease and low frequency shifts an increase in electron densities.

### 2.2.2 Adduct Formation Shifts (**Dd**) in the Presence of **Rh-Rh**

Complexation shifts  $\Delta\delta$  (Table 3) are defined as differences of chemical shifts in the phosphine selenide ... **Rh-Rh** adduct as compared to the respective values in the free ligand. In accordance with the previous observations for other ligands,<sup>39,41</sup>  $\Delta\delta$ -values are small ( $<0.5$  ppm) or even negligible for  $^1\text{H}$  signals. They are larger for  $^{13}\text{C}$  (up to  $-4$  ppm) and  $^{31}\text{P}$  (up to  $+5.9$  ppm), a fact which is expected considering the much larger chemical shift range of these two nuclei. In the case of  $^{77}\text{Se}$  which is the complexation site, considerable shielding, i.e. negative complexation shifts, can be observed if  $\text{Ar} = \text{phenyl}$  whereas the  $\Delta\delta$ -value is negligible in the case of **23** or strongly reduced in **24** with  $\text{Ar} = \text{pentafluorophenyl}$ .<sup>\*</sup> Obviously, the  $\text{P}=\text{Se}$  polarization discussed above leads to a much smaller sensitivity of the selenium atom to complexation. The signs of these  $\Delta\delta$ -values indicate a changed  $\text{P}=\text{Se}$  bond polarization, now introduced by complexation and in the opposite direction. Again, one-bond  $^{77}\text{Se}$ - $^{31}\text{P}$  coupling constants (see values in parentheses in Figure 1) are good probes here; they are reduced by 8-10% in their absolute magnitude. In addition, the one-bond  $^{31}\text{P}$ ,  $^{13}\text{C}$  coupling constants at the P-methyl carbons are also decreased.

<sup>\*</sup>  $^{77}\text{Se}$  chemical shifts and one-bond  $^{77}\text{Se}$ , $^{31}\text{P}$  coupling constants values are not precise because the  $^{77}\text{Se}$  signals are considerably broadened; for the reason see below.

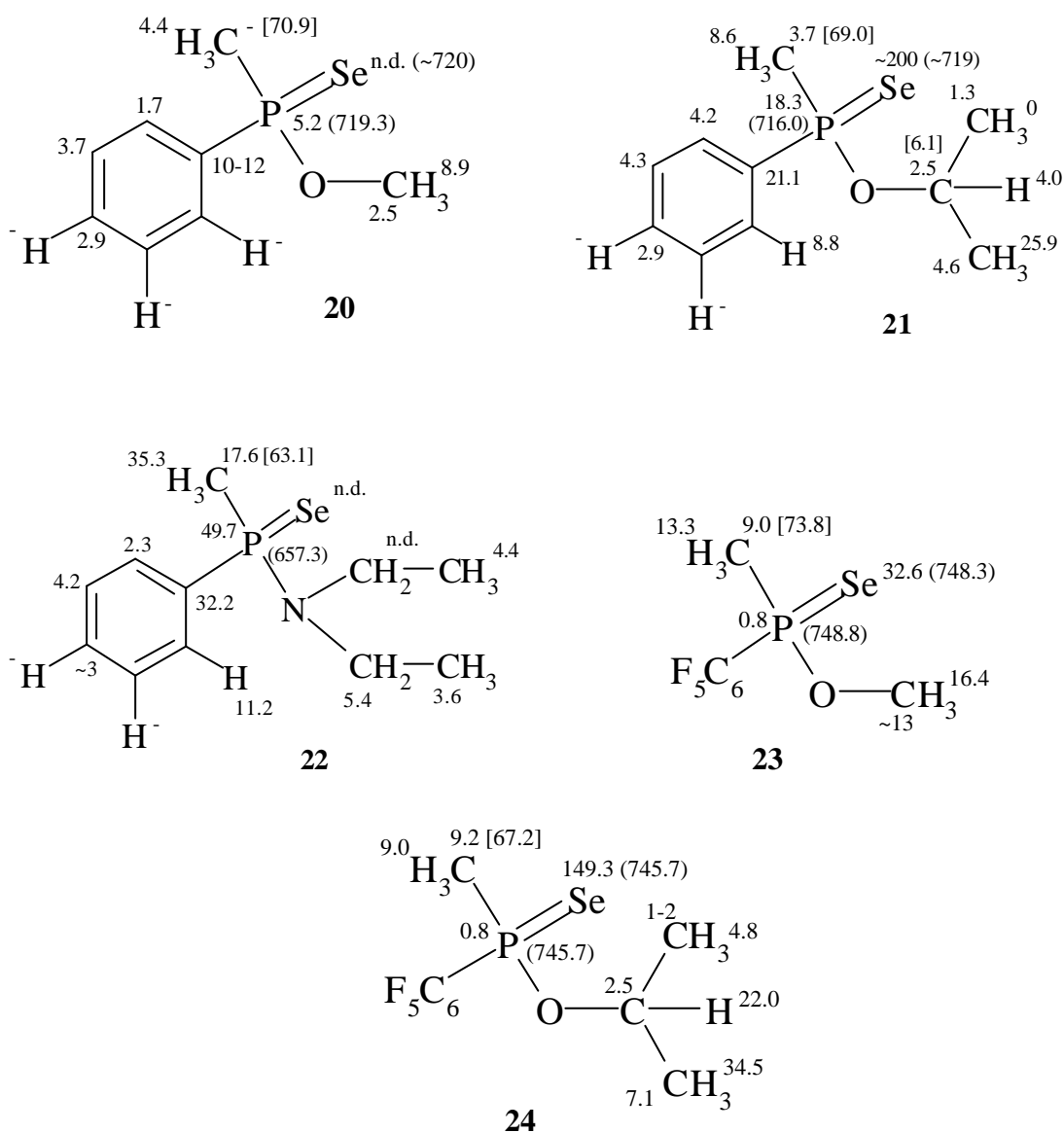


**Figure 1.** Dispersion effects ( $\Delta\nu$ , in Hz) in **20** - **24**, for 9.4 Tesla (400.1 MHz  $^1\text{H}$ , 100.6 MHz  $^{13}\text{C}$ , 161.9 MHz  $^{31}\text{P}$ , and 76.3 MHz  $^{77}\text{Se}$ )<sup>a</sup>; values in squared brackets are  $^{31}\text{P}$ ,  $^{13}\text{C}$  coupling constants and those in parentheses are one-bond  $^{77}\text{Se}$ ,  $^{31}\text{P}$  coupling constants, both in Hz; they are given only if significantly different from the respective values in the uncomplexed substrate.

<sup>a</sup> n.d.: not detectable due to line broadening ( $^{77}\text{Se}$ ) or signal complexity ( $^1\text{H}$ ).

Considerable shielding, i.e. negative complexation shifts can be observed if Ar = phenyl whereas the  $\Delta\delta$ -value is negligible in the case of **23** or strongly reduced in **24** with Ar = pentafluorophenyl. Obviously, the P=Se polarization discussed above leads to a much smaller sensitivity of the selenium atom to complexation. The signs of these  $\Delta\delta$ -values indicate another P=Se bond polarization, now introduced by complexation and in the opposite direction. Again, one-bond  $^{77}\text{Se}$ - $^{31}\text{P}$  coupling constants (see values in parentheses in Figure 1) are good probes here; they are reduced by 8-10% in their absolute magnitude. In addition, the one-bond  $^{31}\text{P}$ ,  $^{13}\text{C}$  coupling constants at the *P*-methyl carbons are also decreased.

### 2.2.3 Signal Dispersion Effects (**Dn**) and Chiral Recognition

The phosphine selenide derivatives **20** - **24** form kinetically instable complexes with the chiral dirhodium tetraacylate **Rh-Rh**. Thus, the observed chemical shifts represent weighted averages between corresponding shifts of the free and complexed ligand (**L**). For sake of simplicity and better comparability, all experiments were conducted for 1 : 1 mixtures of the phosphine selenides and (*R*)-**Rh-Rh** in  $\text{CDCl}_3$  containing small amounts of deuterated acetone for increased solubility<sup>41</sup> (see Experimental Part). Chiral recognition is based on dispersions ( $\Delta\nu$  in Hz), i.e. duplications of NMR signals originated by the existence of two different diastereomeric complexes, (*R*)-**L**...(*R*)-**Rh-Rh** and (*S*)-**L**...(*R*)-**Rh-Rh**. Such effects are listed in Figure 1 and exemplified in Figure 2 for all four nuclei ( $^1\text{H}$ ,  $^{13}\text{C}$ ,  $^{31}\text{P}$  and  $^{77}\text{Se}$ ) of **21** recorded. All four nuclei shows significant signal dispersion in the presence of **Rh-Rh**. It can immediately be seen that chiral recognition and determination of enantiomeric excess is easily accomplished by evaluating the peak intensities of several nuclei. So far, no other direct method – neither spectroscopic nor chromatographic – seems to exist in the literature.

Significant dispersion effects can be extracted for many nuclei. The largest  $\Delta\nu$ -values appear at the selenium atoms which are expected to be the complexation sites; the HOMO of compounds **20** - **24**, as calculated by using PM3 (Figure 6), is essentially the  $\pi$ -bond orbital of the P=Se group. It should be noted that all  $^{77}\text{Se}$  signals in the adducts



are severely broadened. Half-height line widths are mostly in the range of 50-100 Hz; in case of the adducts **20**...**Rh-Rh** and **22**...**Rh-Rh** line broadening is so pronounced that they cannot be distinguished from the noise level safely. We expect that coalescence effects associated with the dynamic process of adduct formation (Figure 3) exist for the  $^{77}\text{Se}$  signals due to their large chemical shifts difference in the two diastereomeric adducts. Very recently, similar effects have been observed by us in the case of diorganyl selenides.<sup>41a</sup>

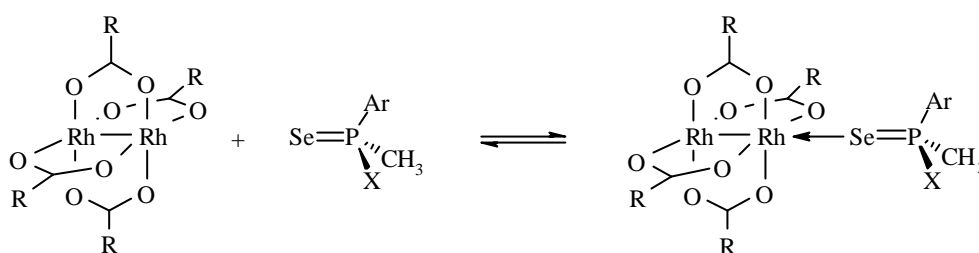


**Figure 3.** Equilibrium of 1:1-adduct formation of phosphine selenides **20** - **24** with **Rh-Rh**.

It is interesting to note that the dispersions at the  $^1\text{H}$  as well as the  $^{13}\text{C}$  signals of the two-diastereotopic isopropyl methyl groups in **21** and **24** are significantly different from each other (Figure 1). This can be originated only in distinct relative orientations with respect to the chiral Mosher acid residues of **Rh-Rh**. The PM3-based geometry (Figure 6) optimizations of both compounds **20** and **24** revealed a strongly preferred conformation with a torsion angle  $\tau(\text{C}^{ipso}\text{-P-O-C}) = 111.7^\circ$  which is apparently stabilized by severe steric constraints if any group is distorted. The dispersion effect in compounds **23** and **24** for  $^1\text{H}$ ,  $^{13}\text{C}$ ,  $^{31}\text{P}$  and  $^{77}\text{Se}$  are presented in Figures 4 and 5. The peaks in all four nuclei are somewhat broadened due to the presence of two, three and four bonds couplings with fluorine atom, Nevertheless we have signal dispersion in all nuclei.

Although it is not taken for granted that a similar conformation exists in the adduct, a marked difference in the relative position of these diastereotopic methyl groups and the chiral dirhodium complex is reasonable. However, despite their large  $\Delta\nu$  differences it is not possible to assign them without having a better understanding of the position of all atoms in the adducts.

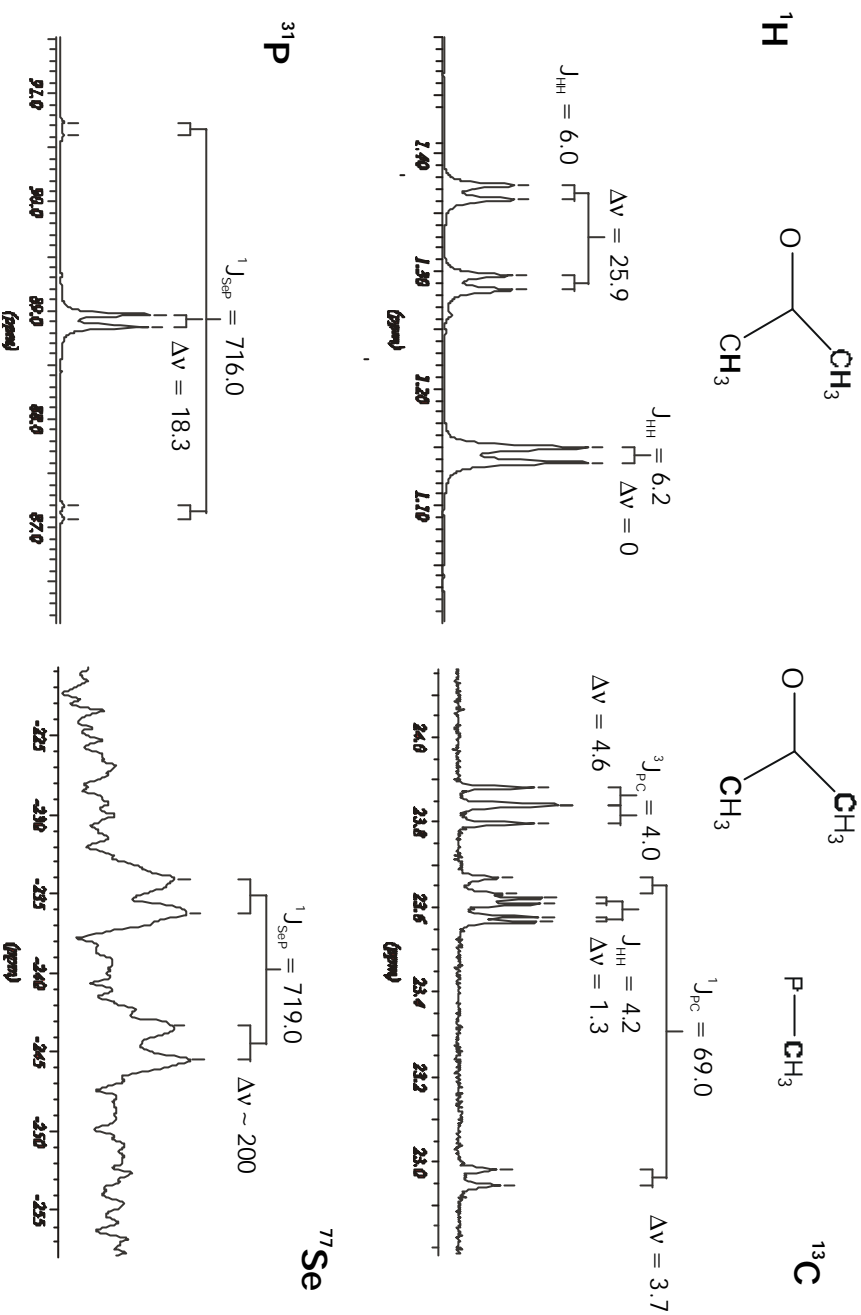


**Figure 2.** Dispersion effects of **21** in the presence of an equimolar amount of **Rh-Rh** ( $\Delta\nu$ , in Hz), as shown by sections of various NMR spectra (as indicated).

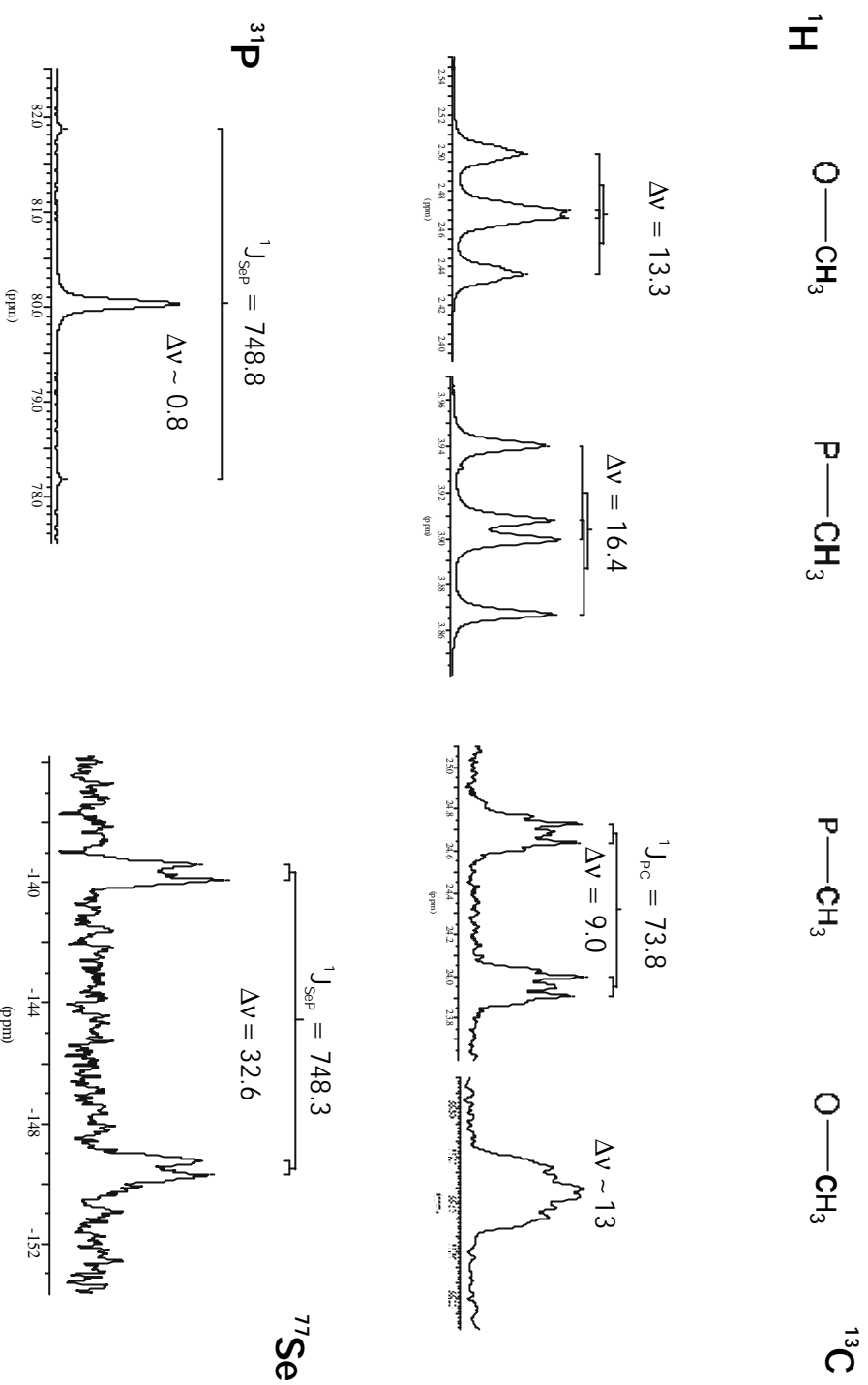


**Figure 4.** Dispersion effects of **23** in the presence of an equimolar amount of **Rh-Rh** ( $\Delta\nu$ , in Hz), as shown by sections of various NMR spectra (as indicated).

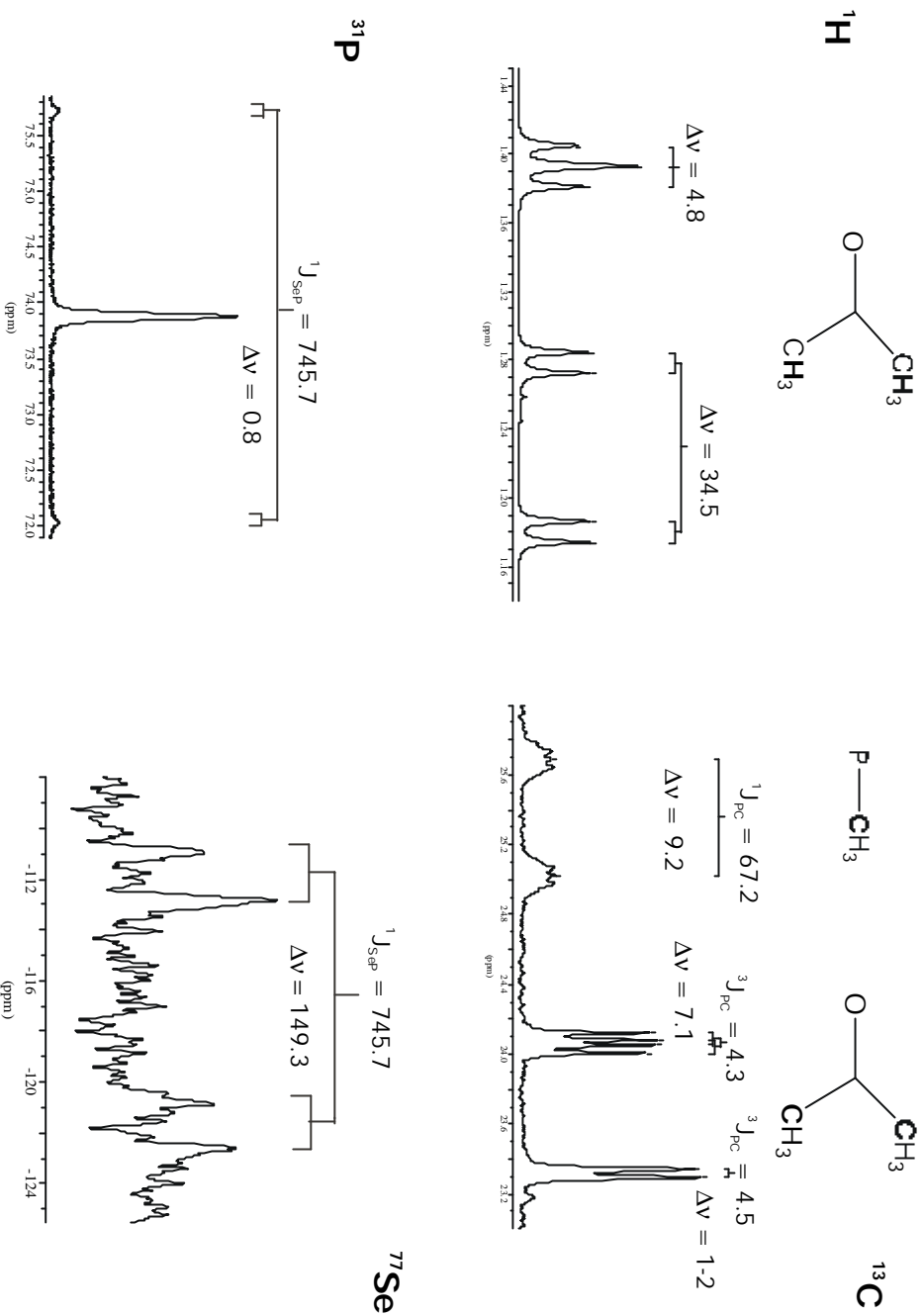
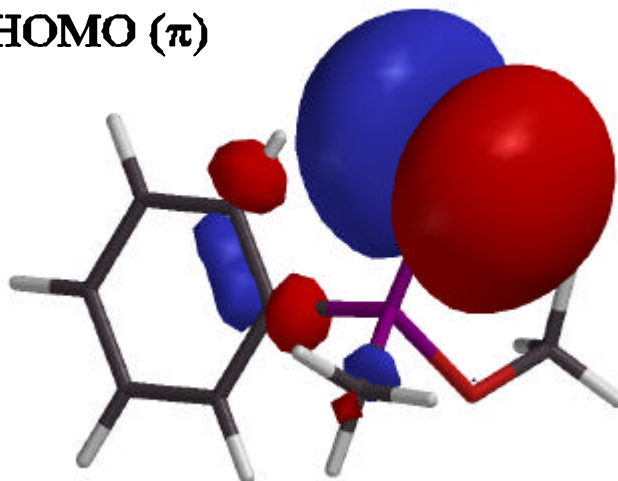


**Figure 5.** Dispersion effects of **24** in the presence of an equimolar amount of **Rh-Rh** ( $\Delta v$ , in Hz), as shown by sections of various NMR spectra (as indicated).

Ph(Me)P(=Se)-OMe (**20**; stable conformer)  
 $\tau(\text{C}^{\text{ipso}}\text{-P-O-C}) = 101^\circ$

**HOMO ( $\pi$ )**



Ph(Me)P(=Se)-O-iPr (**21**; stable conformer)  
 $\tau(\text{C}^{\text{ipso}}\text{-P-O-C}) = 111.7^\circ$

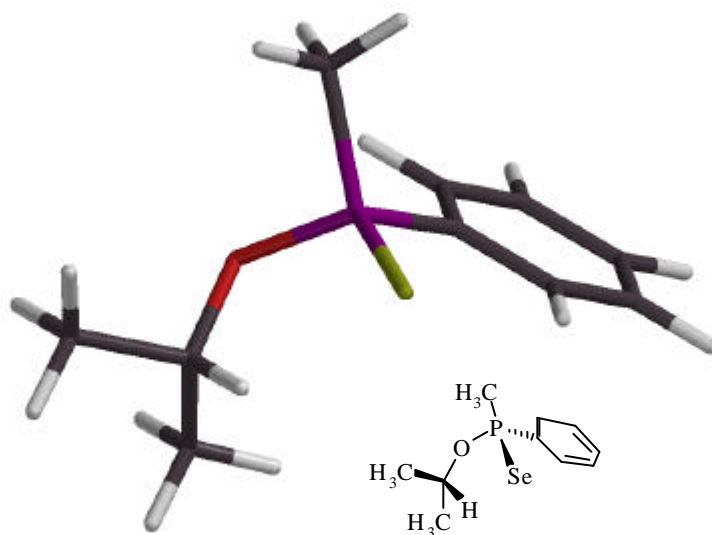


**Figure 6.** Preferred conformation of **21**, as calculated by PM3 methods.

**Table 3.**  $^1\text{H}$  NMR complexation shifts ( $\Delta\delta$ , in ppm) in the phosphine selenides **20** - **24** complexed by **Rh-Rh**.<sup>a,b</sup>

No	20	21	22	23	24
$\text{CH}_3$	+0.07	+0.05	+0.10	+0.05	+0.1
<i>ortho</i> -H	+0.17	+0.24	+1.30		
<i>meta</i> -H	d	d	-0.80		
<i>para</i> -H	d	d	-0.50		
$\text{OCH}_3$	+0.09			+0.02	+0.01/-0.13
$\text{O-CH}(\text{CH}_3)_2$		+0.19			+0.14
$\text{O-CH}(\text{CH}_3)$		+0.06/-0.04			
$\text{NCH}_2\text{-CH}_3$			+0.10		
$\text{NCH}_2\text{-CH}_3$			+0.01		

<sup>a</sup> In 1:1 molar ratios, referred to  $B_0 = 9.4$  Tesla; for details see experimental section.

<sup>b</sup> If the chemical shift differences are  $<0.01$  ppm for  $^1\text{H}$  or  $<0.1$  ppm for  $^{13}\text{C}$  or  $^{31}\text{P}$  and  $^{77}\text{Se}$ , only one  $\Delta\delta$  value is given.

<sup>d</sup> Doublets of multiples; no dispersion effects discernable.

**Table 4.**  $^{13}\text{C}$  NMR complexation shifts ( $\Delta\delta$ , in ppm) in the phosphine selenides **20** - **24** complexed by **Rh-Rh**.<sup>a,b</sup>

No	20	21	22	23	24
$\text{CH}_3$	-2.9	-4.0	-4.0	-3.5	-4.4
<i>ipso</i> -C	-1.4	-2.1	-2.2 <sup>c</sup>	-2.6 <sup>c</sup>	-2.7 <sup>c</sup>
<i>ortho</i> -C	0.0	+0.4	+0.8 <sup>c</sup>	+0.1 <sup>c</sup>	+0.3 <sup>c</sup>
<i>meta</i> -C	+0.1	+0.20	+0.2 <sup>c</sup>	0.0 <sup>c</sup>	+0.3 <sup>c</sup>
<i>para</i> -C	+0.1	+0.4	+0.7 <sup>c</sup>	+0.5 <sup>c</sup>	+0.7 <sup>c</sup>
$\text{OCH}_3$	+0.1			+1.6	
$\text{O-CH}(\text{CH}_3)_2$		+1.5			+1.7
$\text{O-CH}(\text{CH}_3)_2$		+0.1/-0.3			+0.2/-0.5
$\text{NCH}_2\text{-CH}_3$			+0.5		
$\text{NCH}_2\text{-CH}_3$					+0.1

<sup>a</sup> In 1:1 molar ratios, referred to  $B_0 = 9.4$  Tesla; for details see experimental section.

<sup>b</sup> If the chemical shift differences are  $<0.01$  ppm for  $^1\text{H}$  or  $<0.1$  ppm for  $^{13}\text{C}$  or  $^{31}\text{P}$  and  $^{77}\text{Se}$ , only one  $\Delta\delta$  value is given.

<sup>c</sup> Estimated from multiplet signals ( $^{19}\text{F}$ ,  $^{13}\text{C}$  couplings).

**Table 5.**  $^{31}\text{P}$  and  $^{77}\text{Se}$  NMR complexation shifts ( $\Delta\delta$ , in ppm) in the phosphine selenides **20 - 24** complexed by **Rh-Rh**.<sup>a,b</sup>

No	P	Se <sup>c</sup>
<b>20</b>	+3.8	~ -27
<b>21</b>	+3.8	-31.7
<b>22</b>	+4.0	d
<b>23</b>	+5.9	0.0
<b>24</b>	+5.3	-19.6

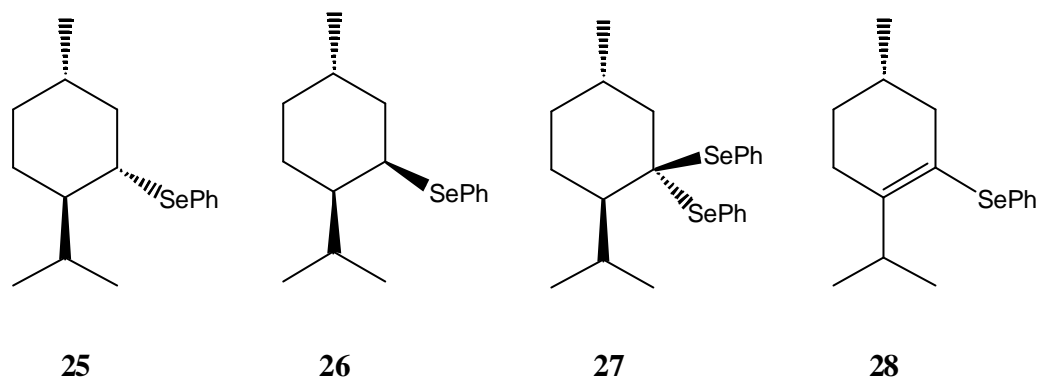
<sup>a</sup> In 1:1 molar ratios, referred to  $B_0 = 9.4$  Tesla; for details see experimental section.

<sup>b</sup> If the chemical shift differences are  $<0.01$  ppm for  $^1\text{H}$  or  $<0.1$  ppm for  $^{13}\text{C}$  or  $^{31}\text{P}$  and  $^{77}\text{Se}$ , only one  $\Delta\delta$  value is given.

<sup>c</sup>  $^{77}\text{Se}$  chemical shifts and one-bond  $^{77}\text{Se},^{31}\text{P}$  coupling constants values are not precise because the  $^{77}\text{Se}$  signals are considerably broadened.

<sup>d</sup> No  $^{77}\text{Se}$  signal found at room temperature.

## 2.3 PHENYSELENYNYLMENTHANE AND -MENTHENE DERIVATIVES (25 – 28)



**Scheme 3.** Structures of the phenylselenenylmenthane derivatives **25-28** investigated.

### 2.3.1 Signal Assignments of the Free Phenylselenenylmenthanes and Menthene 25 - 28

$^1\text{H}$  and  $^{13}\text{C}$  signals (see Tables 6 and 7, respectively) were assigned by using standard correlation techniques (DEPT, COSY, HMQC and HMBC). For  $^1\text{H}$  resonances inspection of the signal multiplicities in terms of  $^1\text{H}$ ,  $^1\text{H}$  couplings and NOE contacts were most helpful. If not obscured by overlap, signals of axial hydrogen's can be identified by large vicinal couplings in *antiperiplanar* configurations ( $J = 10\text{-}12$  Hz) whereas  $^3J$ -values for equatorial hydrogen's are much smaller in the *gauche* orientations (2-5 Hz). Figure 7 shows the  $^1\text{H}$  signal assignments in compound **26**. Except for few cases, unambiguous spectral interpretations including stereochemical hydrogen assignments could be achieved.

Cyclohexane ring inversion is excluded in the menthane derivatives **25-27** because the 1-methyl and the 4-isopropyl groups retain their equatorial position. Therefore, the PhSe substituent is equatorial in **25** and axial in **26** whereas both positions are occupied by the geminal selenium atoms in **27**. However, the conformational preference of the isopropyl groups varies.



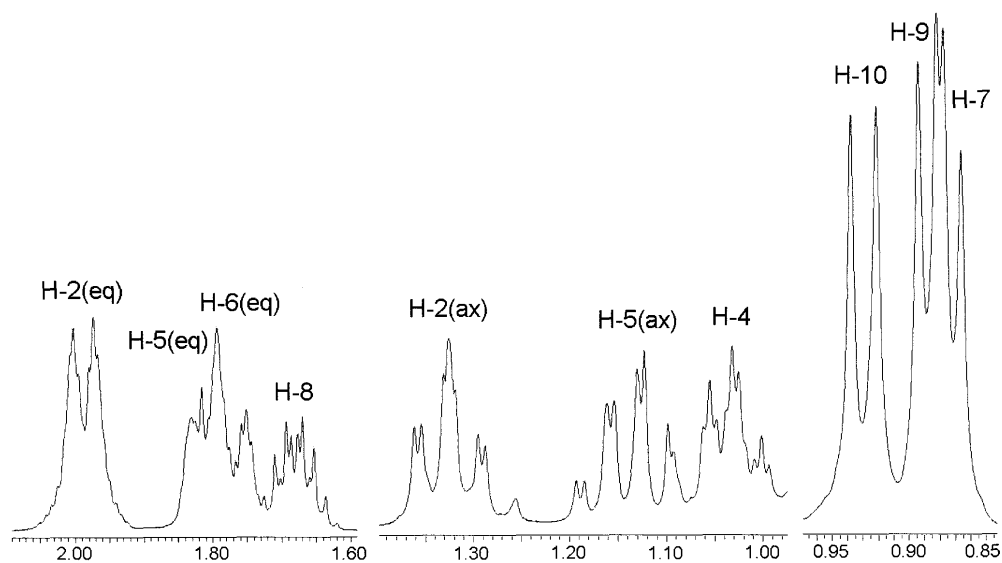
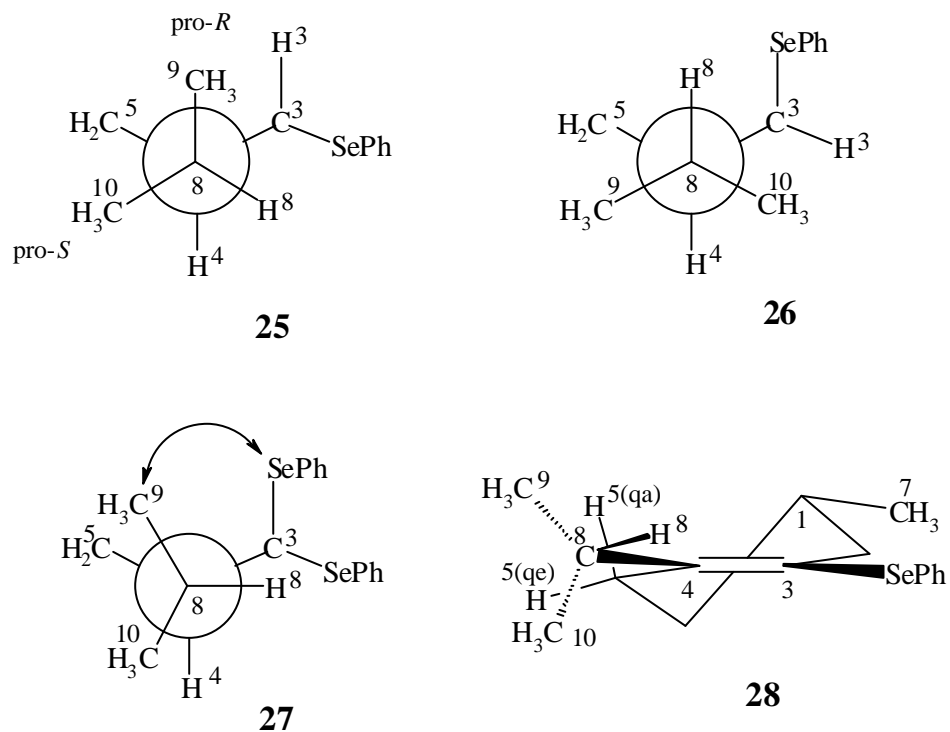


**Figure 7.** Section of the 400 MHz  $^1\text{H}$  NMR spectrum of **26**, in  $\text{CDCl}_3$ .



**Scheme 4.** Preferred conformations of the isopropyl groups in **25-28**.

The equatorial selenium atom in **25** forces the isopropyl group into a position with one methyl (9-CH<sub>3</sub>) to be *antiperiplanar* with respect to H-4 (Scheme 4) in order to avoid a strongly disfavored *skew*-pentane-type arrangement (C-9 – C-8 – C-4 – C-3 – Se). This can be proven by the <sup>13</sup>C chemical shifts of C-9 and C-10; the carbons see a different number of *γ-gauche* oriented groups suffering from different extents of diamagnetic signal shifts: C-9 two *γ-gauche* interactions with  $\delta(^{13}\text{C}) = 15.1$ ; C-10 only one *γ-gauche* interaction with  $\delta(^{13}\text{C}) = 21.4$  (Scheme 4, Table 7).<sup>55</sup> Moreover, the axially positioned H-3 shows a strong NOE contact with H-9 but no NOE with H-10. On the other hand, the same conformation-energy argument (*skew*-pentane) stabilizes the position of both methyl groups C-9 and C-10 *gauche* with respect to H-4 in the neomenthane derivative **26** with only one *γ-gauche* interaction for each and  $\delta(^{13}\text{C}) = 20.6$  and 21.0, respectively (Scheme 4, Table 7). The *vicinal* H-4/H-8 coupling constant is 10.0 Hz in accordance with the *antiperiplanar* orientation of these atoms. Interestingly, the C-9 and C-10 chemical shifts are  $\delta = 24.2$  and 19.0, respectively, in the bis-seleno acetal **27**. This leads to the conclusion that the isopropyl group in **27** prefers a conformation similar to that of **25**, however, somewhat distorted (Scheme 4). The distortion is ca 30° as suggested by AM1 calculations; any other rotamer is at least 15-20 kJ/mol less stable. In **27**, the atom C-9 ( $\delta = 24.2$ ) experiences a deshielding *skew*-pentane-type  $\delta$ -effect<sup>56</sup> from the axial selenium atom instead of the *γ-gauche*-effect from C-3/H-3 in **25**. The chemical shift of C-10 is  $\delta = 19.0$ . Here, a *γ-gauche*-effect smaller than those on C-10 of **25** or C-9 of **26** is effective in accordance with the larger spatial distance by the distortion. A further confirmation comes from the <sup>3</sup>J(H-4, H-8) coupling constant which is very small (0-1 Hz) because the torsion angle is close to 90°.

Finally, the menthene derivative **28** with only one chiral centre adopts a half-chair conformation with a quasi-equatorial methyl at C-1, and the preferred conformation of the isopropyl group is as shown in Scheme 4. I.e., H-8 points towards the selenium atom and is a little out-of-plane (15-20° according to AM1 calculations). This allowed to assign the two diastereotopic methyl groups 9 and 10: whereas irradiation of the methyl signal at  $\delta = 1.00$  produces NOE responses for both H-5 protons, that at  $\delta = 0.98$  enhanced the

intensity of the quasi-equatorial H-5(qe) only. Thus, the former signal was assigned to H-9 and the latter to H-10.

The  $^{77}\text{Se}$  NMR signals of **25-28** showed significant line broadenings due to coalescence effects. This phenomenon may provide information about the adduct formation processes<sup>41a</sup> and is discussed in chapter 3.2.3.<sup>41c</sup>

### 2.3.2 Complexation Shifts (**Dd**) in the Presence of **Rh-Rh**

The complexation site in the ligand molecules **25-28** is the selenium atom; phenyl rings are not able to bind at the rhodium atom(s)<sup>34-41</sup>. (It should be noted that chiral recognition of aromatic substrates by  $^{31}\text{P}$  NMR spectroscopy has been claimed for some mononuclear rhodium complexes containing phosphine ligands.)<sup>57</sup> As mentioned above<sup>41a</sup>, phenylselenides form 1:1- and 2:1- complexes with **Rh-Rh** which are in a fast-exchange equilibrium with free **Rh-Rh** because both partners exist in equimolar ratios. Therefore, this ratio was chosen for the present study.

Unambiguous signal assignment is mandatory for a reliable evaluation of complexation shifts and dispersion effects by adduct formation of the selenides **25-28** with **Rh-Rh**. In these experiments, signal assignment are based on the same 1D and 2D experiment as for the free selenides and were secured by comparative experiments with pure enantiomers under identical conditions. Nevertheless, some signals could not be identified beyond doubt, in particular those of the aromatic hydrogen's which are obscured by the much larger  $^1\text{H}$  signals of **Rh-Rh**.

$^1\text{H}$  and  $^{13}\text{C}$  chemical shifts in the ligand molecules may be changed by forming adducts between **Rh-Rh** and the selenide ligands. By definition, complex or adduct formation shifts ( $\Delta\delta$ ) are the differences between chemical shifts of ligand atoms in the adducts relative to the respective ones in the free ligands. In agreement with all previous observations for selenides and other monofunctional ligands  $\Delta\delta$  are moderately deshielding for atoms close to the complexed atom in terms of intervening bonds. This can indeed be observed for the selenides **25-28**; typical positive  $\Delta\delta$ -values exist only for the H3 and H-4 atoms (+0.09 to +0.70) and for the C-3 atoms (+2.1 to +4.0 ppm), see Tables 8 and 9.

However, negative  $\Delta\delta$ -values (shielding) of  $^1\text{H}$  signals may be observed in certain regions of the molecules, particularly for atoms further away from the complexation site. This is the case for H-6(eq) and H-7, the atoms with the largest distance to the complexation site (Se). A reasonable explanation is as follows: The nuclei experience a diamagnetic ring current effect if they come into close contact with the phenyl groups within the Mosher acid residues; electric field effects from the methoxy and/or the trifluoromethyl groups may be active as well.

Alternatively, significant  $\Delta\delta$ -values may arise from conformational distortions of parts of the ligand molecules during adduct formation, compared to the free ligand molecule. However, it is evident from the  $^1\text{H}$  and  $^{13}\text{C}$  signals that the isopropyl groups in the compounds **25-28** do not experience significant complexation shifts. Thus, it can be concluded that the conformational preferences of this group is hardly affected by complexation with **Rh-Rh**. This is different for H-1 and C-1 in **26** as well as for H-2(eq) and C-2 in most compounds **25-28**. A tentative explanation is the flexibility of the phenyl group at the selenium atom leading to different average orientations with respect to the C-1/C-2 fragments of **25-28**. In particular, the C-2/H-2(eq) bond being close in space with respect to the selenium atom(s) appears to suffer from a distinct bond polarisation from the hydrogens ( $\Delta\delta > 0$ ) towards the carbons ( $\Delta\delta < 0$ ).

Among the phenyl protons only those in *ortho*-position are significantly affected; they are deshielded in the adduct with respect to the free ligands. The *ipso*-carbons, however, are somewhat shielded whereas slight deshielding is observed for most of the *ortho*- and *para*- carbons but not for the *meta*-carbons. This suggests a change of the inductive and mesomeric properties of the selenium atoms by binding to rhodium.

### 2.3.3 Diastereomeric Dispersion Effects (**Dn**) - Determination of Absolute Configuration?

Even a brief overview of the data in Table 10 shows that most hydrogen and carbon atoms reflect the stereochemical difference in the diastereomeric adducts, some hydrogens display signal splittings up to 35 Hz. As an example, Figure 8 shows signal dispersions of methyl groups (CH<sub>3</sub>-7, CH<sub>3</sub>-9 and CH<sub>3</sub>-10) in <sup>1</sup>H NMR spectrum of **25**. Figure 9 shows signal dispersion of methyl groups (CH<sub>3</sub>-7, CH<sub>3</sub>-9, CH<sub>3</sub>-10 and H<sub>ax</sub>-6) in <sup>1</sup>H NMR spectrum of **27**. Two methyl groups (CH<sub>3</sub>-7 and CH<sub>3</sub>-9) shows significant signal dispersion 35.6 and 15.0 Hz. Figure 10 shows signal dispersion in <sup>13</sup>C NMR spectrum of **27**, all most all <sup>13</sup>C signal shows dispersion. It can be seen that it is easy to determine the enantiomeric purity of selenides by inspecting the intensity ratios of <sup>1</sup>H NMR signals.

Short-lived adducts like those of **Rh-Rh** with selenides and other ligands<sup>33,34,36</sup> appear to be very flexible so that any effect on NMR signals ( $\Delta\delta$  or  $\Delta\nu$ ) is time-averaged. Generally, within the series **25-28** the magnitudes and particularly the signs of the  $\Delta\nu$  values vary strongly for most of the <sup>1</sup>H and <sup>13</sup>C atoms. Since the carbon skeletons are very similar we are left with the assumption that the four ligands **25-28** adopt very divergent average orientations relative to **Rh-Rh** owing to the different stereochemical positions of the selenium atoms acting as binding sites. Therefore, we have to state that it is not very promising to read absolute configurations<sup>58</sup> from the signs of  $\Delta\nu$ -values of the NMR signals.

### 2.3.4 Conclusions

Phenylselenenylmenthanes and -menthenes form short-lived adducts with **Rh-Rh** easily. Thereby, deshielding effects of nearby hydrogens and carbons (in terms of the number of intervening bonds) are observed ( $\Delta\delta$ ), whereas some more remote nuclei are shielded. The phenyl orientation is changed whereas the isopropyl conformations are retained.

Many NMR signals are dispersed due to the existence of diastereomeric adducts ( $\Delta\nu$ ) when the chiral phenylselenenylmenthanes and -menthenes are bound to **Rh-Rh**. A determination of enantiomeric ratios is facile irregardless of the stereochemical position

of the selenium atom as the complexation site. This constitutes a simple and valuable method for chiral recognition in this class of compounds which is gaining increasing importance in developing new methodologies of asymmetric synthesis.

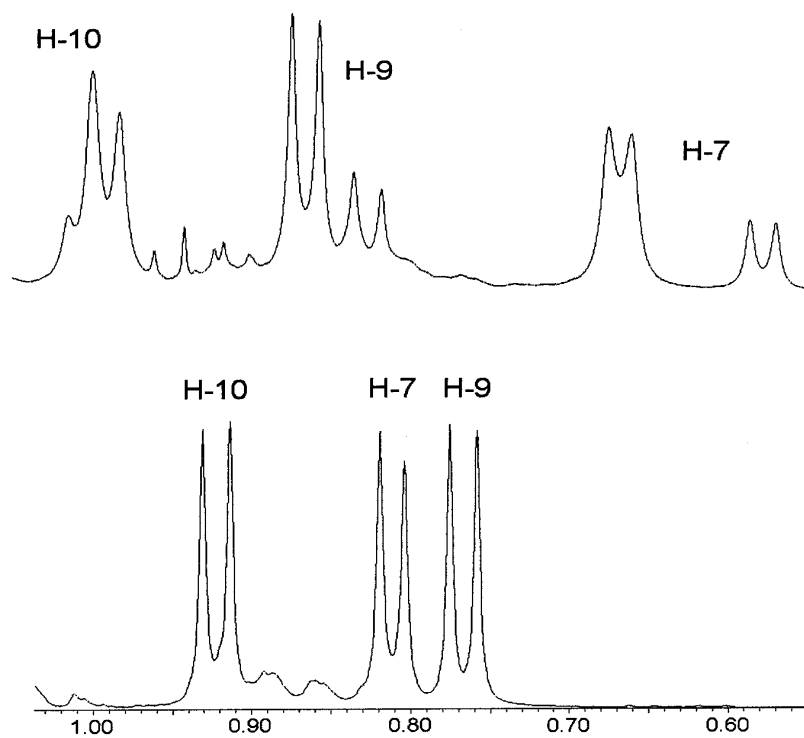


**Figure 8.** Section of the 400 MHz  $^1\text{H}$  NMR spectrum of **25**; in the absence (bottom) and in the presence (top) of an equimolar amount of **Rh-Rh**.

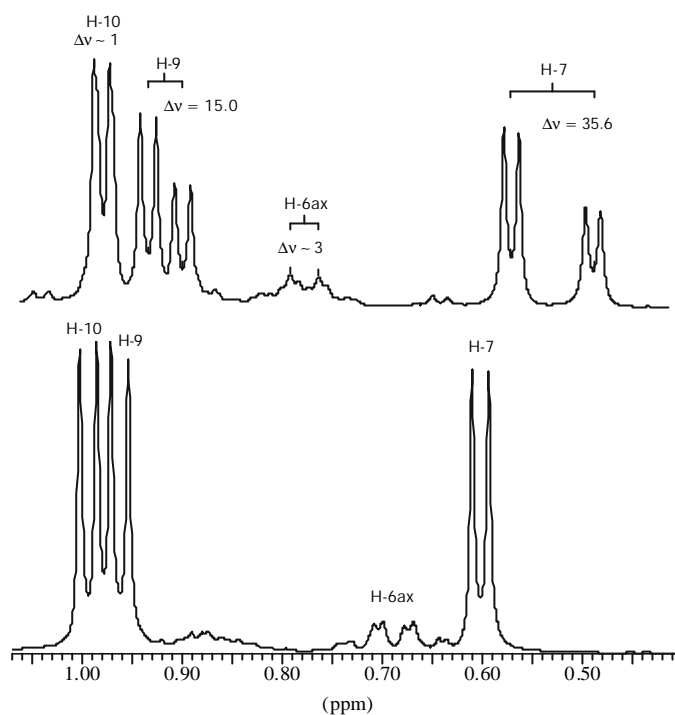


**Figure 9.** Section of the 400 MHz  $^1\text{H}$  NMR spectrum of **27**; in the absence (bottom) and in the presence (top) of an equimolar amount of **Rh-Rh**.

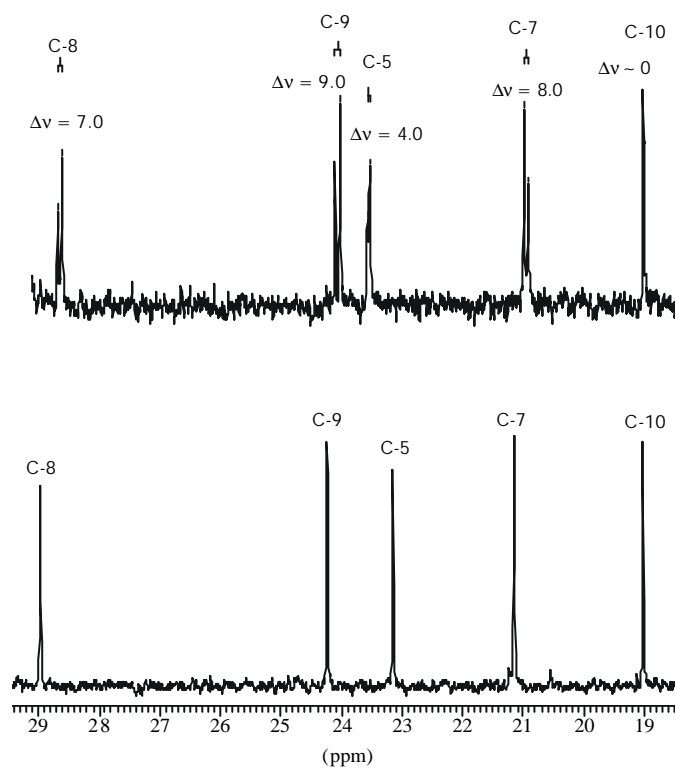


**Figure 10.** Section of the 400 MHz  $^{13}\text{C}$  NMR spectrum of **27**; in the absence (bottom) and in the presence (top) of an equimolar amount of **Rh-Rh**.

**Table 6.** <sup>1</sup>H chemical shifts of **25-28**, in CDCl<sub>3</sub>; samples with **Rh-Rh** contain a small amount of acetone-d<sub>6</sub> (for details see Experimental Part).<sup>a-c</sup>

No.	25		26		27		28	
H-1	1.29	m	1.99	m	2.01	m	1.68	m
H-2 (eq)	2.07	dm	1.99	dm	1.79	dt	2.34	dm
H-2 (ax)	1.25	m	1.33	ddd	1.23	dd	1.94	ddm
H-3 (eq)	-		3.71	m	-			
H-3 (ax)	3.07	td	-		-		-	
H-4	1.29	tm	1.04	ddt	1.38	dd	-	
H-5 (eq)	1.70	dm	1.82	dm	1.72	dm	2.23	dm
H-5 (ax)	1.06	td	1.15	qm	1.49	dddd	2.14	tm
H-6 (eq)	1.70	dm	1.77	dm	1.73	dm	1.77	dm
H-6 (ax)	0.87	qm	0.91	m	0.69	qd	1.22	m
H-7	0.81	d	0.87	d	0.61	d	0.88	d
H-8	2.42	sept d	1.69	m	3.02	sept	3.40	sept
H-9	0.77	d	0.89	d	0.97	d	1.00	d
H-10	0.92	d	0.93	d	1.00	d	0.98	d
H-ortho (eq)	7.55	dm			7.57	dm	7.37	dm
H-ortho (ax)			7.55	dm	7.82	dm		
H-meta (eq)	7.27	tm			7.26	tm	7.24	tm
H-meta (ax)			7.24	tm	7.34	tm		
H-para (eq)	7.27	tm			7.25	tm	7.21	tm
H-para (ax)			7.24	tm	7.33	tm		

<sup>a</sup> Recorded at 400.1 MHz.<sup>b</sup> Vicinal coupling constants involving methyl groups are ca 7 Hz.<sup>c</sup> Abbreviations “d”, “t”, “q”, “sept”, “m” indicate doublet, triplet, quartet, septet and (unresolved) multiplet, respectively.



**Table 7.**  $^{13}\text{C}$  chemical shifts of **25-28**, in  $\text{CDCl}_3$ ; samples with **Rh-Rh** contain a small amount of acetone- $\text{d}_6$  (for details see Experimental Part).<sup>a</sup>

No	25	26	27	28
C-1	34.3	27.7	29.9	30.6
C-2	44.9	41.8	48.0	42.6
C-3	48.3	50.4	66.8	120.7
C-4	47.7	49.5	51.7	148.3
C-5	25.0	27.2	23.1	24.8
C-6	34.7	35.2	34.8	30.9
C-7	22.1	22.1	21.1	21.2 <sup>b</sup>
C-8	29.1	31.3	28.9	34.5
C-9	15.1	20.6	24.2	20.5
C-10	21.4	21.0	19.0	21.1 <sup>b</sup>
<i>C-ipso</i> (eq)	129.0		129.5	131.6
<i>C-ipso</i> (ax)		130.8	126.6	
<i>C-ortho</i> (eq)	135.5		138.1	131.2
<i>C-ortho</i> (ax)		134.1	138.3	
<i>C-meta</i> (eq)	128.8		128.5	128.9
<i>C-meta</i> (ax)		128.8	128.5	
<i>C-para</i> (eq)	127.3		128.6	126.0
<i>C-para</i> (ax)		126.9	128.9	

<sup>a</sup> Recorded at 100.6 MHz.

<sup>b</sup> Not resolvable from HMQC; may be interchanged.

**Table 8.** Complexation effects ( $\Delta\delta$ , in ppm) on the  $^1\text{H}$  chemical shifts of **25-28**; in  $\text{CDCl}_3$  containing a small amount of acetone- $\text{d}_6$  (for details see Experimental Part).<sup>a,b</sup>

No	25		26		27		28	
	1 <i>R</i> ( <i>maj</i> )	1 <i>S</i> ( <i>min</i> )	1 <i>R</i> ( <i>maj</i> )	1 <i>S</i> ( <i>min</i> )	1 <i>R</i> ( <i>min</i> )	1 <i>S</i> ( <i>maj</i> )	1 <i>R</i> ( <i>min</i> )	1 <i>S</i> ( <i>maj</i> )
H-1	~ +0.4	~ +0.4	-0.68	-0.68	n.d.	n.d.	~ -0.1	~ -0.1
H-2 (eq)	+0.45	+0.40	+0.71	+0.63	+0.17	+0.17	+0.24	+0.17
H-2 (ax)	+0.18	+0.25	+0.16	n.d.	n.d.	n.d.	~ +0.1	~ +0.1
H-3 (eq)	-	-	+0.70	+0.68	-	-		
H-3 (ax)	+0.55	+0.57	-	-	-	-	-	-
H-4	~ +0.4	n.d.	+0.09	+0.11	n.d.	n.d.	-	-
H-5 (eq)	~ 0	~ 0	-0.03	-0.03	+0.11	+0.07	+0.02	-0.02
H-5 (ax)	+0.02	n.d.	+0.22	+0.22	+0.02	+0.02	~ -0.1	~ -0.1
H-6 (eq)	-0.11	n.d.	-0.20	-0.16	n.d.	n.d.	-0.13	-0.13
H-7 (ax)	~ -0.1	~ -0.1	-0.09	-0.09	+0.08	+0.07	~ -0.5	~ -0.5
H-7	-0.16	-0.25	-0.30	-0.30	-0.17	-0.08	-0.24	-0.27
H-8	+0.51	+0.51	+0.25	+0.25	n.d.	n.d.	+0.38	+0.39
H-9	+0.08	+0.04	-0.11	-0.03	-0.08	-0.04	0.00	-0.02
H-10	+0.05	+0.07	0.00	0.00	-0.02	-0.02	+0.07	+0.07
H- <i>ortho</i> (eq)	+0.34	+0.36			-0.04	+0.02	+0.43	+0.41
H- <i>ortho</i> (ax)			+0.43	+0.38	n.d.	n.d.		
H- <i>meta</i> (eq)	n.d.	n.d.			n.d.	n.d.	-0.05	-0.05
H- <i>meta</i> (ax)			n.d.	n.d.	n.d.	n.d.		
H- <i>para</i> (eq)	n.d.	n.d.			n.d.	n.d.	-0.08	-0.08
H- <i>para</i> (ax)			n.d.	n.d.	n.d.	n.d.		

<sup>a</sup> For each compound left: (1*R*)-enantiomer, right: (1*S*)-enantiomer; “major”: major constituent, “minor”: minor constituent in the non-racemic mixture; n.d.: not detectable safely.

<sup>b</sup> Recorded at 400.1 MHz.

**Table 9.** Complexation effects ( $\Delta\delta$ , in ppm) on the  $^{13}\text{C}$  chemical shifts of **25-28**; in  $\text{CDCl}_3$  containing a small amount of acetone- $d_6$  (for details see Experimental Part).<sup>a,b</sup>

No	25		26		27		28	
	1R (maj)	1S (min)	1R (maj)	1S (min)	1R (min)	1S (maj)	1R (maj)	1S (min)
C-1	-0.5	-0.6	-0.7	-0.9	+0.1	+0.1	0.0	0.0
C-2	-4.0	-3.7	-1.2	-1.6	+0.1	+0.1	-2.6	-2.8
C-3	+4.0	+3.8	+2.7	+2.4	+3.2	+2.9	+2.1	+2.2
C-4	-2.3	-2.3	+0.8	+0.8	+0.2	+0.3	+1.5	+1.4
C-5	-0.1	-0.1	-0.5	-0.5	+0.6	+0.6	+0.9	+1.3
C-6	-0.5	-0.3	+0.1	+0.1	-0.5	-0.7	0.0	0.0
C-7	-0.5	-0.5	-0.3	-0.3	-0.2	-0.1	+0.1 <sup>c</sup>	-0.2 <sup>c</sup>
C-8	0.0	0.0	-0.2	-0.2	+0.3	+0.2	0.0	0.0
C-9	-0.3	-0.3	+0.3	+0.2	+0.1	0.0	+0.3	+0.3
C-10	-0.2	-0.2	0.0	0.0	-0.1	-0.1	+0.6 <sup>c</sup>	+0.8 <sup>c</sup>
C- <i>ipso</i> (eq)	n.d.	n.d.			-2.5	-2.5	+1.2	+1.3
C- <i>ipso</i> (ax)			-1.9	-1.7	+0.1	+0.2		
C- <i>ortho</i> (eq)	+0.8	+0.9			-0.1	-0.2	+2.0	+2.1
C- <i>ortho</i> (ax)			+2.1	+2.2	-0.1	-0.1		
C- <i>meta</i> (eq)	n.d.	n.d.			+0.2	+0.2		
C- <i>meta</i> (ax)			-0.2	-0.2	+0.2	+0.3	+0.6	+0.4
C- <i>para</i> (eq)	n.d.	n.d.			-0.3	-0.3		
C- <i>para</i> (ax)			+1.7	+1.7	-0.4	-0.4	n.d.	n.d.

<sup>a</sup> For each compound left: (1R)-enantiomer, right: (1S)-enantiomer; “major”: major constituent, “minor”: minor constituent in the non-racemic mixture; n.d.: not detectable safely.

<sup>b</sup> Recorded at 100.6 MHz.

<sup>c</sup> Values for C-7 and C-10 may be interchanged pairwise for each enantiomer.

**Table 10.** Dispersion effects ( $\Delta\nu$ , in Hz) at the  $^1\text{H}$  and  $^{13}\text{C}$  chemical shifts of **25-28**;<sup>a,b</sup> in  $\text{CDCl}_3$  containing a small amount of acetone- $d_6$  (for details see Experimental Part).<sup>a,b</sup>

No	$^1\text{H}$				$^{13}\text{C}$			
	25	26	27	28	25	26	27	28
1	n.d.	~ 0	n.d.	0.0	+14	+21	~ 0	-29
2 (eq)	+17.8	~ +33	n.d.	-21.2	-23	+26	-5	+13
2 (ax)	~ +45	n.d.	n.d.	n.d.				
3 (eq)	-	+10.8	=	-	+24	+28	+34	-15
3 (ax)	~ -10 <sup>c</sup>	-	-	-				
4	~ +17 <sup>c</sup>	~ -6	n.d.	-	0	+6	-9	+8
5 (eq)	<2	~ 0	n.d.	n.d.	-5	-5	+4	-22
5 (ax)	<2	~ 0	n.d.	n.d.				
6 (eq)	n.d.	~ -15	n.d.	0.0	-15	0	-18	0
6 (ax)	n.d.	~ 0	~ +3	0.0				
7	+35.4	-3.1	-35.6	-7.3	0	0	-8	-12
8	~ 0	~ 0	n.d.	-2.4	~ -1	+4	+7	0.0
9	+15.4	-31.2	-15.0	-6.4	+3	+2	+9	+8
10	-7.8	0	~ -1	~ -1	0	0	~ 0	-12
<i>ipso</i> (eq)	-	-	-		n.d.		~ +1	
<i>ipso</i> (ax)		-	-	-		~ +16	-6	-12
<i>ortho</i> (eq)	-10.0		-26.8		-14		+7 <sup>d</sup>	-12
<i>ortho</i> (ax)		+14	n.d.	~ -7		-3	~ 0 <sup>d</sup>	
<i>meta</i> (eq)	n.d.		n.d.		n.d.		-7 <sup>e</sup>	+15
<i>meta</i> (ax)		n.d.	n.d.	n.d.		-2	-10 <sup>e</sup>	
<i>para</i> (eq)	n.d.		n.d.		n.d.		-6	n.d.
<i>para</i> (ax)		n.d.	n.d.	n.d.		0	-2	

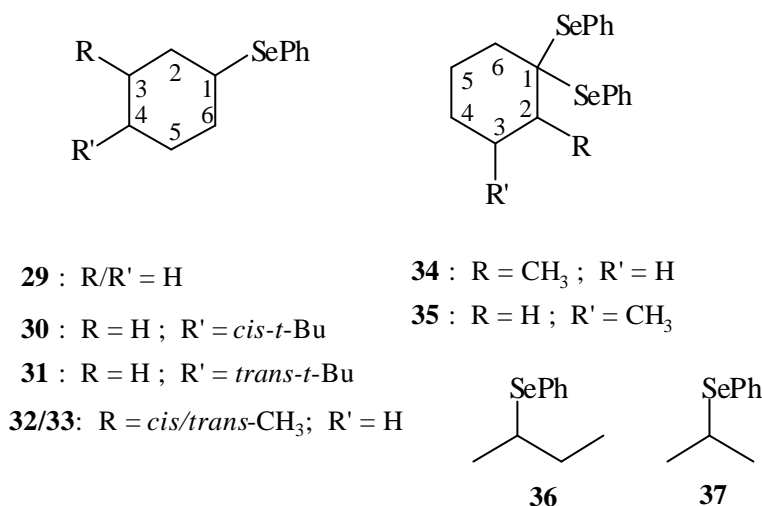
<sup>a</sup> The  $\Delta\nu$ -values (in Hz, at 400.1 and 100.6 MHz, respectively) are defined as follows: the chemical shift (in Hz) of the (1*S*)-enantiomer is subtracted from the respective one in the (1*R*)-enantiomer irregardless which is the major and which the minor constituent.

<sup>b</sup> Note that  $\Delta\nu$ -values are field-dependent; in this study they are referred to 400.1 MHz ( $^1\text{H}$ ) and 100.6 MHz ( $^{13}\text{C}$ ); n.d.: not detectable safely.

<sup>c</sup> Signal of the 1*S*-enantiomer is not detectable in the 1D spectrum. However, from the HMQC experiment and/or by signal overall-width comparisons we expect a dispersion as indicated.

<sup>d,e</sup> May be interchanged pair wise.

## 2.4 PHENYLSELENYNYLCYCLOHEXANE DERIVATIVES AND OTHER SECONDARY SELENIDES (29-37)



**Scheme 5.** Structures of the phenylselenenylalkane derivatives investigated **29-37**.

### 2.4.1 Signal Assignments and Conformational Analyses of 29-37

<sup>1</sup>H and <sup>13</sup>C signals of the phenylselenenylcyclohexane derivatives **29-35**, 2-phenylselenenylbutane (**36**) and 2-phenylselenenylpropane (**37**) (Scheme 5 and Tables 11 and 12, respectively) were assigned by using standard correlation techniques (DEPT, COSY, HMQC and HMBC) as well as by inspecting <sup>77</sup>Se,<sup>13</sup>C and <sup>77</sup>Se,<sup>1</sup>H coupling constants. For <sup>1</sup>H resonances inspections of the signal multiplicities in terms of <sup>1</sup>H,<sup>1</sup>H couplings were most helpful. If not obscured by overlap, signals of axial hydrogens appear as triplets or double doublets due to large *geminal* and *vicinal* couplings in *antiperiplanar* configurations (<sup>3</sup>J = 10-12 Hz) whereas equatorial hydrogens give doublet-typed resonances because all *vicinal* couplings are from *gauche* orientations (<sup>3</sup>J ≈ 3 Hz). Except for few cases, unambiguous spectral interpretations including stereochemical hydrogen assignments could be achieved. This was important for a reliable evaluation of complexation shifts and dispersion effects by adduct formation of the selenides **29-37** with **Rh-Rh**.

Although, the cyclohexane derivative **29** is not chiral, it has been included in this study as the parent compound. Its conformational behaviour has been described before.<sup>59</sup> As for other monosubstituted cyclohexanes, a ring inversion equilibrium exists with a strong preference for the equatorial SePh conformer ( $A = 1.1$ ).<sup>59</sup> Thus, the NMR signals which are conformation-averaged can be expected to be close to those of a conformationally rigid cyclohexane with an equatorial PhSe-group. This is confirmed by comparison of the data with those of the 4-*tert.*-butylcyclohexanes **30** (axial PhSe) and **31** (equatorial PhSe) which are achiral as well.

In *cis*-3-methylcyclohexylphenylselenide (**32**) both substituents are in equatorial position; the inverted conformer with two substituents in *syn*-diaxial position can be excluded because of the steric compression. However, the situation in the *trans*-isomer (**33**) is not as clear-cut; in each conformer one substituent is axial and the other equatorial. Since the A-value of CH<sub>3</sub> is clearly larger (1.7),<sup>60</sup> than that of SePh (1.1)<sup>59</sup>, the conformer with the axial selenium atom prevails.

Likewise, the methyl groups in the diselenoacetal derivatives **34** and **35** govern the conformational behaviour in that they strongly prefer the equatorial position; in the case of the 1,3-isomer **35** any invertomer can even be excluded for the same reason as for **32** (diaxial interaction).

Therefore, we can assume that all conformational equilibria are strongly biased. As we have shown for the menthane derivatives **25** - **28** (chapter 2.3).<sup>41b</sup> It can be expected that this is not severely changed by **Rh-Rh** adduct formation so that it is allowed to compare chemical shifts of the ligands **29** - **37** in absence and presence of an equimolar amount of the complex **Rh-Rh**.

#### 2.4.2 Adduct Formation Shifts (**Dd**) and Diastereomeric Dispersion (**Dn**) - Chiral Recognition

The complexation site in the ligand molecules is the selenium atom<sup>41a,b</sup>; phenyl rings are not able to bind at the rhodium atom(s).<sup>34,40</sup> In agreement with previous observations for selenides and other functionalities, adduct formation shifts ( $\Delta\delta$ ; Table 13 and 14), i.e. differences between chemical shifts of ligand atoms in the adduct (1:1 molar ratios) relative to the respective ones in the free ligands, are generally positive but small for atoms in one to three bond distances from the complexation site Se ( $\Delta\delta = +0.3$  to  $+0.8$  for  $^1\text{H}$  and  $\Delta\delta = +1.5$  to  $+6.0$  for  $^{13}\text{C}$ ). On the other hand, they are low or practically absent for atoms further away. We interpret this deshielding as a change in the inductive effect of Se in the adduct as compared to the free ligand to a C( $\alpha$ )-Se bond polarization.<sup>33,36,40</sup> Correspondingly, the  $^{77}\text{Se}$  nuclei are shielded. Occasionally, significant negative  $\Delta\delta$ -values ( $\Delta\delta$  up to  $-0.2$  for  $^1\text{H}$  or up to  $-3.5$   $^{13}\text{C}$ ) can be observed, particularly for atoms far away from the complexation site. These observations have been discussed before.<sup>35,41b</sup> Apparently, these are the atoms coming close to the anisotropic groups of the Mosher acid residues in **Rh-Rh**.

Dispersion effects ( $\Delta\nu$ ) are collected in Table 15 ( $^1\text{H}$  NMR) and Table 16 ( $^{13}\text{C}$  NMR). Since we used racemates, there is no possibility to determine which belongs to the (*R*)- and which to the (*S*)-isomer so that in a given entry of Tables 13 and 14 the values with the larger chemical shifts were noted on the left and those with the lower on the right-hand side. Consequently, all  $\Delta\nu$ -data in Tables 15 and 16 are absolute values. In chapter 2.3, we have shown in a similar investigation on non-racemic mixtures of menthene compounds **25-28** that **Rh-Rh**-adducts and signs of  $\Delta\nu$ -values are not appropriate for the determination of absolute configuration.

The  $^1\text{H}$  signals are often complex and overlapping in the adduct formation experiment. Often, it is nearly impossible to extract dispersion effects unless the signals are unobscured. This holds for the aromatic protons and carbons as well, whose signals interfere with those of the Mosher acid phenyl groups; only the *ortho*-proton and -carbon signals are exceptions.

As can be seen from the data in Table 15, all methyl proton signals are well suited for chiral recognition; strong dispersion effects can be observed in most cases. Incidentally, the diselenoacetal **32** was a particularly fortunate case in that many signals could be tested for  $\Delta\nu$ -values although their precision was not too good. Nevertheless, it is clear that even the protons in the cyclohexane ring are very sensitive to diastereomerism in the adducts; see for example in compound **35**, the two H-2 atoms whose  $\Delta\nu$ -values are in the range of 80 to 90 Hz. These are among the largest  $^1\text{H}$  dispersion effects ever recorded by the “Dirhodium Method” for any kind of ligands. Most of the  $^{13}\text{C}$  signals in compound **32** and **36** show splittings as well which are presented in Table 16. Here, however, the  $\Delta\nu$ -values of the methyl carbons are surprisingly low compared to other carbon atoms in the cyclohexane rings.



**Table 11.** <sup>1</sup>H chemical shifts of the phenylselenenylalkane derivatives **29-37**.<sup>a</sup>

No	29	30	31	32	33	34	35	36	37
H-1 (eq)	-	3.76	-	-	3.70	-	-	1.40	1.43
H-1 (ax)	3.25	-	3.09	3.17	-	-	-		
H-2 (eq)	2.04	2.10	2.13	2.05	1.93	-	2.06	3.24	3.45
H-2 (ax)	1.51	1.70	1.45	1.14	1.49	1.70	1.40		
H-3 (eq)	1.74	1.65	1.79	0.86	-	1.52	-	1.70	
								1.61	
H-3 (ax)	1.33	1.50	1.02	-	1.89	1.75	1.98		
H-4 (eq)	1.60	1.05	-	2.03	1.67	1.72	1.69	1.00	
H-4 (ax)	1.25	-	1.01	1.34	1.01	1.21	0.65		
H-5 (eq)	1.74	1.65	1.79	1.76	1.71	1.65	1.46		
								-	-
H-5 (ax)	1.33	1.50	1.02	1.29	1.56	1.02	1.90		
H-6 (eq)	2.04	2.10	2.13	1.88	1.84	1.87	2.02	-	-
H-6 (ax)	1.51	1.90	1.45	1.67	1.75	1.57	1.65		
CH <sub>3</sub>	-	-	-	0.87	0.90	1.34	0.78	-	-
<i>t</i> -Bu-CH <sub>3</sub>	-	0.87	0.81	-	-	-	-	-	-
H- <i>ortho</i> <sub>(ax)</sub>	-	7.53	-	-	7.53	7.86	7.80	7.55	7.55
H- <i>meta</i> <sub>(ax)</sub>	-	7.25	-	-	7.25	7.37	7.33	7.26	7.25-
H- <i>para</i> <sub>(ax)</sub>	-	7.24	-	-	7.27	7.40	7.40	7.26	7.28
H- <i>ortho</i> <sub>(eq)</sub>	7.55		7.54	7.55	-	7.60	7.61	-	-
H- <i>meta</i> <sub>(eq)</sub>	7.27		7.25	7.25	-	7.27	7.28	-	-
H- <i>para</i> <sub>(eq)</sub>	7.25		7.24	7.27	-	7.33	7.36	-	-

<sup>a</sup> Recorded at 400.1 MHz in CDCl<sub>3</sub> with two drops of acetone-d<sub>6</sub>. Notations s, d, t, q, m, br indicate singlet, doublet, triplet, quartet, multiplet and broad, respectively. Asterisked values may be interchanged.

**Table 12.**  $^{13}\text{C}$  chemical shifts of the phenylselenenylalkane derivatives **29-37**.<sup>a</sup>

No	29	30	31	32	33	34	35	36	37
C-1	43.2	44.6	42.9	42.5	43.5	65.6	56.8	21.6	24.3
C-2	34.2	32.6	34.9	43.0	40.5	41.4	47.1	41.5	33.8
C-3	26.9	23.1	28.6	34.1	28.5	31.3	29.7	30.5	-
C-4	25.7	48.3	47.3	34.0	34.3	23.8	33.7	12.3	-
C-5	26.9	23.1	28.6	27.3	22.2	25.9	23.7	-	-
C-6	34.2	32.6	34.9	32.2	32.2	38.7	37.9	-	-
CH <sub>3</sub>	-	-	-	22.5	21.6	20.2	21.9	-	-
<i>t</i> -Bu-C	-	32.6	32.5	-	-	-	-	-	-
<i>t</i> -Bu-CH <sub>3</sub>	-	27.5	27.5	-	-	-	-	-	-
<i>C-ipso</i> <sub>(ax)</sub>	-	130.9	-	-	130.6	126.2	127.5	129.5	129.5
<i>C-ortho</i> <sub>(ax)</sub>	-	133.8	-	-	133.9	138.3	137.8	134.9	134.8
<i>C-meta</i> <sub>(ax)</sub>	-	128.9	-	-	128.9	128.6	128.7	128.8	128.8
<i>C-para</i> <sub>(ax)</sub>	-	126.9	-	-	127.0	128.8	128.9	127.3	127.3
<i>C-ipso</i> <sub>(eq)</sub>	129.1	-	129.1	129.1	-	129.4	129.0	-	-
<i>C-ortho</i> <sub>(eq)</sub>	134.7	-	134.8	134.8	-	138.0	138.2	-	-
<i>C-meta</i> <sub>(eq)</sub>	128.8	-	128.8	128.8	-	128.6	128.6	-	-
<i>C-para</i> <sub>(eq)</sub>	127.2	-	127.2	127.2	-	128.7	128.8	-	-

<sup>a</sup> Recorded at 100.6 MHz in CDCl<sub>3</sub> with two drops of acetone-d<sub>6</sub>.

**Table 13.** Adduct formation shifts  $\Delta\delta$  (<sup>1</sup>H) on hydrogen atoms in the phenylselenenylalkane derivatives **29** – **37**.<sup>a</sup>

No	29	30	31	32	33	34	35	36	37	
		<i>cis</i>	<i>trans</i>	<i>cis</i> (minor)	<i>trans</i> (major)					
H-1 (eq)	-	+0.78	-	-	+0.72/+0.72	-	-	-	+0.10/+0.10	+0.10/+0.09 <sup>d</sup>
H-1 (ax)	+0.54	-	+0.65	+0.66/+0.64	-	-	-	-		
H-2 (eq)	+0.06	0.0	+0.16	~+0.23	~+0.02		+0.33/+0.12		+0.63/+0.62	+0.57
H-2 (ax)	+0.08	-0.41	+0.13	~+0.10			+0.53/+0.29			
H-3 (eq)	-0.15	-0.10	-0.12	~ -0.10	~+0.17		-		+0.33/+0.33	~+0.12
H-3 (ax)	-0.20	+0.10	-0.07			~+0.10				
H-4 (eq)	-0.13	-	-				~ -0.16		-0.02/-0.03	
H-4 (ax)	-0.13	-0.03	-0.06		~+0.02		~ -0.06		~ 0.02	
H-5 (eq)	-0.15	+0.01	-0.12				~ -0.14			
H-5 (ax)	-0.20	-0.14	-0.07			~+0.05				
H-6 (eq)	+0.06	+0.06	+0.16	~+0.38	~+0.11	~+0.43	+0.27/+0.12			
H-6 (ax)	+0.08	+0.03	+0.13			~+0.58				
CH <sub>3</sub>	-	-	-	-0.10/-0.13	-0.11/-0.13	+0.02/-0.05	-0.15/-0.20			
<sup>t</sup> Bu-CH <sub>3</sub>	-	-0.03	-0.05							
H- <i>ortho</i>	+0.15	+0.16	+0.25						+0.26	+0.25
H- <i>meta</i>	-0.15	+0.23	-0.04						~ -0.1	not evaluated
H- <i>para</i>	-0.24	-	+0.05						~+0.04	not evaluated

<sup>a</sup> Recorded at 400.1 MHz in CDCl<sub>3</sub> with two drops of [D<sub>6</sub>]acetone.<sup>b</sup> Empty entries indicate that the respective signals could not be identified safely.<sup>c</sup> Entries with “~”: signal could be identified but not the dispersion. Therefore, the  $\Delta\delta$ -values are not accurate ( $\pm$  ca 0.02).<sup>d</sup> since H-1 and H-3 in are prochiral in the free ligand, two different signals appear in the adduct. No stereodifferentiation.

**Table 14.** Adduct formation shifts  $\Delta\delta(^{13}\text{C})$  on carbon atoms in the phenylselenenyalkane derivatives **29** - **37**.<sup>a</sup>

No	29	30	31	32	33	34	35	36	37
		<i>cis</i>	<i>trans</i>	<i>cis</i> (minor)	<i>trans</i> (major)				
C-1	+3.8	+2.8	+4.4	+3.9/+3.9	+2.6/+2.6	+6.0/+6.0	~ +6.2	-2.8/-2.9	-1.7 <sup>c</sup>
C-2	-1.9*	-2.7	-2.1 <sup>†</sup>	-2.1/-2.2	-2.8/-2.8	+0.7/+0.1	-1.8/-2.0	+4.5/+4.5	+4.8
C-3	-0.2*	-0.4	-0.5*	-0.2/-0.3	-0.4/-0.5	+0.6/+0.6	+0.1/-0.1	-1.9/-1.9	-
C-4	-0.3	-0.2	-0.4	+0.2/+0.1	~ -0.3	0.0/-0.1	-0.1/-0.2	-0.5/-0.6	-
C-5	-0.2	-0.4	-0.4*	~ -0.4	-0.3/-0.4	-0.8/-0.9	-0.1/-0.3	-	-
C-6	-2.0	-2.7	-2.2 <sup>†</sup>	-0.1/-0.2	-2.5/-2.6	-0.1/-0.3	-1.5/-1.7	-	-
CH <sub>3</sub>	-	-	-	~ -1.5	+0.7/+0.6	0.0	-0.3/-0.4	-	-
<sup>t</sup> Bu-C	-	-0.1	-0.2	-	-	-	-	-	-
<sup>t</sup> Bu-CH <sub>3</sub>	-	-0.1	-0.1	-	-	-	-	-	-
C- <i>ipso</i>	-2.8	-3.5	-2.1	-0.5/-0.5	-2.2/-2.2			-0.9/-0.9	-1.0
C- <i>ortho</i>	+0.3	+0.4	+0.2	+0.5/+0.5	+0.7/+0.6			0.0	+0.1
C- <i>meta</i>	-0.1	0.0	+0.1	0.0/0.0	0.0/0.0			+0.2	0.0
C- <i>para</i>	+1.3	+0.9	+1.6					+0.4	-0.3

<sup>a</sup> Recorded at 100.6 MHz in CDCl<sub>3</sub> with two drops of [D<sub>6</sub>]acetone.<sup>b</sup> Empty entries indicate that the respective signals could not be identified safely; entries with “~”: signal could be identified but not the dispersion. Therefore, the  $\Delta\delta$ -values are not accurate ( $\pm$  ca 0.02); values marked by “\*” or “<sup>†</sup>” may be interchanged.<sup>c</sup> Separate signals for C-1 and C-3:  $\delta = 22.53$  and  $22.46$ .

**Table 15.** Selected  $^1\text{H}$  dispersion effects ( $\Delta\nu$ , in Hz) in the phenylselenenylalkane derivatives **32-36**; recorded at 400.1 MHz.<sup>a</sup>

No	32	33	34	35	36
H-1 (eq)	-	~ 5*			
H-1 (ax)	11.3	-			1.6
H-2 (eq)				~ 83	
H-2 (ax)				88±5	6-7
H-3					2.0
					>1
H-4 (eq)				~ 10*	
H-5 (eq)				~ 15*	3.4
H-6 (eq)				60±5	
CH <sub>3</sub>	11.7	3.0	27.9	~ 21	
<i>ortho</i> -H			<sup>b</sup>	<sup>c</sup>	<1
<i>meta</i> -H					
<i>para</i> -H					

<sup>a</sup> Asterisked values were estimated from HMQC spectra and/or signal widths.

<sup>b</sup> There are two doublets at  $\delta = 7.890$  and  $7.843$  (distance (18-19 Hz). Very probably, they belong to the different phenyl groups (axial and equatorial PhSe). However, it cannot be completely excluded that the two kinds of *ortho*-protons are isochronous and the existence of two signals is due to diastereomeric dispersion.

<sup>c</sup> There are two signals at  $\delta$  7.845 and 7.805/7.785 for the two kinds of *ortho*-protons (axial and equatorial PhSe). The latter shows a dispersion of ca 7 Hz whereas the first does not. The dispersed  $^1\text{H}$  signal correlates (HMQC) to a dispersed *ortho*- $^{13}\text{C}$  signal at  $\delta = 138.1/138.0$  ( $\Delta\nu = 8$  Hz; at 100.6 MHz); the other one correlates to a non-dispersed carbon peak at  $\delta = 137.2$ .

**Table 16.** Selected  $^{13}\text{C}$  dispersion effects ( $\Delta\nu$ , in Hz) in the phenylselenenylcyclohexane derivatives **32-36**; recorded at 100.6 MHz.<sup>a</sup>

No	32	33	34	35	36
C-1	<1	<1	<2	3	8
C-2	12	4	53	24	0
C-3	5	7	3	14	2
C-4	4	~2*	9	10	3
C-5	6	4	11	20	-
C-6	12	4	21	27	-
CH <sub>3</sub>	<2	3	0	6	-
<i>ipso-C</i>	3	~1			0
<i>ortho-C</i>	5	5	b	c	<1
<i>meta-C</i>	<1	1			0
<i>para-C</i>					

<sup>a</sup> Asterisked values were estimated from signal widths.

<sup>b</sup> Four peaks at  $\delta = 138.2, 138.0, 137.9$  and  $137.7$ ; for explanation see footnote b of Table 15.

<sup>c</sup> See footnote c of Table 15.

### 3 ADDUCT FORMATION - STOICHIOMETRY

Dirhodium and other dinuclear complexes have been studied intensively during the last few decades.<sup>61</sup> Important applications are the use of dinuclear complexes as homogeneous catalysts<sup>62</sup> and as auxiliaries in the chirality determination of compounds with various functional groups by circular dichroism.<sup>63</sup> Although much work has been done on the structure of such adducts in the solid state<sup>61,64</sup> knowledge about the structure and formation of adducts and eventual oligomers in solution is still scarce.<sup>61</sup> In a first approach, we have recently studied by <sup>1</sup>H and <sup>13</sup>C NMR as well as IR spectroscopy how chiral xanthine derivatives are ligated to the axial position of **Rh-Rh** and how this differs in solution and in the solid state.<sup>65</sup> During the course of our previous studies on various monovalent functionalities<sup>33-41</sup> we had encountered evidences which partly appeared to be contradictory with in terms of diverging adduct formation modes. Therefore, we regarded it necessary to perform a surveying study and gain a more comprehensive understanding of the various kinds of kinetically instable adducts which may exist in solution depending on the experimental conditions. The results of this study are described in this chapter.

#### 3.1 Stoichiometry of the adducts

Very recently, we found that selenium atoms are the first ligands in our project where the adducts are stable enough to see them separately in a low-temperature NMR experiment.<sup>41a</sup> These measurements allowed to identify two existing types of adducts: **L→Rh-Rh** and **L→Rh-Rh←L**, the 1:1- and 2:1-adducts, respectively (see Scheme 6). This promoted us to start a study to see what the experimental conditions for a maximum concentration of the respective adducts are. Thereby, we wanted to find out the best molar ratio of the constituents (the ligand **L** and **Rh-Rh**) for the detecting diastereomeric dispersions.





As stated above, it is possible to observe separately the adducts of selenides and **Rh-Rh** with varying stoichiometries by NMR spectroscopy at low temperatures. The experiments proved that the equilibria are shifted strongly towards the adducts (large binding constants); i.e., practically no free selenide will be observed as long as free rhodium sites are available. Moreover, the 2:1-adduct **36**→**Rh-Rh**←**36** is energetically favoured.

There is, however, another parameter to observe the existence of the adducts: the  $^1\text{H}$  signals of the Mosher acid methoxy groups display clearly different chemical shifts for the various adducts species (Figure 11).

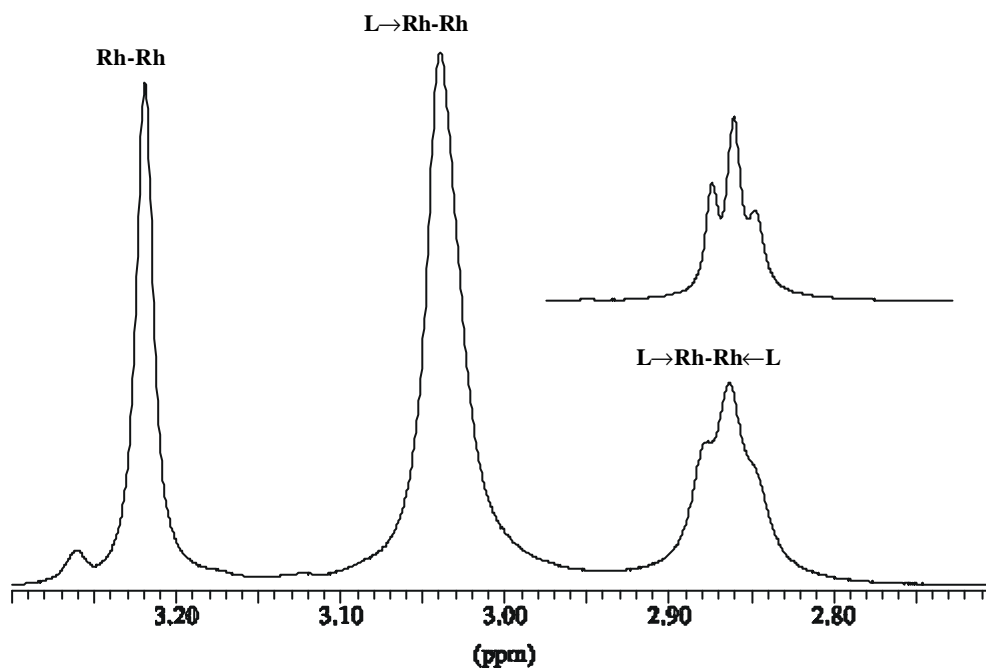


**Figure 11.**  $^1\text{H}$  NMR signals of the methoxy groups in the Mosher acid residues of the various adducts of with **36**, in  $\text{CDCl}_3$  at 215 K; molar ratio **36** : (**Rh-Rh**) = 1 : 1.3. The inserted signal corresponding to the **L**⊗**Rh-Rh**⊖**L** adduct, is resolution-enhanced.

### 3.1.1 NMR Titration Experiments

This allows to follow the changes of the relative concentration of the dirhodium species involved by increasing the amount of selenide (NMR titration). This is exemplified in Figure 12 for the chiral 2-phenylselenenylbutane (**36**).

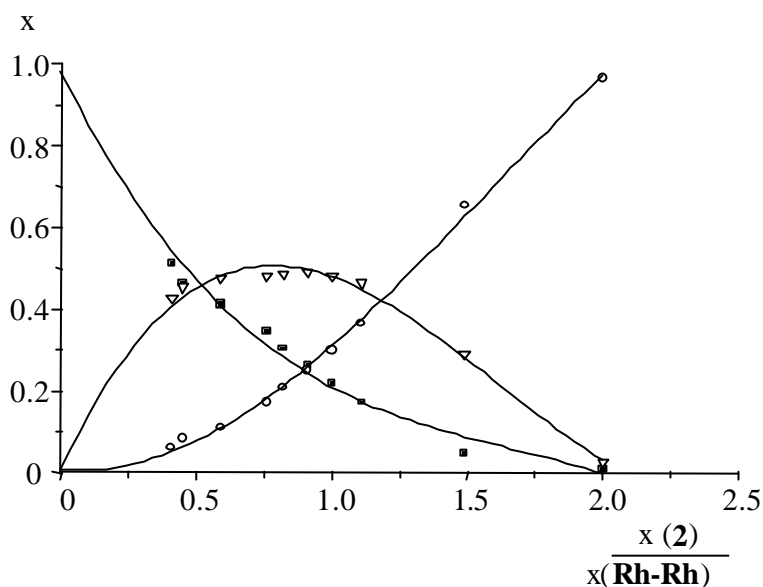


**Figure 12.** Molar fractions  $x$  of free **Rh-Rh** (■), its **L→Rh-Rh** (∇) and **L→Rh-Rh←L** (○) adducts depending on the molar ratios of **36**: (**Rh-Rh**), observed from  $^1\text{H}$  signals of the Mosher acid methoxy groups.

It can be seen that at low proportions of **36** (0.5 - 1 molar) the major components are **Rh-Rh** and **36→Rh-Rh**, the latter going up quickly to ca 50%. As the content of **36** increases, the concentration of the 2:1-adduct **36→Rh-Rh←36** increases as well, paralleled by a corresponding decrease for the free **Rh-Rh** complex which nearly disappears at ca 1.5 mole. Finally, at two moles all rhodium sites are occupied by ligands molecules of **36** (**36→Rh-Rh←36**).

As a conclusion, it is advisable to restrict the **36** : **Rh-Rh** ratio to ca 0.5 : 1 for avoiding unwanted high proportion of **36→Rh-Rh←36** adducts. However, dispersion effects are not very sensitive as to which type of adducts exists so that a higher amount of **36** may

even be advantageous; it affords a higher overall-concentration of **36** and hence a shorter experimental recording times.

It is interesting to note that the methoxy  $^1\text{H}$  signal of the Mosher acid residues in the **36**→**Rh-Rh**←**36** adduct (Figure 11;  $\delta \approx 2.86$ ) consists of three signals because there are four different diastereoisomers adducts **I-IV**:

**I**: (*R*)-**36**→**Rh-Rh**<sup>(*R*)</sup>←(*R*)-**36**, **II**: (*S*)-**36**→**Rh-Rh**<sup>(*R*)</sup>←(*S*)-**36**, and

**III**: (*R*)-**36**→**Rh-Rh**<sup>(*R*)</sup>←(*S*)-**36** **IV**: (*S*)-**36**→**Rh-Rh**<sup>(*R*)</sup>←(*R*)-**36**.

Note that **III** and **IV** are not identical because the two rhodium atoms in **Rh-Rh** are diastereotopic. The same is valid for **36**→**Rh-Rh** as compared to **Rh-Rh**←**36**; they are diastereomers. However, the chemical shift difference associated to this kind of diastereomerism seems to be so low that it could not be observed before in any experiment using **Rh-Rh** as a chiral auxiliary. In Figure 11 the methoxy  $^1\text{H}$  line width of the 1:1-adduct ( $\delta = 3.04$ ) is about 10 Hz whereas that of the free **Rh-Rh** ( $\delta = 3.22$ ) is only 5 Hz. Although coalescence effects cannot be excluded, this may be an indication that the former signal consists of two overlapping singlets.

Thus, the methoxy signal of the Mosher acid residues in **Rh-Rh** is able to reflect the chirality of both ligand molecules in the **36**→**Rh-Rh**←**36** adduct since they are flanked by these ligand molecules. In contrast, the atoms of a given ligand cannot identify the chirality of the second ligand molecule on the opposite side of the **Rh-Rh** moiety (in terms of chemical shift sensitivity). We assign the most intensive central peak to the adducts **III** and **IV** with ligands of both enantiomeric forms of **36** inside the adduct because it cannot be expected that their chemical shift difference is large enough to be detected (see above). The assignment of the two flanking signals to the diastereomeric 2:1-adducts **I** and **II** can be performed only by using a non-racemic mixture of **36** which was not available.

Analogous results were obtained for the achiral selenide **37** (see next page).

Molar fractions of different adducts for various ratios of compound **36** and **Rh-Rh** in  $\text{CDCl}_3$  solution at 215 K.

$X(2)/X(\text{Rh-Rh})$	Molar fraction of <b>Rh-Rh</b>	Molar fraction of <b>L<sup>®</sup> Rh-Rh</b>	Molar fraction of <b>L<sup>®</sup> Rh-Rh- L</b>
2	0.008	0.026	0.966
1.49	0.047	0.29	0.653
1.11	0.172	0.463	0.365
1	0.219	0.481	0.3
0.91	0.262	0.489	0.249
0.82	0.304	0.487	0.209
0.76	0.345	0.482	0.172
0.59	0.412	0.477	0.111
0.45	0.462	0.454	0.084
0.41	0.513	0.425	0.062

Molar fractions of different adducts for various ratios of compound **37** and **Rh-Rh** in  $\text{CDCl}_3$  solution at 215K.

$X(2)/X(\text{Rh-Rh})$	Molar fraction of <b>Rh-Rh</b>	Molar fraction of <b>L<sup>®</sup> Rh-Rh</b>	Molar fraction of <b>L<sup>®</sup> Rh-Rh- L</b>
1.29	0.0152	0.026	0.959
0.97	0.17	0.465	0.365
0.91	0.182	0.51	0.31
0.85	0.226	0.517	0.257
0.79	0.267	0.512	0.221
0.73	0.304	0.505	0.191
0.67	0.347	0.509	0.145
0.39	0.515	0.418	0.067
0.32	0.585	0.357	0.058
0.25	0.63	0.328	0.042

### 3.1.2 Job's Method

In the method of continuous variation,<sup>66,67</sup> one mixes equal concentration solutions of two species, A and B, in varying ratios and measures a property characteristic of the complex formed. Because the total concentration,  $[A] + [B]$ , is constant in all solution, the concentration of an AB complex will reach a maximum value when  $[A] = [B]$  and the concentration of an  $A_2B$  complex will reach a maximum values when  $[A] = 2[B]$ , etc. A plot of concentration of complex as a function of the mole fraction of A in solution is constructed; the maximum amount of complex is found at the point corresponding to the mole-fraction of A in the complex. With rapidly exchanging free ligand and complex studied by NMR spectroscopy, we are interested in the number of ligands bound by the host in the complex. Self-association of the hosts is not important, so the ligand species present are the ligand (L) and the complex (C).

The following derivation applies where  $C_i$  is the concentration of species  $i$ ,  $C_{H(0)}$  is the initial concentration of host,  $\delta_i$  is the chemical shift of species  $i$ , and  $\delta_{\text{obs}}$  is the observed chemical shift.

$$\begin{aligned}
 C_L &= C_{L(0)} - C_C \\
 \delta_{\text{obs}} &= (\delta_L C_L + \delta_C C_C) / C_{L(0)} \\
 \delta_{\text{obs}} &= (\delta_L C_{L(0)} - \delta_L C_C + \delta_C C_C) / C_{L(0)} \\
 \delta_{\text{obs}} &= C_C (\delta_C - \delta_L) / C_{L(0)} + \delta_L C_{L(0)} / C_{L(0)} \\
 \delta_{\text{obs}} - \delta_L &= C_C (\delta_C - \delta_L) / C_{L(0)} \\
 C_C &= (\delta_{\text{obs}} - \delta_L) C_{L(0)} / (\delta_C - \delta_L)
 \end{aligned}$$

Because  $(\delta_C - \delta_L)$  is a constant, the concentration of the complex is proportional to  $\Delta\delta$  (the observed chemical shift minus the chemical shift of the free ligand) multiplied by the initial concentration of ligand. An appropriate Job plots for our situation would be  $\Delta\delta$  times the initial concentration of ligand as a function of the mole fraction of ligand ( $X_L$ ). However, because of the constraint of the method of continuous variation that the sum of the ligand and complex concentrations are equal in all measurements,  $C_{L(0)}$  in the

final expression above can be replaced by the  $X_L$  in the ligand-complex mixture. Thus we used plots of  $\Delta\delta X_L$  as a function of the  $X_L$ .

The favoured stoichiometry of an adduct can then be determined by identifying the mole fractions of the adduct components at the curve maximum. Sharp breaks in the curve indicate high formation constants whereas flat maxima point to loose binding. Figure 13 shows a representative Job-plot for one of the two diastereotopic H-3 atoms in the racemic mixture of **36** ( $\delta = 1.73$ ); analogous curves are observed for the two methyl proton signals. As expected, it turns out that the curve is quite sharp and the maximum exists at a mole fraction of ca 0.65 for **36**, a value which is close to that expected for a molar ratio of **36** : **Rh-Rh** = 2 : 1. This is in complete agreement with the statements above concerning the binding constants and the existence of **36**→**Rh-Rh** and **36**→**Rh-Rh**←**36** adducts (Figure 12) and confirms the reliability of the Job plot method in the present molecular systems. For the further confirmation of Job-plot we drew more graphs, e.g., Figures 14 and 15 represent the H-1 and H-2 protons in compound **36**.

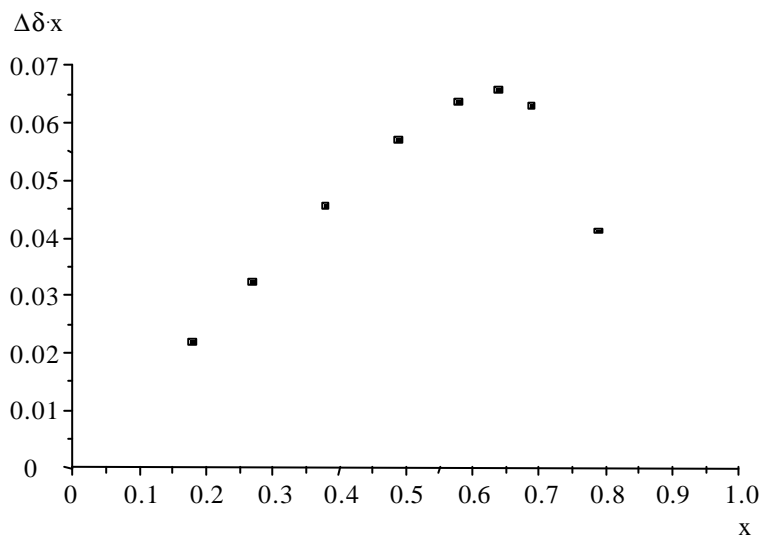


**Figure 13.** Job plot for H-3 in the adducts of **36**; for explanation see text.

Ratio L:Rh-Rh	L		Rh-Rh	
	vol (ml)	mass (mg)	vol.(ml)	mass (mg)
8:2	0.56	3.99	0.14	5.32
7:3	0.49	3.49	0.21	7.98
6.5:3.5	0.455	3.24	0.245	9.31
6:4	0.42	2.99	0.28	10.64
5.5:4.5	0.385	2.74	0.315	11.97
5:5	0.35	2.49	0.35	13.3
4:6	0.28	1.99	0.42	15.96
3:7	0.21	1.49	0.49	18.62
2:8	0.14	1.00	0.56	21.28

Real mole fraction of **36** ( $X_L$ ), chemical shifts  $\delta$  (in ppm) signal shifts  $\Delta\delta$  (in ppm) and  $\Delta\delta \times X_L$  for H-3 proton.

$X_L$ <sup>a)</sup>	d	Dd	Dd $\times X_L$
0.79	1.6627	0.0520	0.0411
0.69	1.7016	0.0909	0.0627
0.64	1.7132	0.1025	0.0656
0.58	1.7204	0.1097	0.0636
0.55	b)		
0.49	1.7270	0.1163	0.0570
0.38	1.7302	0.1195	0.0454
0.27	1.7308	0.1201	0.0324
0.18	1.7314	0.1207	0.0217

a) Real molar fractions of the host were calculated on the basis of the integral values of the methoxy signal of the Mosher's acid and signal of the host from  $^1\text{H}$  NMR spectra.

b) Overlapped.

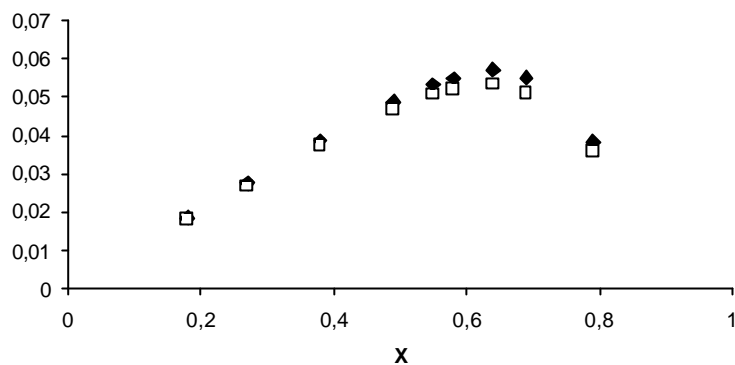


**Figure 14.** Job's plot for methyl group protons of **36** (H-1).

Real mole fraction of **36** ( $X_L$ ), chemical shifts  $\delta$  (in ppm) signal shifts  $\Delta\delta$  (in ppm) and  $\Delta\delta \times X_L$  for H-1 protons (methyl group).

$X_L^a$	d	Dd	Dd $\times$ $X_L$
0.79	1.4484	0.0486	0.0384
	1.4451	0.0453	0.0358
0.69	1.4796	0.0798	0.0551
	1.4737	0.0739	0.0510
0.64	1.4894	0.0896	0.0573
	1.4832	0.0834	0.0534
0.58	1.4945	0.0947	0.0549
	1.4894	0.0896	0.0520
0.55	1.4967	0.0969	0.0533
	1.4922	0.0924	0.0508
0.49	1.4994	0.0996	0.0488
	1.4956	0.0958	0.0469
0.38	1.5014	0.1016	0.0386
	1.4981	0.0983	0.0374
0.27	1.5017	0.1019	0.0275
	1.4988	0.0990	0.0267
0.18	1.5019	0.1021	0.0184
	1.4992	0.0994	0.0179

a) Real molar fractions of the host were calculated on the basis of the integral values of the methoxy signal of the Mosher's acid and signal of the host from  $^1\text{H}$  NMR spectra.



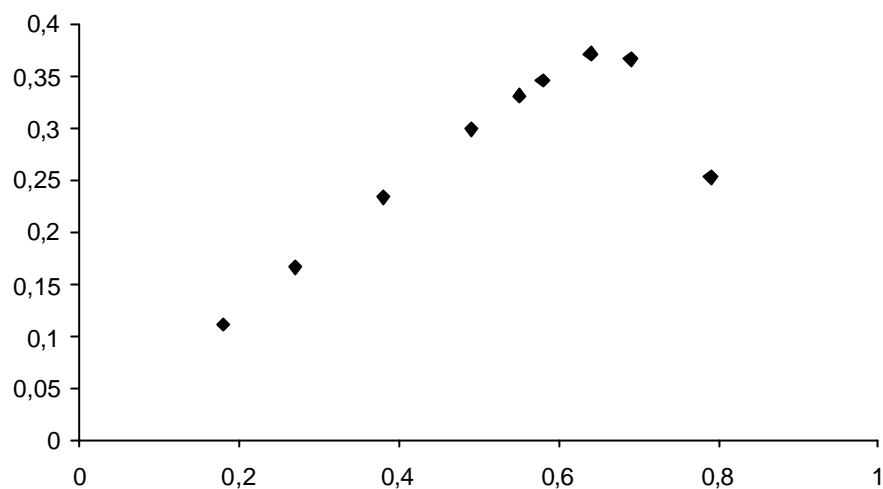


**Figure 15.** Job's plot for proton H-2 of **36**.

Real mole fraction of **36** ( $X_L$ ), chemical shifts  $\delta$  (in ppm) signal shifts  $\Delta\delta$  (in ppm) and  $\Delta\delta \times X_L$  for H-2 proton.

$X_L$ <sup>a)</sup>	d	Dd	Dd $\times$ $X_L$
0.79	3.5632	0.3192	0.2522
0.69	3.7740	0.5300	0.3657
0.64	3.8238	0.5798	0.3711
0.58	3.8398	0.5958	0.3456
0.55	3.8454	0.6014	0.3308
0.49	3.8528	0.6088	0.2983
0.38	3.8579	0.6139	0.2333
0.27	3.8591	0.6151	0.1661
0.18	3.8594	0.6154	0.1108

a) Real molar fractions of the host were calculated on the basis of the integral values of the methoxy signal of the Mosher's acid and signal of the host from  $^1\text{H}$  NMR spectra.

The following conclusions can be drawn from experiments described in this work:

- a) NMR titration experiments can be monitored only with strongly ligating functional groups, i.e. if the life-time of an adduct molecule is large on the NMR time-scale. This is the case for selenoethers at 215 K in chloroform.<sup>68</sup> **Se**→**Rh-Rh** (1:1-adducts) are formed first but **Se**→**Rh-Rh**←**Se** (2:1-adducts) appear already at low molar concentrations of **Se**. If two moles of **Se** are added, only **Se**→**Rh-Rh**←**Se** exists. Job plots confirm this result; the curve maximum appears at a **Se** molar fraction of ca 0.65, i.e. 2 : 1. Thus, Job plots give reliable results in this adduct system.
  
- b) The Mosher acid residues in **Rh-Rh** are able to differentiate the chirality of both ligands in **Se**→**Rh-Rh**←**Se** *via* their methoxy <sup>1</sup>H signals but, in contrast, a ligand cannot recognize the configuration of the second ligand molecule because they are isolated on opposite sides of the dirhodium complex.
  
- c) Therefore, for chiral recognition experiments it is not necessary to restrict the molar ratio of **Se** : **Rh-Rh** to low values (ca 0.5) in order to keep the concentration of 2:1-adducts (**Se**→**Rh-Rh**←**Se**) low. Rather, it is advisable to choose ratios of 1 - 1.5 where the concentration of the ligand is higher giving greater sensitivity in the NMR experiment (Scheme 8).

### 3.2 Adduct Formation and Thermodynamics Investigated by Variable-Temperature NMR Spectroscopy

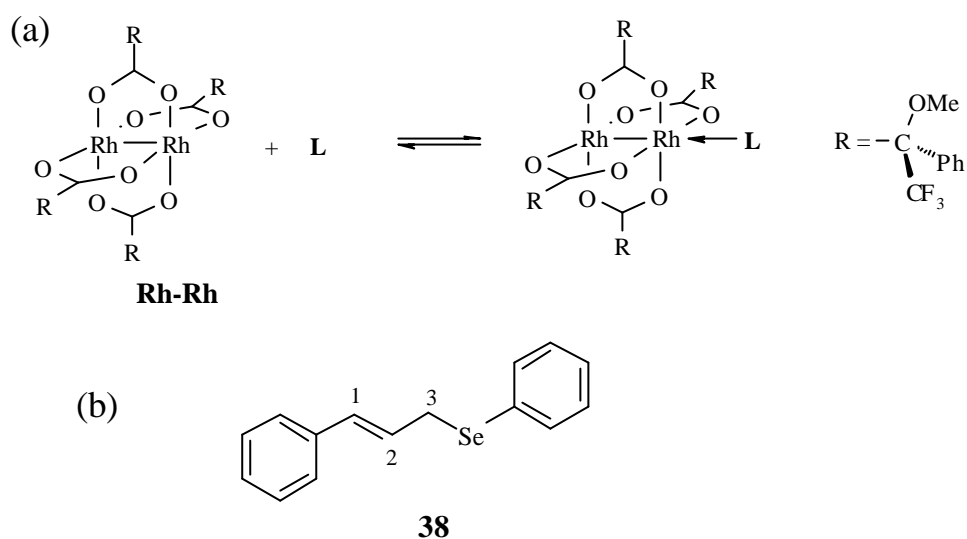
Variable temperature NMR spectroscopy, also known by the term dynamic NMR (DNMR), deals with the effects in a broad sense of chemical exchange processes on NMR spectra. If a chemical system consists of interchanging species, the exchange rates can be manipulated by varying the sample temperature. Thereby the appearance of the NMR signals can be influenced,

Generally, signals are severally broadened in the range of coalescence temperature ( $T_c$ ). At lower temperature, the species can be monitored separately. At higher temperatures well-resolved signals appear which, however, represent averages. From a series of spectra with varying the temperature around  $T_c$ , kinetic and thermodynamic parameter (rate constant, energy barrier) can be extracted.<sup>69</sup>

Conformational analysis of selenium-containing compounds by variable- temperature NMR spectroscopy (DNMR) is facilitated by the great sensitivity of  $^{77}\text{Se}$  chemical shifts. Generally, the chemical shift differences of selenium atoms in different conformers (at low temperatures) are much larger than those of carbon or hydrogen atoms. Therefore, the coalescence temperature in  $^{77}\text{Se}$  NMR spectra is usually higher than in the  $^1\text{H}$  or  $^{13}\text{C}$  NMR spectra of the same compounds. However, it should be noted that the temperature range between the high- and the low-temperature regime, i.e., in which line broadening occurs, is large than that observed in  $^1\text{H}$  and  $^{13}\text{C}$  NMR spectra. So, the temperature rise is smaller in the low-temperature limit than for the observation of coalescence. This diminishes the advantages of  $^{77}\text{Se}$  DNMR to some extent. On the other hand, a large temperature range for changes in the appearance of the signals allows a higher precision in the computer simulation for evaluating the thermodynamic and kinetic data of the conformational process.

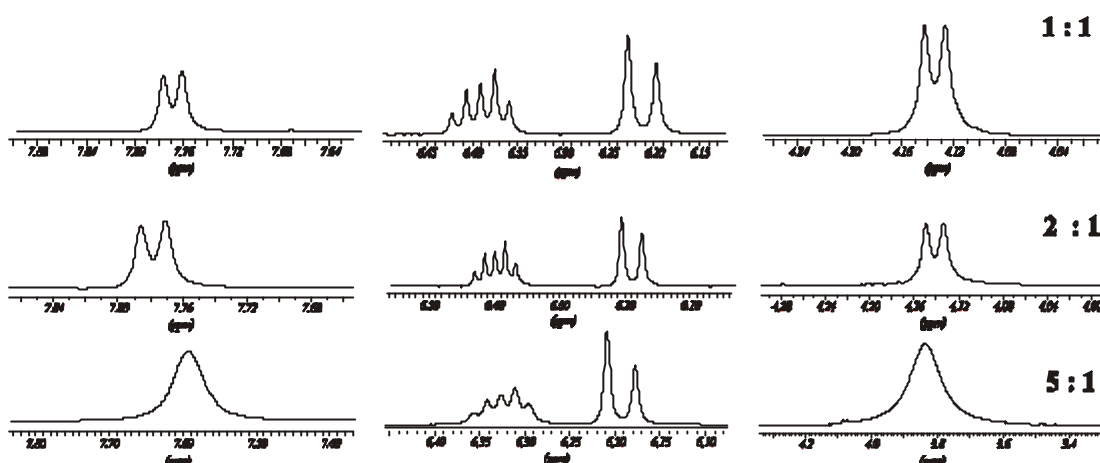
### 3.2.1 A Primary Selenide

Variable-temperature  $^1\text{H}$  and  $^{77}\text{Se}$  NMR data of the primary 3-phenylselenenyl-1-phenyl-1-propene (**38**) in the presence of  $\text{Rh}_2(\text{MTPA})_4$  (**Rh-Rh**) prove that the equilibria are strongly shifted towards the adduct **Rh-Rh**  $\leftarrow$  **38**; free selenide molecules cannot be detected as long as uncomplexed rhodium atoms are available (Scheme 8).



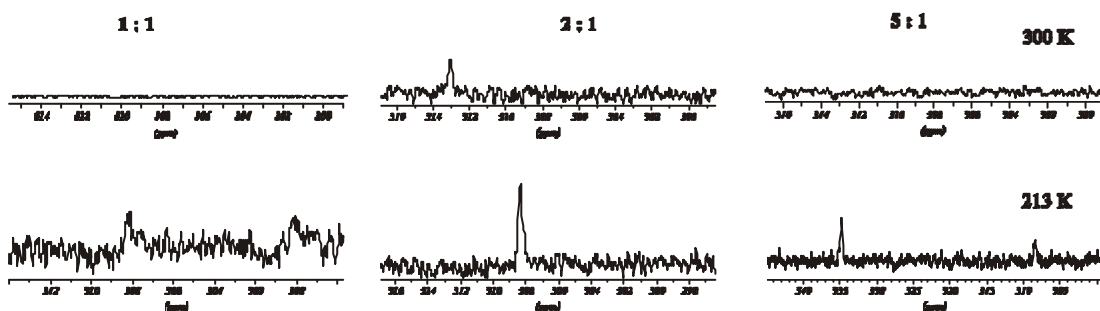
**Scheme 8.** (a) Structure of **Rh-Rh** and the equilibrium of **Rh-Rh** and **L** (**38**); (b) Structure of 3-phenylselenenyl-1-phenyl-1-propene (**38**).

Figure 16 shows sections of the room-temperature  $^1\text{H}$  NMR spectra of **38** in the presence of **Rh-Rh** at various ratios. For ratio 5:1 it can be seen that all  $^1\text{H}$  signals are broadened due to coalescence effects arising from the exchange of free and ligated selenide molecules; at lower temperatures these signals display the full coalescence evolution (Figure 18). In contrast, for the cases of 1:1 and 2:1 ratios the  $^1\text{H}$  signals exhibit only moderate line broadening even at low temperatures.



**Figure 16.** 500.1 MHz  $^1\text{H}$  NMR spectral sections at various ratios **38** to **Rh-Rh**, as indicated; left: *ortho*-H of Se-Ph, middle: H-2 and H-1, right: H-3; all recorded at room temperature.

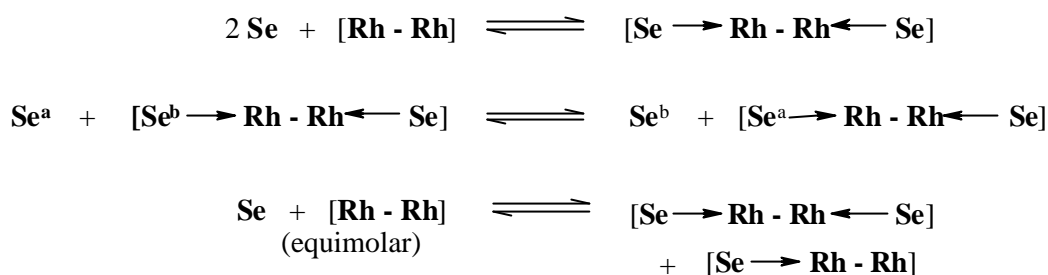
For a closer insight we recorded  $^{77}\text{Se}$  NMR spectra at lower temperatures. Figure 17 shows the results for 300 K and 213 K. It can be seen that only one sharp  $^{77}\text{Se}$  signal exists for all temperatures if the ratio is 2:1.\* This indicates the preference of the corresponding 2:1-adducts, schematically designated as  $[\text{Se} \rightarrow \text{Rh-Rh} \leftarrow \text{Se}]$ , where each rhodium atom carries one selenium, and proves that practically no free selenide **38** exists; i.e. the equilibrium Eq-1 in Scheme 9 is completely on the right-hand side.



**Figure 17.** 95.4 MHz  $^{77}\text{Se}$  signals with various ratios of **38** to **Rh-Rh**, as indicated; top: at 300 K, bottom: at 213 K; in  $\text{CDCl}_3$ .

\* The chemical shift difference is due to the temperature dependence of  $\delta(^{77}\text{Se})$ .

The situation is different for the ratio 5:1. Here, we find extensive line broadening due to coalescence, and at 213 K two signals at  $\delta = 335$  and 308 are observed with an intensity ratio of ca 3:2. Clearly, the high-frequency signal belongs to the free ( $\delta = 342$  at room temperature) and the low-frequency signal to the complexed selenide molecule. The dynamics have to be interpreted as an intermolecular exchange process (Eq-2 in Scheme 9).



**Scheme 9.** Equilibria of **38** and **Rh-Rh** at various ratios; “Se“ stands for **38**.

Finally, the 1:1 mixture shows coalescence effects of the  $^{77}\text{Se}$  signals as well; no signal can be observed at 300 K. At 213 K, however, two broad  $^{77}\text{Se}$  signals at  $\delta = 308$  and 300 emerge. Whereas the first ( $\delta = 308$ ) can be attributed to the  $[\text{Se} \textcircled{\text{R}} \text{Rh-Rh} \leftarrow \text{Se}]$ -adduct (2:1), the second ( $\delta = 300$ ) arises from a 1:1-adduct  $[\text{Se} \textcircled{\text{R}} \text{Rh-Rh}]$  (Eq-3 in Scheme 9). The  $^{77}\text{Se}$  signal intensity ratio is ca 1:1 (only rough estimation due to low signal-to-noise ratio). On the basis of the above signal assignment and the different number of selenium atoms in each adduct we are led to a molar ratio of ca 1:2 for the two adducts. This indicates a significant but low energy difference so that the equilibria can be shifted easily towards complex  $[\text{Se} \textcircled{\text{R}} \text{Rh-Rh} \leftarrow \text{Se}]$  by adding further selenide.

The intermolecular exchange process for the 5:1 ratio (Eq-2 in Scheme 9) is nicely revealed by the  $^1\text{H}$  NMR spectra at various temperatures (Figure 18). At low temperatures, all four  $^1\text{H}$  signals displayed are splitted into two with an intensity ratio of 2:3 (for the complexed and the free selenide, respectively), and coalescence temperatures can be estimated.<sup>69</sup> A preliminary estimation of the energy barrier,  $\Delta G_c^\ddagger$ , for each spin system at its coalescence temperature leads to a surprisingly high value of 54-55 kJ/Mol for this equilibrium.

The fact that no "free" rhodium sites exist if more than two selenides per **Rh-Rh** are present, and also shows that acetone- $d_6$  used to increase the solubility of the complexes plays no significant role as a ligand.

As a conclusion, we were able to freeze equilibria and to estimate the thermodynamics of the complexation when the ligand is a selenide. The results are:

If an excess of uncomplexed rhodium atoms is available, no free selenide molecules will remain in the equilibria.

If less than two selenide molecules per **Rh-Rh** molecule exist, a dynamic mixture of 2:1- and 1:1- adducts with comparable thermodynamic stabilities will be formed.

With an excess of selenide molecules, only 2:1- adducts plus remaining free selenide molecules can be observed. Here, an intermolecular selenide exchange exists for which a barrier of 54-55 kJ/Mol can be estimated (in a molar ratio of **1 : Rh-Rh = 5:1**).

Acetone- $d_6$  used for enhancing the solubility of **Rh-Rh** does not significantly compete with **38** as a ligand in the equilibria and hence, has no harmful effect to the experiment

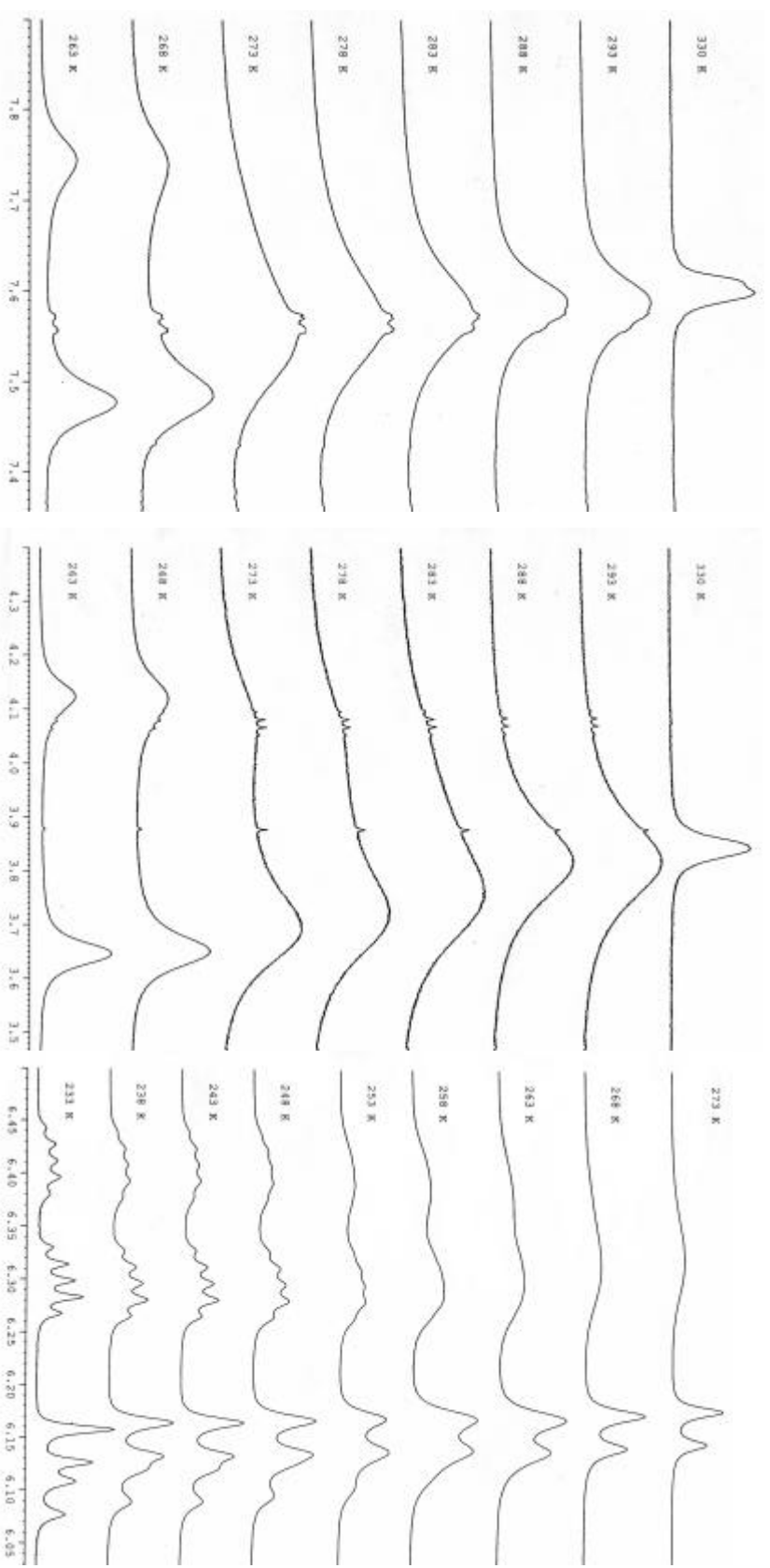


**Figure 18.** <sup>1</sup>H NMR sections at variable temperature, **38** : Rh-Rh = 5:1; left: *ortho*-H of Se-Ph, middle: H-3, right: H-2 and H-1; in CDCl<sub>3</sub>, 500.1 MHz.



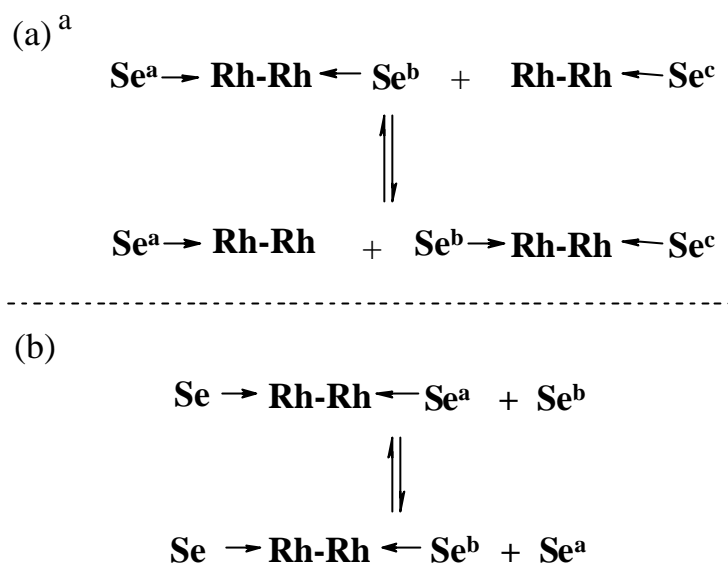
### 3.2.2 Secondary Selenides

It has been shown<sup>41a</sup> that equilibria consisting of complexes **Rh-Rh** and primary seleno-ether 3-phenylselenenyl-1-phenyl-1-propene as a ligand molecule (**Se**) are strongly shifted towards the adducts (large formation constants) i.e., no selenium ligand remains free if sufficient rhodium sites are available. If **Rh-Rh** is in excess, there is a mixture of inter-converting 1:1- and 2:1-adducts (**Se**Ⓢ**Rh-Rh** and **Se**Ⓢ**Rh-Rh**→**Se**, respectively). At room temperature and in the presence of an excess of **Se** only 2:1-adducts (**Se**Ⓢ**Rh-Rh**→**Se**) exist forming an equilibrium with excessive free ligand selenides (Scheme 10a). The exchange barrier has been estimated to 54-55 kJ mol<sup>-1</sup>.<sup>41a</sup>

#### 3.2.2.1 "Switch" Equilibria

At 1:1-molar ratios, fast exchange "switch" equilibria exist between 1:1- and 2:1-adducts (**Se**Ⓢ**Rh-Rh** and **Se**Ⓢ**Rh-Rh**→**Se**, respectively) involving free **Rh-Rh** complex molecules which may be called "0:1-adducts" (cf. Scheme 10b). This was studied only by <sup>77</sup>Se NMR spectroscopy<sup>41a</sup>.

In order to inspect the adduct formation processes in more detail we recorded a series of variable-temperature NMR spectroscopy of the 4-*tert.*-butylcyclohexane derivatives **30** and **31**. These two compounds have been chosen because they offer particular advantages: (a) they are achiral so that no confusion by diastereomerism is possible, (b) the cyclohexane rings are conformationally stable due to *tert.*-butyl substitution; (c) they differ only in the relative position of the phenylselenenyl residue with respect to the cyclohexane ring.



**Scheme 10.** "Switch" (a) and "replacement" equilibria (b) of a selenoether ligand **Se** and a complex **Rh-Rh** in (a) an excess of **Rh-Rh** or (b) an excess of **Se**.

<sup>a</sup> Switches between 1:1- and "0:1-adducts" as well as 2:1-adducts and "0:1-adducts" have also to be considered but were not displayed here.

The discussion of the spectroscopic results starts with *cis*-1-phenylselenenyl-4-*tert*-butylcyclohexane (**30**) having the selenium atom in a fixed axial position. The easiest way to detect the composition of the adducts of **30** (symbol: **Se**) and **Rh-Rh** is the observation of the methoxy protons and carbons – as well as the carboxyl carbons – of **Rh-Rh** itself in an experiment with a 1:1-molar ratio of the two components **30** and **Rh-Rh**. At room temperature the <sup>1</sup>H signal of the methoxy group is a somewhat broadened singlet at  $\delta = 3.04$  because there is a fast exchange between all adduct species at this temperature (Figure 19).

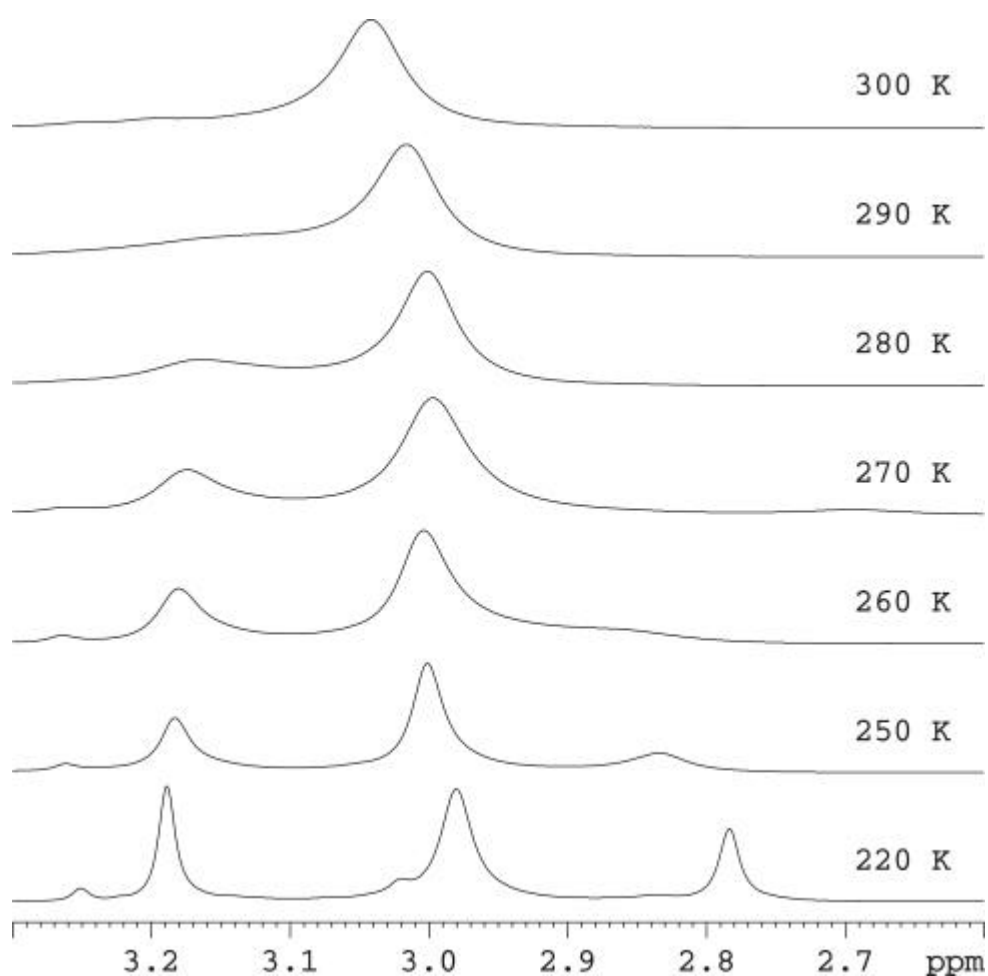


**Figure 19.** Methoxy proton signals of **RhRh** in the presence of **30** at variable temperatures; **30 : Rh-Rh = 1:1**.

If, however, the exchange rate is decreased by lowering the sample temperature to 220 K, typical coalescence phenomena appear which can be seen in Figure 19. At a 1:1-molar ratio of **30** and **Rh-Rh**, two rhodium sites per selenium atom available exist statistically. Consequently, three signals can be observed at  $\delta = 3.19$ , 2.98 and 2.78 which are attributed to the free **Rh-Rh** complex ("0:1-adduct"), the 1:1-adduct and the 2:1-adduct, respectively. Analogously, three carbon signals for carboxyl and the methoxy carbon of the MTPA residues appear in an  $^{13}\text{C}$  NMR experiment using the same solution are presented in Figure 20.

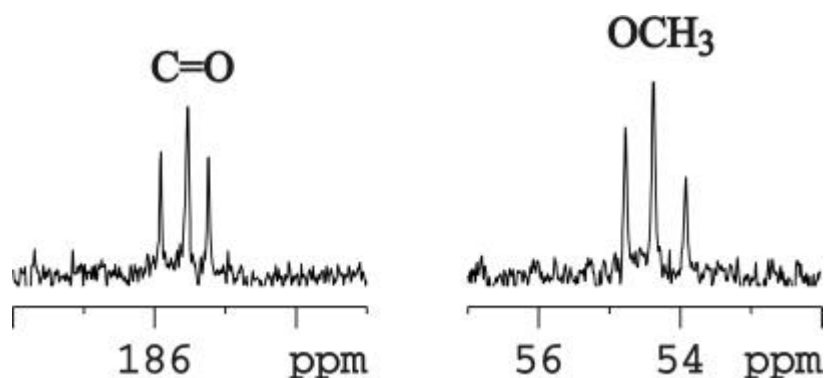


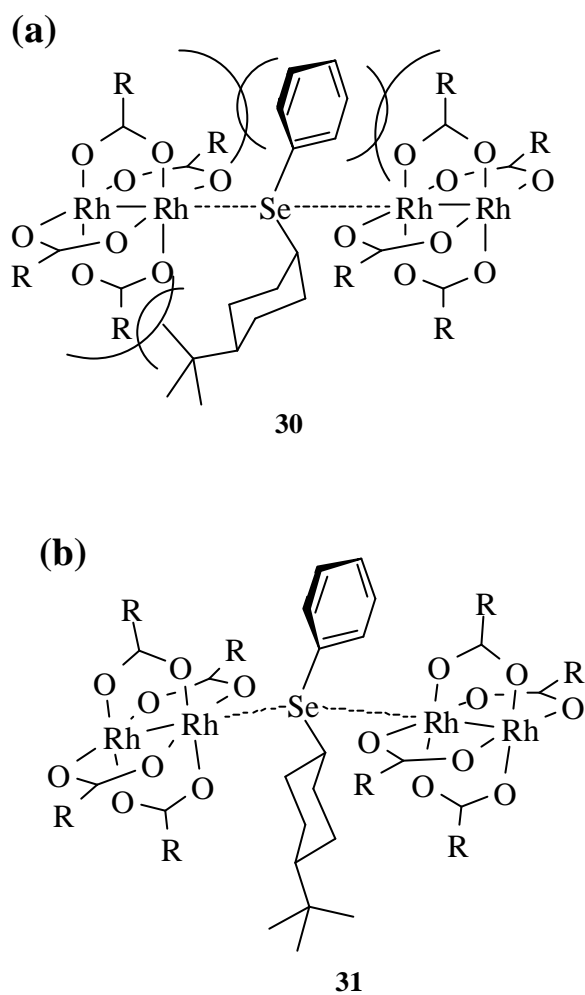
**Figure 20.** Carboxyl (left) and methoxy carbon signals (right) of the MTPA residues in **Rh-Rh; 30** : **Rh-Rh** = 1:1; at 213 K.

The underlying mechanism of intermolecular reaction is a "switch"-exchange under these conditions (1:1 molar ratio), i.e., a selenium ligand leaves its rhodium site if a close-by free rhodium atom is available. (Note that practically no free **Se** ligand can exist in 1:1 molar ratios). However, the spectra recorded allow a more detailed look at the situation close to the transition state of this **Se** switch.

As expected, the *ortho*-proton signal of **30** (at 300 K a doublet due to scalar coupling with *meta*-protons) divides into two doublets on temperature decreases because of the slower exchange between the 1:1- and the 2:1-adducts (Figure 21). Although the 1:1-adduct prevails over the 2 : 1 adduct (ca 5:3, as taken by integration of the signals in Figure 19, at 220 K), the intensities of the two doublets are nearly equal (Figure 21) because the 2:1-adduct contains four *ortho*-protons (2 **Se**) whereas that of the 1:1-adduct has only two (1 **Se**). An estimation of this "switch" barrier by inspecting the signal distance at ca 235 K and a coalescence temperature of ca 250 K the provides 52-53 kJ mol<sup>-1</sup>, a value which is not far away from the barrier observed for the primary selenide.

At temperatures lower than 240 K, however, the two proton signals begin to undergo a second exchange process. Although it is not possible to reach the corresponding low-temperature range (the solution solidifies at temperatures lower than 213 K), it is evident from the significant widening of the whole signal group that this process involves both doublets and that each of them splits into more. A reasonable explanation is to assume that during the approach of the two adducts – i.e., during passing the transition state – the

phenyl group in **30** is jammed in by the voluminous Mosher acid residues (R) of the two **Rh-Rh** complexes and thereby hindered in its internal rotation (Scheme 11a).



**Scheme 11.** Schematic view of the transition state in the switch mechanism; (a) with **30** and (b) with **31**.

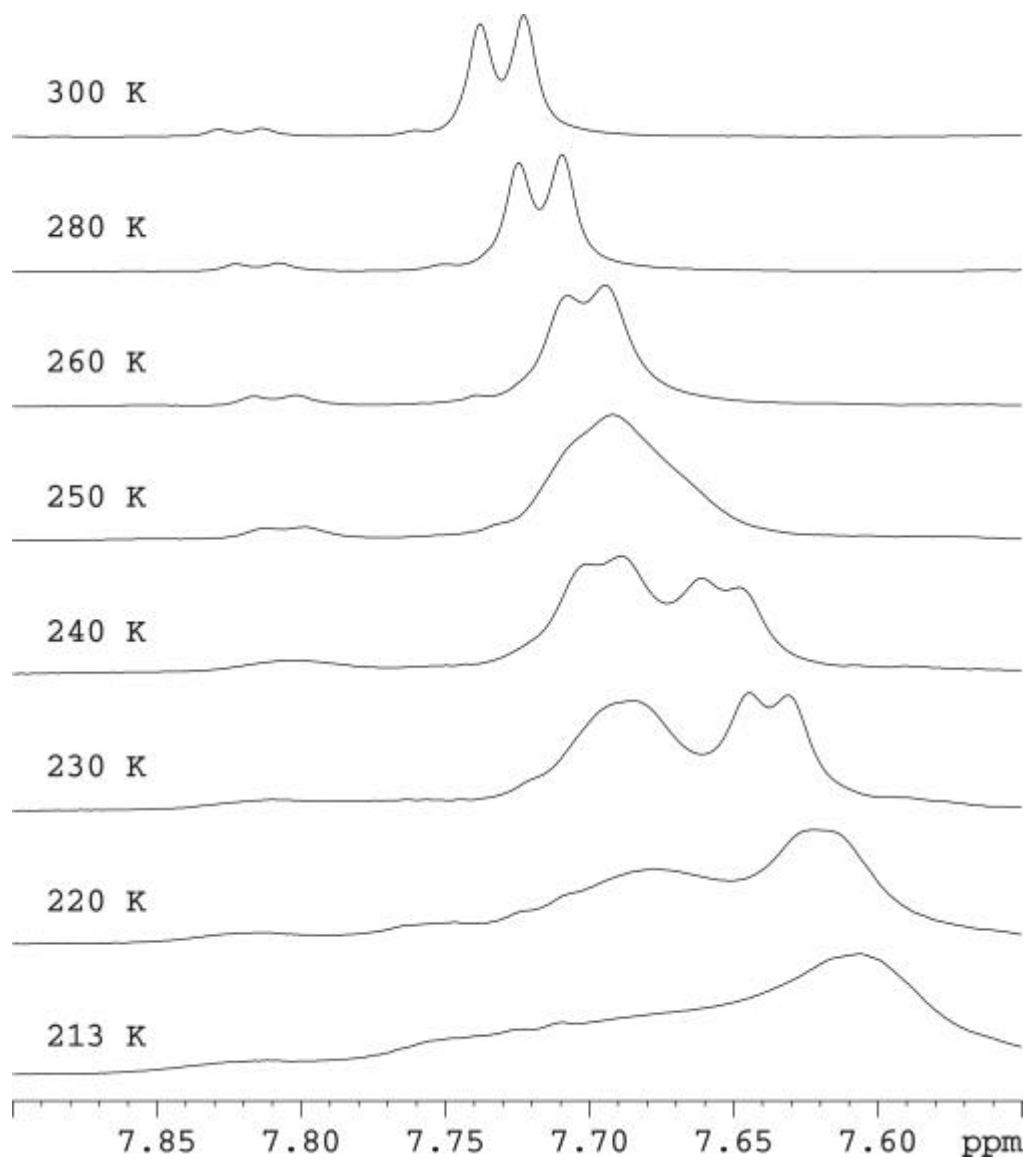


**Figure 21.** *Ortho*-proton signals of **30** at variable temperature; equimolar amount of **Rh-Rh** (**30** : **Rh-Rh** = 1:1).

This interpretation is supported by the fact that this second coalescence has not been discovered for 3-phenylselenenyl-1-phenyl-1-propene (**38**)<sup>41</sup> or for 2-phenylselenenyl-butane (**36**),<sup>69</sup> molecules with the much smaller steric demand of their alkyl residue. Moreover, this interpretation is confirmed by the behaviour of analogous signals in the adduct with the *trans*-isomer **31**. Whereas the methoxy <sup>1</sup>H signals undergo the same separation on lowering the temperature as shown for **30** in Figure 19, a second coalescence process for the *ortho*-protons cannot be identified. Apparently, the approach of the partners during the “switch” process is easier and steric compression on the phenyl group lower (Scheme 11b).

The most striking difference between **30** and **31** is observed for the *tert.*-butyl singlets: that of **30** splits into two indicating the two adducts with a ratio similar as that shown by the methoxy protons (Figure 22a). There is, however, no noticeable *tert.*-butyl signal splitting in **31** (Figure 22b). Apparently, the *tert.*-butyl group is not able to reflect the difference between 1:1- and 2:1-adducts because there is no severe steric compression, such as for **30** (Scheme 11b).

#### 3.2.2.2 “Replacement” Equilibria

In accordance with our previous discussion<sup>41a</sup> the low-temperature NMR experiment with an excess of **Se** (**30** : **Rh-Rh** = 4:1) revealed only the peaks of the 2:1-adduct beside those of the excessive free **30** indicating that all rhodium sites in the **Rh-Rh** complex molecules are involved in **Se**-adduct formation. This is in accordance with the “replacement” mechanism as shown in Scheme 10b.

Again, typical coalescence phenomena were observed for the *ortho*- and the *tert.*-butyl-protons. In each case, however, the signals of the 2:1-adduct undergo a second coalescence, similar to that discussed above for the 1:1-molar ratio. We are led to the conclusion that this is a consequence of steric compression due the transition state of the replacement of a ligated molecule **30** by a free one, analogous to that depicted in Scheme 11 for the “switch” transition.

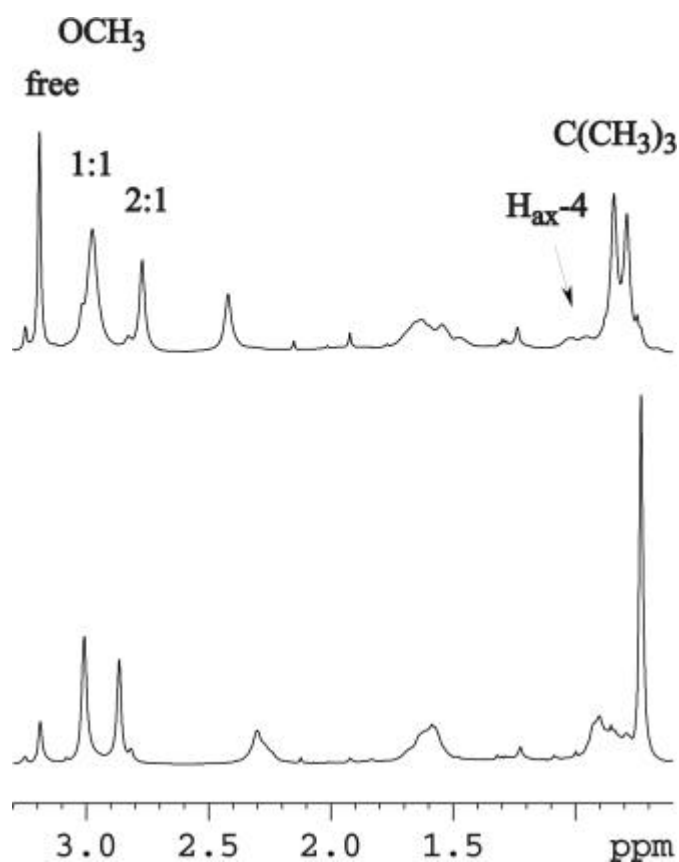


**Figure 22.** <sup>1</sup>H signals of the *tert.*-butyl groups in **30** (top) and **31** (bottom) at 213 K; equimolar with respect to **Rh-Rh**.

Indeed, the coalescence behaviour for *ortho*-proton is much more simple for **31** (**31** : **Rh-Rh** = 2.5 : 1, Figure 23) than for **30**; no second coalescence appears at low temperatures. The estimated “replacement” barrier is 53-54 kJ mol<sup>-1</sup>. Thus, the  $\Delta G^\ddagger$ -values in both mechanisms and for both isomeric cyclohexane selenides are similar in their magnitudes.



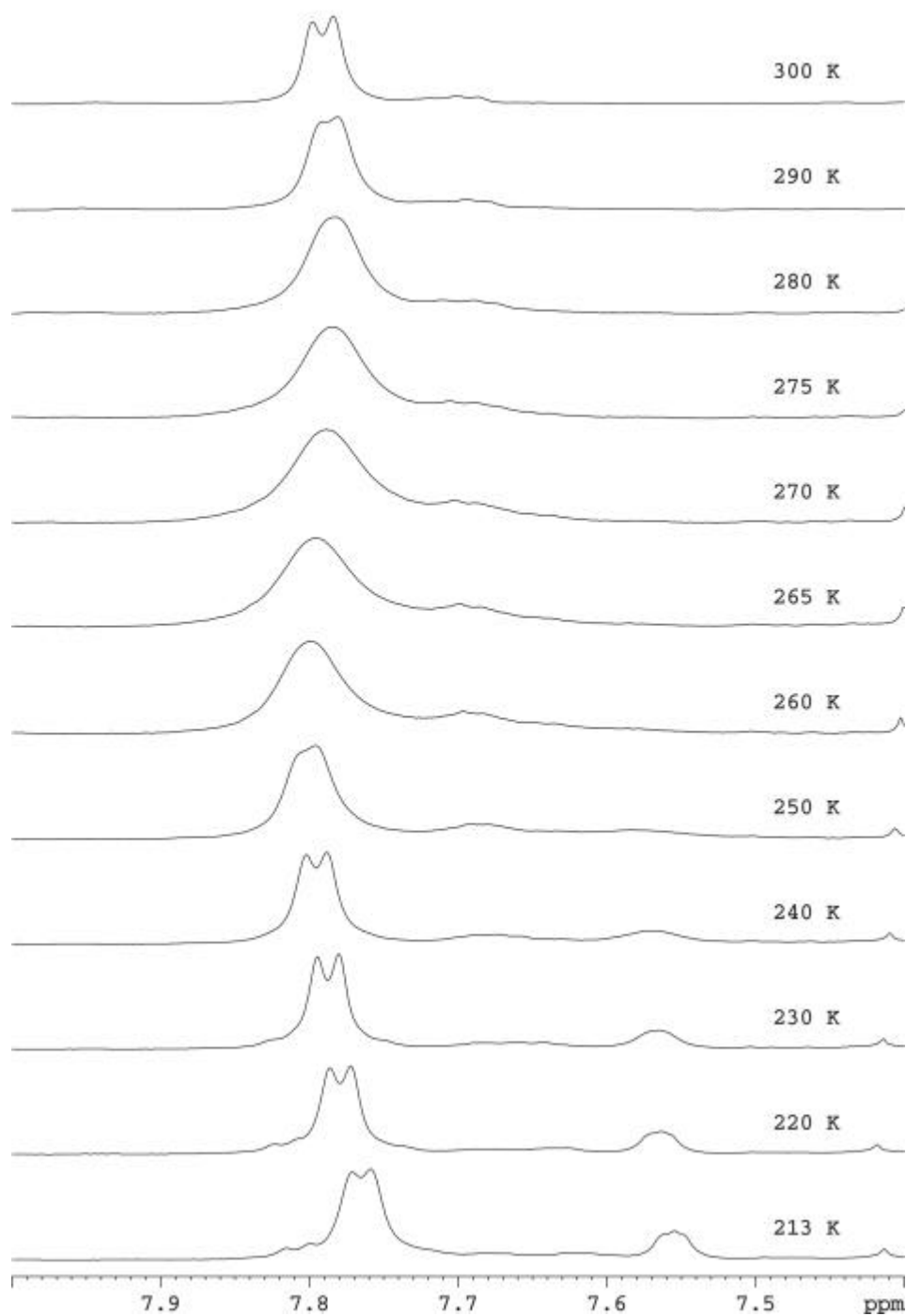


**Figure 23.** *Ortho*-proton signals of **31** at variable temperature; equimolar amount of **Rh-Rh** (**31** : **Rh-Rh** = 2.5:1).

### 3.2.2.3 Activation Barriers

For comparison, analogous variable-temperature  $^1\text{H}$  NMR experiments were performed for the 2-phenylselenenylbutane (**36**). Although this compound is chiral and shows dispersion effects, it was possible to determine the barriers of the “switch” (molar ratio **36** : **Rh-Rh** = 1 : 1) and the “replacement” exchange (molar ratio **36** : **Rh-Rh** = 4 : 1) as well. Interestingly, in this selenide which is sterically much less hindered than **30** and **31** the two barriers  $\Delta G^\ddagger$  are significantly different: ca 45 kJ/mol for the “switch” and ca 54 kJ/mol for the “replacement”. For the latter mechanism (“replacement”) involving the approach of a free selenide molecule (**Se**) to one bulky adduct with subsequent dislodging of a complexed ligand molecule -all three values for **30**, **31** and **36** are quite similar; the shape the ligand molecules and the steric congestion around the selenium atom seems not to play a decisive role. However, there is a clearly lower “switch” barrier for **36** as compared to **30** and **31**. Apparently, the bulkiness of the ligand molecule, which has to be flanked between two voluminous **Rh-Rh** residues during the transition, is important; the larger the ligand the higher the barrier to overcome by switching. This observation strongly supports our interpretation of the existence of the two different mechanisms and the absence of a noticeable concentration of free ligand molecules under rhodium excess conditions (large adduct formation constants) as stated above. So, a simple  $\text{Rh} \leftarrow \text{Se}$  contact separation is not sufficient to explain both mechanisms; in the “switch” situation the hindrance of the approach of the two **Rh-Rh** residues by the intervening ligand molecule is important as well.

### 3.2.3 Characterisation of Phenylselenenylcyclohexanes and -Menthanes and Their $Rh_2(MTPA)_4$ -Adducts by $^{77}Se$ NMR Spectroscopy

$^{77}Se$  NMR spectra of the free ligands **29** - **36** were recorded in the 1D direct mode or indirectly by  $\{^{77}Se\}$   $^1H$ -detected HMBC optimized for  $J(^{77}Se,^1H) = 7$  Hz. These data accompanied by analogous 1D data of the menthane derivatives **25** - **28** are collected in Table 17.

Due to the low concentration of the adduct solutions, signal-to-noise ratios were sometimes a problem and required several hours of spectrometer time per measurement. In such cases the HMBC experiment was clearly superior in its sensitivity. Figure 24 shows a representative example of  $\{^{77}Se\}$   $^1H$ -detected HMBC experiments in compound **31**. It is evident that at 2.5:1 molar ratio of (**31** : **Rh-Rh**) the  $^{77}Se$  signals can be assigned easily by correlating them to the *ortho*-protons of the 2:1-adduct (left) and those of the free ligand (right). Figures 25 and 26 also represent the  $\{^{77}Se\}$   $^1H$ -detected HMBC experiments in compound **25** and **36**. It can be clearly seen in Figure 26 that at 4:1 molar ratio of (**36** : **Rh-Rh**) two  $^{77}Se$  signals at  $\delta$  385 for the free Se (ligand) and at  $\delta$  357 for 2:1-adduct were obtained.

The signals of the adducts of **32** could not be observed due to the fact that **32** and **33** were a mixture with a composition of ca 30% and ca 70%, respectively. The concentration which could be achieved was too low for **32**.

As expected,  $^{77}Se$  chemical shifts are strongly temperature-dependent. For the free ligands values of  $-12$  to  $-16$  ppm can be found. This is in accordance to other acyclic and cyclic selenides reported before.<sup>59</sup> However, there are two cases which deviate from these observation:

- (a) Nearly equal chemical shifts are found for **29** ( $\delta = 400$ ). At room temperature this signal is averaged over the signal for the equatorial (ca 90%) and the axial conformer (ca 10%) whereas that at 213 K represents only the equatorial conformer<sup>59</sup>; here the separate signal of the axial conformer could not be identified from the noise level.

Apparently, the share of the axial conformer compensates the expected temperature shift in the room-temperature experiment.

- (b) The chemical shift difference for **33** is much larger (-27 ppm) than all others. This may be attributed to the fact that **33** exists in two different conformations with only a small  $\Delta G_0$  difference (ca 0.6 kcal/mol as the difference of the A-values, *vide infra*). If the ground state entropy  $\Delta S_0$  is different, the equilibrium varies by temperature change. Then, the value of -27 ppm would consist of ca 50% of normal temperature effect and ca 50% of an additional diamagnetic shift indicating a higher content of the conformer with the axial PhSe group at 213 K.

Substituent effects on the  $^{77}\text{Se}$  chemical shift have been described before.<sup>59</sup> Here, diamagnetic  $\gamma$ -gauche effects are most significant and range up to ca -40 to -60 ppm; note that an axial selenium atom experience two  $\gamma$ -gauche interactions whereas a  $\gamma$ -anti oriented Se has none.<sup>59</sup> Likewise, the differences of the  $\delta$ -values of corresponding selenium atoms in the two selenoacetals **34** and **35** can be explained semi quantitatively by the existence of a methyl in  $\gamma$ -gauche position with respect to both selenium atoms in **34** whereas the methyl group in **35** is in one bond further away ( $\delta$ -position). The exceptionally large difference between the  $^{77}\text{Se}$  chemical shifts of the two menthyl selenides **25** and **26** ( $\Delta\delta = 377 - 288 = 89$ ) may be explained by the additional effect of the conformational behaviour of the isopropyl group.

Adduct formation shifts  $\Delta\delta$  can be extracted by comparing the  $^{77}\text{Se}$  chemical shifts of the 1:1-adducts with those of the corresponding free ligands (Table 17). In most examples, these values are shielding (-28 to -59) in agreement with previous observations for other selenides<sup>41a</sup> and phosphine selenides (with selenium as the complexation site). It is interesting to observe that these  $\Delta\delta$ -values allow to state which of the two selenium atoms of **35** is the preferred complexation site in the 1:1-adduct: clearly it the equatorial Se which is offers an easier approach of the rhodium atom. Simultaneously, this explains why the adduct formation shifts of the axial Se in **35** are so low (-6 at room temperature and -9 at 213 K); there is only a small contribution of this Se in the adduct formation.

Such clearly differentiation can be observed by no other NMR parameter ( $^1\text{H}$  or  $^{13}\text{C}$ ) in the molecule because Se is the only atom involved directly.

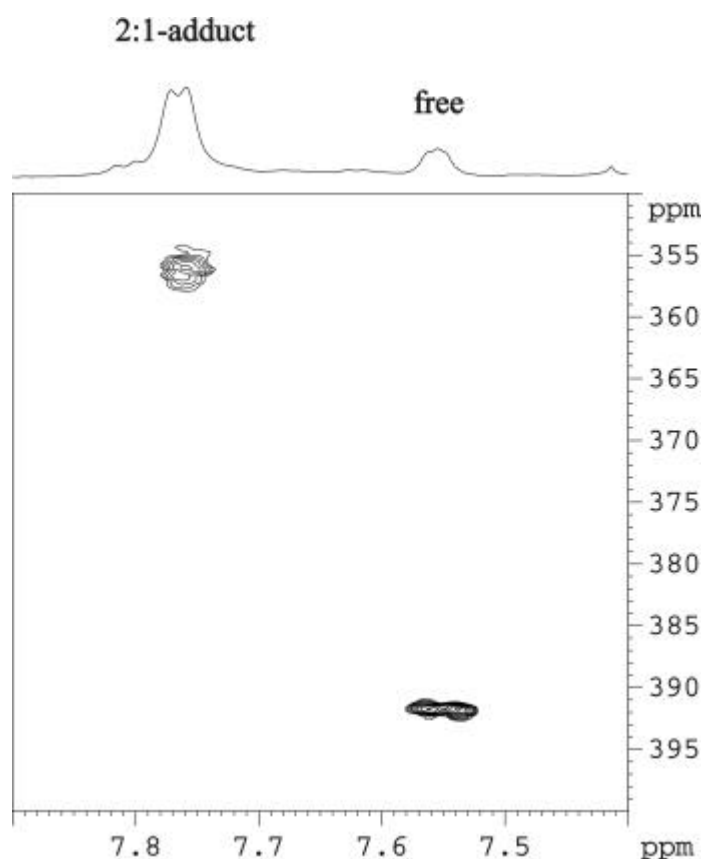


**Figure 24.** Section of the  $\{^{77}\text{Se}\}$   $^1\text{H}$ -detected HMBC spectrum of **31** and **Rh-Rh** (2.5 : 1 molar ratio of **31** : **Rh-Rh**).<sup>a</sup>

<sup>a</sup> The  $^{77}\text{Se}$  atom of the free **31** shows two further correlation peaks (not depicted) with H-1 ( $\delta = 3.09$ ) and H-2(ax) / 6(ax) ( $\delta = 1.45$ ) confirming the  $^{77}\text{Se}$  signal assignment.

On the other hand, there are a few compounds (**26**, **27** and **34**) which present positive  $\Delta\delta$ -values, i.e., deshielding adduct formation shifts. The reason is not clear but an explanation suggesting the absence of any adducts and a deshielding of  $^{77}\text{Se}$  nuclei simply by differences in the susceptibilities of the probes can be excluded because significant

dispersion effects ( $\Delta\nu$ ) are present (see below) proving the existence of an intramolecular interaction between the ligand molecules and **Rh-Rh**. Inspecting the present family of selenides, a sign reversal seems to occur only if a combination of two structural features in the molecule exists, namely an axial selenium atom and an equatorial alkyl substituent at the neighbouring carbon. Whether or not this indicates a principal difference in the underlying adducts/clusters is currently under investigation in our laboratory.

We have reported previously that diastereomeric dispersion effects  $\Delta\nu$  at  $^{77}\text{Se}$  nuclei to be the largest ever found, an experience confirmed again in this series of phenylselenenylcyclohexane derivatives. Values up to 230 Hz are found (Table 17), and in one particular case (the equatorial selenium atom of **34**) it is even 636 Hz. Undoubtedly, such eminent magnitudes of dispersions are originated in the greater shielding sensitivity of heavy nuclei on structural influences in the molecule. In some cases we observed broad  $^{77}\text{Se}$  signals, and no dispersion was visible. We expect that coalescence phenomena are responsible. It should be noted that observing low-temperature NMR signals without line broadening means that the ligand exchange rate is low on the NMR time-scale but it is not necessarily zero. In such case one would observe  $^{77}\text{Se}$  signal splitting due to  $^{103}\text{Rh}$ - $^{77}\text{Se}$  coupling, in analogy to  $^{31}\text{P}$  signals in phosphine adducts.

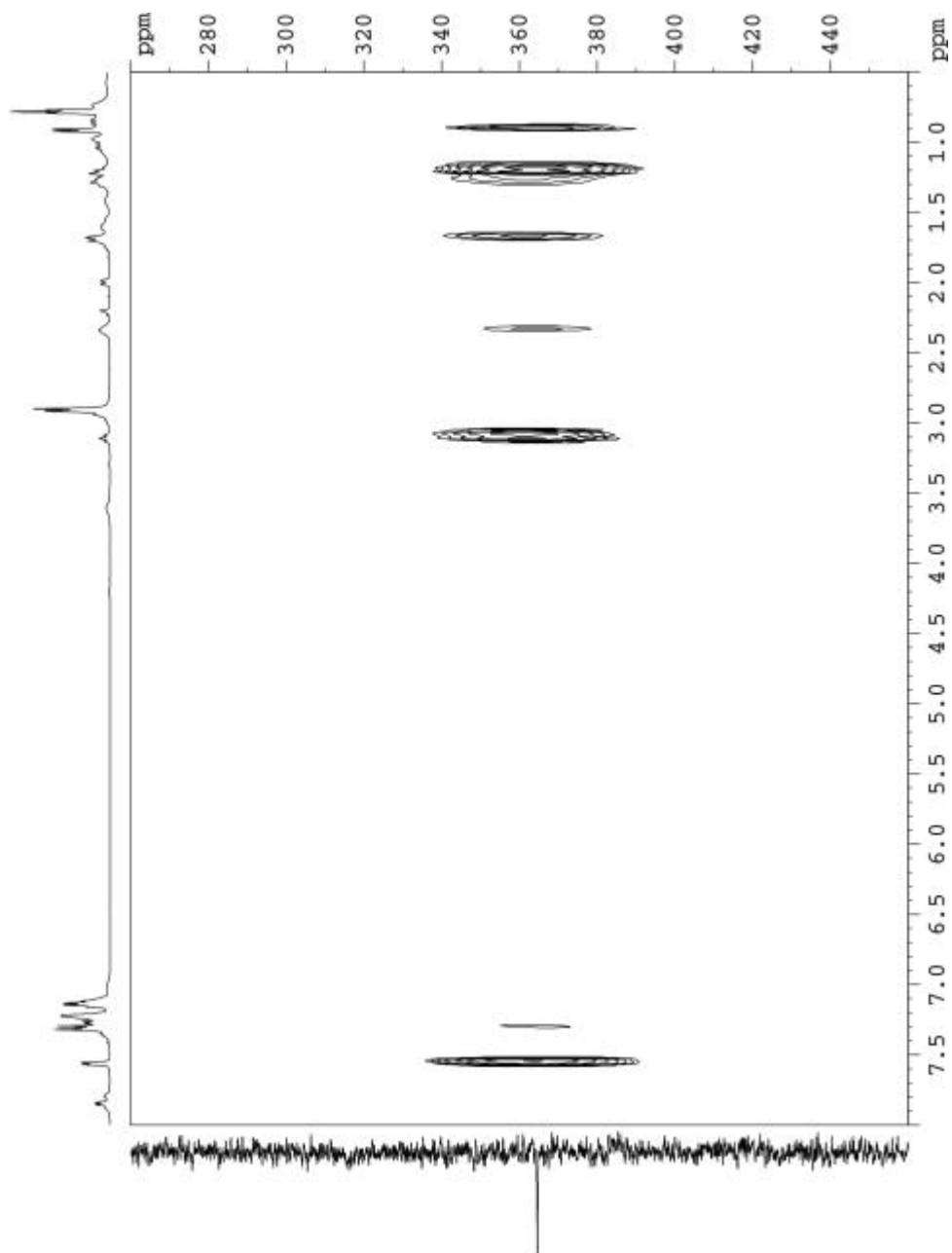


**Figure 25.** Section of the  $\{^{77}\text{Se}\}$   $^1\text{H}$ -detected HMBC spectrum of **25** and **Rh-Rh** (4 : 1 molar ratio of **25** : **Rh-Rh**).

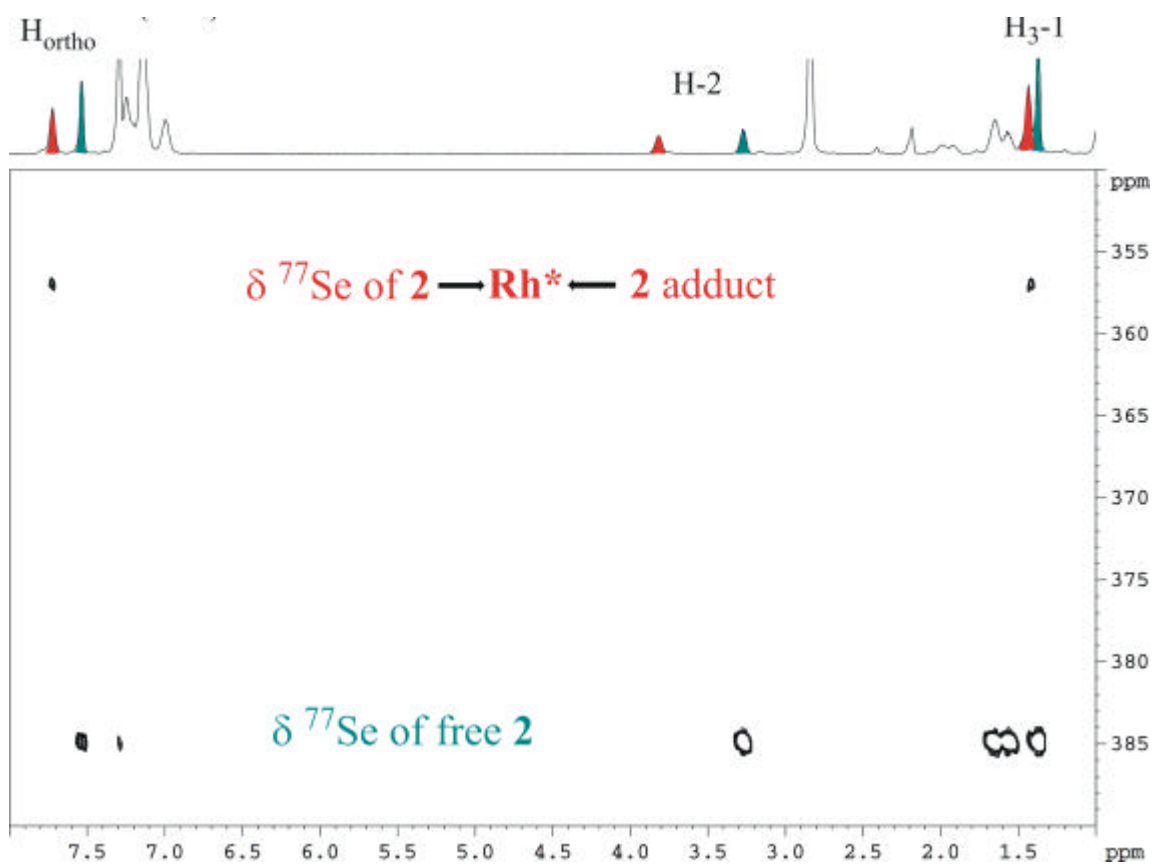


**Figure 26.** Section of the  $\{^{77}\text{Se}\}^1\text{H}$ -detected HMBC spectrum of **36** and **Rh-Rh** (4 : 1 molar ratio of **36** : **Rh-Rh**).



**Table 17.**  $^{77}\text{Se}$  chemical shifts ( $\delta$ ) and adduct formation shifts ( $\Delta\delta$ ) for compounds **25-36**; numbers in italics are chemical shifts from 2D HMBC experiments. Values in squared brackets are diastereomeric dispersion effects ( $\Delta\nu$ , in Hz; referred to 76.31 MHz).<sup>a</sup>

		$\delta$		$\delta$		$\Delta\delta$	
		free ligand <b>L</b>		1:1 adducts of <b>L : Rh-Rh</b> (equimolar)			
		r.t.	213 K	r.t.	213 K	r.t.	213 K
<b>25</b>		377	365	325 (br)		ca -52	
<b>26</b>		288		293, 291 [210]		+5, +3	
<b>27</b>	ax	401		408, 405 [211]		+7, +4	
	eq	495		508 (br)		+13	
<b>28</b>		364		330 (br)		-34	
<b>29</b>		400 <sup>b</sup>	400 (eq) <sup>c</sup>	n.d. <sup>d</sup>	354 (eq) 364 <sup>e</sup>		-46 -36
<b>30</b>		338	325 / 324	284	268	-54	-57 / -56
<b>31</b>		406	392 / 392	362 / 361	357 356 <sup>e</sup>	-44 / -45	-35 -36
<b>32</b>		411	399	n.d.	n.d.		
<b>33</b>		360	333	n.d.	282 291 <sup>e</sup>		-51 -42
<b>34</b>	ax	379	366	402 (br) <sup>f</sup>		ca +23	
	eq	500	486	512/504 [636]		+12/+4	
<b>35</b>	ax	431	422 <sup>g</sup>	425, 424 [127]		-7, -6	
	eq	568	558	509 (br)		ca -60	
<b>36</b>		398	385		357 <sup>h</sup>		-28

<sup>a</sup> In  $\text{CDCl}_3$ ; relative to external  $(\text{PhSe})_2$   $\delta = 463$ , corresponding to  $(\text{CH}_3)_2\text{Se}$   $\delta = 0$ ; r.t.: room temperature; for spectral conditions see experimental part.

<sup>b</sup> Averaged signal, equatorial and axial conformer (ca. 9:1).

<sup>c</sup> Signal of the equatorial conformer (eq); that of the axial was not detectable.

<sup>d</sup> Not detectable due to signal-to-noise ratio.

<sup>e</sup> Signal smaller than that of the 1:1-adduct; it was assigned to the 2:1-adduct.

<sup>f</sup> (br): broadened signal, presumably by coalescence effects.

<sup>g</sup> At 243 K.

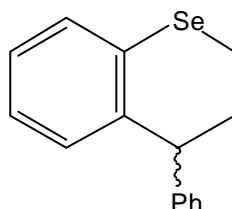
<sup>h</sup> Recorded with 4 mole equivalents of **Rh-Rh**; i.e. data correspond to 2:1-adducts.

## 4 SELENOCHROMANS

Heterocyclic compounds containing a selenium atom have attracted much attention in recent years because of their high reactivity and unique chemical properties.<sup>70</sup> The chemistry of selenium-containing molecules, as well as the tellurium analogs, have been intensively studied.<sup>71</sup> However, compared with sulphur heterocyclic compounds,<sup>72</sup> the preparative methods for selenium-containing heterocyclic molecules are quite limited. For example, only a few methods for the preparation of benzoselenane derivatives such as selenochromans and isoselenochromans have been reported.<sup>73</sup>

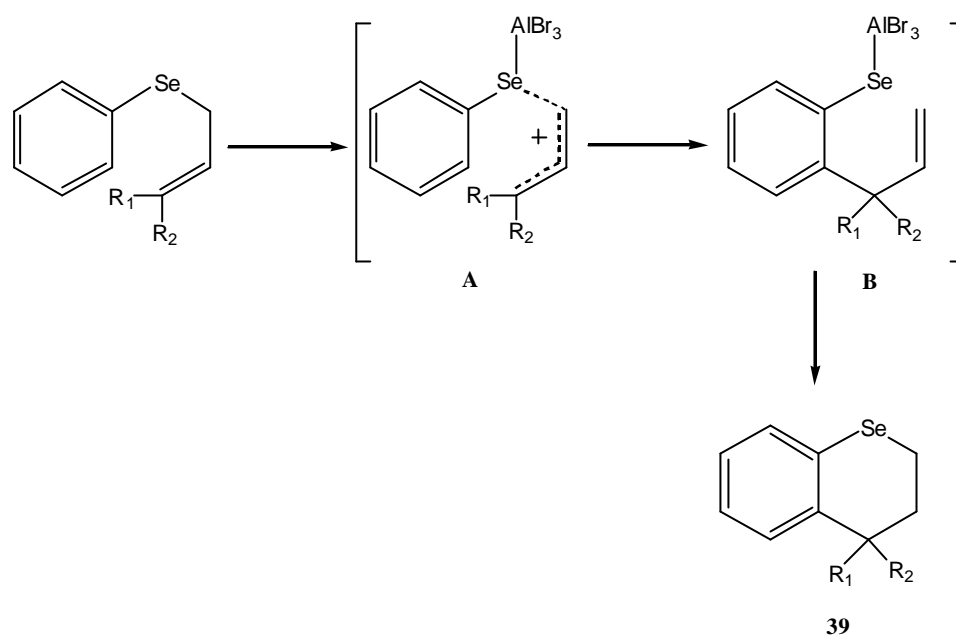
### 4.1 Synthesis of Selenochromans

Cinnamoyl phenyl selenide (**38**) was used for the synthesis of chiral 3,4-dihydro-4-phenyl-2*H*-benzoselenin (**39**), which was prepared from allylic halides by nucleophilic substitution reactions<sup>74</sup> with the phenylseleno group (Scheme 13). The reactions of this substrate in the presence of an equimolar ratio of AlBr<sub>3</sub> at room temperature smoothly proceeded to afford the corresponding selenochromans in moderate yield. The cinnamoyl selenides generally showed good reactivity towards AlBr<sub>3</sub>.

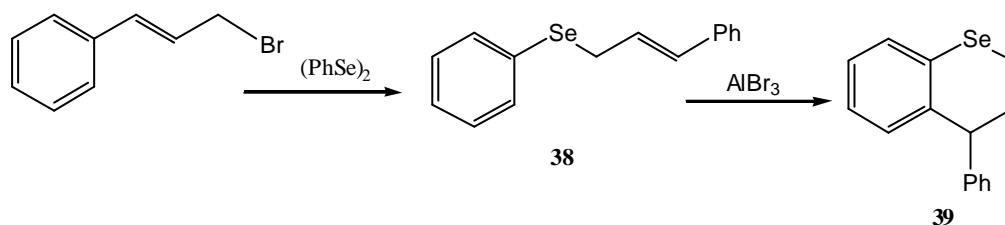


**39**

The reaction pathway can be explained as shown in Scheme 12.<sup>75</sup> Initial coordination of selenium atom to aluminium bromide activates the allylic selenide to generate a positively charged allyl group (**A**). Then the Friedel-Crafts type C-C bond formation between the aromatic ring and the allyl group, followed by nucleophilic attack of aluminium selenolate (**B**) to the olefinic carbon leads to the selenochroman.



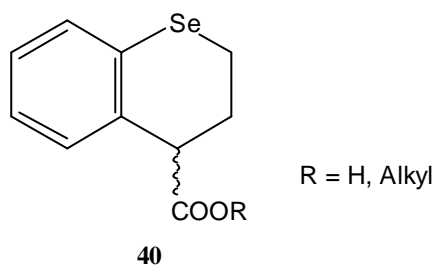
**Scheme 12.** Reaction pathway of benzoselenochromanes.



**Scheme 13.** Synthesis of 3,4-dihydro-4-phenyl-2H-benzoselenin (**39**).

## 4.2 Chiral Discrimination By the Dirhodium Complex Rh-Rh

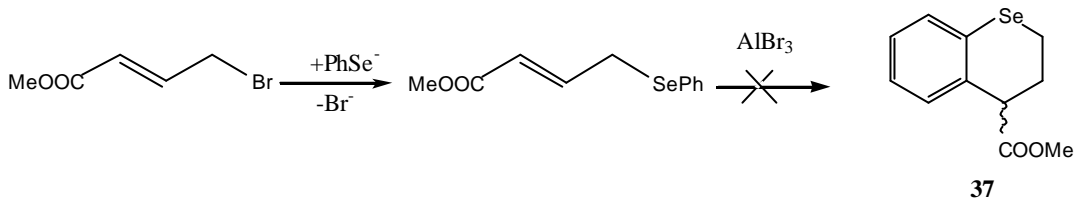
After the successful synthesis of **39** we were interested to determine the chiral discrimination through NMR in the presence of the dirhodium complex **Rh-Rh**. Table 18 shows complexation shift and dispersion effect in compound **39** in the presence of dirhodium complex. We planned to modify this reaction with commercially available methyl 4-bromocrotonate for the synthesis of chiral selenochroman-4-carboxylic acid derivatives **40**.



Compound **40** was planned to be further converted into diastereomeric ester and amides by the reacting with enantiomerically pure alcohols and amines. Then after record  $^1\text{H}$ ,  $^{13}\text{C}$  and  $^{77}\text{Se}$  NMR spectra in the presence of dirhodium complex to differentiate enantiomers in such class of compounds in which functional groups ( $\text{OH}$  and  $\text{NH}_2$ ) are far from chirality centre.

Unfortunately, we could not succeed to synthesis selenochroman methyl ester by using equal molar amount of  $\text{AlBr}_3$  or double the amount of the reagent.

Therefore, we stopped this sub-project at this stage in favor of the other projects described in the sections 2 and 3.



**Scheme 14.** Proposed reaction for the synthesis of selenochroman methyl ester.

**Table 18.** Complexation shift and dispersion effect in **39** in the presence of **Rh-Rh**

$^1\text{H}^{\text{a}}$				$^{13}\text{C}^{\text{b}}$			
No.	d (ppm)	dD (ppm)	dn (Hz)	No.	d (ppm)	dD (ppm)	dn (Hz)
H-2	2.89/2.85	+0.49/+0.44		C-2	16.6	+1.3	50
H-3	2.45/2.29	-0.04/+0.02		C-3	30.6	-1.3	32
H-4	4.21	-0.04	56	C-4	45.7	-0.4	34
H-5	6.89			C-5	131.3	+0.2	9.0
H-6	7.10			C-6	127.2		
H-7	6.97			C-7	124.9	-0.1	7.0
H-8	7.32	+0.20	3	C-8	128.9		
H-ortho	7.07			C-9	128.4		
H-meta	7.26			C-10	138.2	+1.1	27
H-para	7.20			C- <i>ipso</i>	143.7	+0.1	8.0
				C- <i>ortho</i>	128.3		
				C- <i>meta</i>	128.4		
				C- <i>para</i>	126.3		
$^{77}\text{Se}^{\text{c}}$	220	-31					

<sup>a</sup> At 400.1 MHz; room temperature; in  $\text{CDCl}_3$ .

<sup>b</sup> At 100.6 MHz; room temperature; in  $\text{CDCl}_3$ .

<sup>c</sup> At 76.3 MHz; room temperature; in  $\text{CDCl}_3$ .

## 5 EXPERIMENTAL SECTION

### 5.1 General Methods

#### 5.1.1 Infrared Spectroscopy (IR)

The IR-spectra (neat) were obtained using a PERKIN-ELMER FT 1710 spectrometer. The following abbreviations were used to indicate the intensity of the absorption bands: s = strong, m = middle, w = weak. The characteristic IR absorptions are presented in  $\text{cm}^{-1}$ .

#### 5.1.2 Mass Spectrometry (MS)

Mass spectrometry was carried out using a FINNIGAN AM 400 mass spectrometer (Ionization potential 70 eV). The characteristic EI MS peaks are given m/z (mass to charge ratio) and relative percentage intensity of base peak (100 %).

#### 5.1.3 Melting Points (m.p.)

Melting points were measured by using a Büchi apparatus and are not corrected.

#### 5.1.4 Solvents

Diethyl ether and THF were distilled over sodium-potassium alloy/benzophenone. Ethanol and methanol were dried over calcium hydride. Dichloromethane, Petroleum ether and *n*-pentane were dried over calcium chloride. Pyridine was dried over KOH.

#### 5.1.5 Chromatographic Techniques

Thin layer chromatography (TLC) was carried out using aluminum TLC plates coated with the silica gel 60F<sub>254</sub> from Merck. The column chromatography was carried out using silica gel 60 (40-60  $\mu\text{m}$ ) and 60 A (20-45  $\mu\text{m}$ ) from Merck. Preparative column chromatography was carried out using the silica gel<sup>76</sup> (J. T. Baker with particle size 30-60  $\mu\text{m}$ ). The detection of substance over the TLC was done with the help of the UV-lamp ( $\lambda = 254 \text{ nm}$ ) and developed in Ce(IV) sulfate/Molybdato-phosphoric acid-solvent.<sup>77</sup>

### 5.1.6 Specific Rotation

The specific rotation,  $[\alpha]_{\lambda}^c$  were determined on polarimeter PERKIN-ELMER 341. C is the concentration of the sample and  $\lambda$  is the wavelength of light used to determine the specific rotation.

### 5.1.7. Molecular Geometry Calculations

Molecular geometries and orbitals were calculated on an IBM PC using spectran-Pro® package. Generally, calculations took 5 to 10 minutes.

## 5.2 Nuclear Magnetic Resonance Spectroscopy (NMR) Parameters

**Table 19.** Employed NMR Spectrometers.

	Field Strength $B_0$	Resonance frequency			
	[Tesla]	$^1\text{H}$ [MHz]	$^{13}\text{C}$ [MHz]	$^{31}\text{P}$ [MHz]	$^{77}\text{Se}$ [MHz]
Bruker AVANCE-400 <sup>a</sup>	9.40	400	100.577	161.923	76.27
Bruker AVANCE-500 <sup>b</sup>	11.74	500	125.721	202.404	100.6

<sup>a</sup> DPX 400; Probe head: 5 mm QNP  $^1\text{H}/^{77}\text{Se}/^{13}\text{C}/^{31}\text{P}$  Z-grad.

<sup>b</sup> DRX 500; Probe head: 5 mm multinuclear inverse Z-grad.

All NMR- measurements were carried out at room or low temperature in 5 mm NMR tubes, and in deuterated solvents. Tetramethylsilane (TMS,  $\delta = 0.00$ ) was used as internal standard.<sup>78</sup> The chemical shifts  $\delta$  are represented in (ppm) and the coupling constant over n bond ( $^nJ$ ) are represented in Hertz (Hz).

The multiplicity of the peaks were abbreviated as s = singlet, d = doublet, t = triplet, q = quartet, m = multiplet, br = broad signal, dm = doublet of multiplet, dd = doublet of doublets, ddd = doublet of double doublets, dt = doublet of triplets, dq = doublet of

quartets ddq = doublet of doublet of quartet, ttt = triplet of triplet of triplet, tm = triplet of multiplet.

All  $^{13}\text{C}$ -NMR spectra were measured under  $^1\text{H}$  broad-band decoupling. The multiplicities of the signals were determined with DEPT90 (pulse angle  $q = 90^\circ$  gave a CH-subspectrum with positive signal amplitudes) and the DEPT135 (pulse angle  $q = 135^\circ$  gave a CH/CH<sub>3</sub>-subspectrum with positive as well as the CH<sub>2</sub>-subspectrum in negative signal amplitudes). Direct and indirect connectivities between  $^1\text{H}/^1\text{H}$  and  $^1\text{H}/^{13}\text{C}$  were established with the help of two-dimensional  $^1\text{H}/^1\text{H}$ -COSY, NOESY, gs-HMQC and gs-HMBC correlations. In some compounds the  $^1\text{H}$  signal assignments were carried out with the help of NOE experiments.

The  $^{31}\text{P}$  NMR spectra were recorded using 202.4 MHz resonance frequency, and aqueous phosphoric acid ( $\delta = 0$  ppm) was used as a internal reference.

The room temperature  $^{77}\text{Se}$  NMR spectra were recorded using 76.27 MHz resonance and at low temperature  $^{77}\text{Se}$  NMR spectrum were recorded out using 100.6 MHz resonance frequency. Diphenyldiselenide ( $\text{PhSe}$ )<sub>2</sub> ( $\delta = 463$  ppm) was used as a external reference.

Two-dimensional  $\{^{77}\text{Se}\} ^1\text{H}$ -detected HMBC spectra were recorded at 95.4 MHz using the standard Bruker HMBC program but without a low-pass filter. The experiment was optimized for long-range couplings  $^nJ(^{77}\text{Se}, ^1\text{H}) = 7$  Hz. No decoupling was performed during acquisition. Gradient ratios were 60 : 35 : 43.13. 128 rows were sampled in F1. The number of scans was 2 – 16 depending on the signal-to-noise ratio required, the relaxation delay was 1.5 s and the gradient pulse 1 ms. The data were processed with 512 data points in F1 after zero-filling and 2 k in F2, no zero-filling.

Generally, the number of transients and recording times were 32 to 80 scans/ca 4-6 min for  $^1\text{H}$  and  $^{31}\text{P}$ , 1K to 2K scan/1.5-2 hours for  $^{77}\text{Se}$  and 7K to 20K scan/5-15 hours for  $^{13}\text{C}$  in the **Rh-Rh**-complexation experiments. Digital resolutions were 0.24 Hz/point in the  $^1\text{H}$  and 1.53 Hz/point in the  $^{13}\text{C}$  NMR spectra



Variable-temperature  $^1\text{H}$  (500.1 MHz) spectra were recorded in the presence of **Rh-Rh** on a Bruker DRX-500. Digital resolutions were 0.37 Hz/point in the  $^1\text{H}$  NMR spectra. Temperatures varied from 213 to 333 K and were read from the instrument panel; no further measures for more precise temperature determinations were taken.

### 5.3 NMR Samples Preparation

In typical chiral recognition experiments, 45.2 mg **Rh-Rh** (0.04 mmol) and a molar equivalent of the respective ligands **L** in 0.7 ml  $\text{CDCl}_3$ , and 7  $\mu\text{l}$  (one drop) of acetone- $\text{d}_6$  were added to increase the solubility of **Rh-Rh**. Addition of acetone- $\text{d}_6$  does not significantly compete with the ligands in adduct formation <sup>41a</sup>.

#### 5.3.1 Samples Preparation for Job Plots

Equimolar solutions (0.026-0.048 M) of ligand and dirhodium complex in  $\text{CDCl}_3$  (containing a trace of acetone- $\text{d}_6$ ) were prepared in volumetric flasks and mixed in various amounts. These mixed solutions were subjected to  $^1\text{H}$  NMR measurements at 400.1 MHz and room temperature.

#### 5.3.2 Stock Solutions for Job Plot

Ligand: 0.167 mmol of the ligand are dissolved in 5.0 ml of  $\text{CDCl}_3$  (in volumetric flask).

**Rh-Rh**: 190.0 mg (0.167 mmol) of dirhodium complex with 5 drops of acetone- $\text{d}_6$  was dissolved in 5.0 ml of  $\text{CDCl}_3$  (in volumetric flask).

## 5.4 Synthetic Procedures

### 5.4.1 Synthesis of Dirhodium Carbonate Sodium Salt $[Na_4Rh_2(CO_3)_4]$ <sup>79</sup>

Dirhodium (II) tetra-acetate  $[Rh_2(OCOCH_3)_4]$  (1.0 g, 2.26 mmol) was dissolved in 20 ml of 2M sodium carbonate solution and heated to 100 °C for 50 min until a blue purple color appeared. The reaction mixture was cooled to room temperature and filtered, the residue being washed with small portions of distilled water, methanol and diethyl ether. Drying at 50 °C in *vacuo* overnight afforded a light blue-purple crystal powder of dirhodium carbonate sodium salt in 90 % yield.

### 5.4.2 Tetrakis-[(*R*)-(+)- $\alpha$ -methoxy- $\alpha$ -trifluoromethylphenyl-acetate]-dirhodium(II)]<sup>80</sup>

Rhodium carbonate sodium salt (1.0 g, 1.62 mmol) and (*R*)-(+)- $\alpha$ -methoxy- $\alpha$ -trifluoromethylphenylacetic acid (Mosher acid) (3.126 g, 13.35 mmol, 8 eq, e.e. = 97 %) were dissolved in 100 ml of distilled water under nitrogen and heated to 100 °C for 50 min. until a blue green sticky solid separated. After cooling, the water was decanted, the residue dissolved in methylene chloride and the organic layer washed three times with 2M sodium carbonate solution (20 ml each time) and dist. water (20 ml each time) to remove the excess of Mosher acid. At the end the organic layer was washed with brine solution and dried over  $MgSO_4$ . Further chromatographic purification on silica gel with methylene chloride / ethyl acetate (9.5 : 0.5) as eluents gave green complex crystals. The complex was shaken with benzene to remove ethyl acetate and dried under high vacuum at 110 °C for three days. The overall yield was 77 %.

### 5.4.3 Synthesis of Phosphine Selenides

The phosphine selenides **20-24** were prepared by Dr. J. Omelanczuk, Lodz, Poland, by oxidation of the corresponding methylphenylphosphinites  $C_6H_5(Me)P-OR$ ,  $C_6F_5(Me)P-OR$  and *N,N*-diethyl-methylphenyl phosphine  $C_6H_5(Me)P-N(C_2H_5)_2$  with selenium in diethyl ether at room temperature (exothermic reaction). All compounds were isolated by vacuum distillation at ca 0.1 Torr. The phosphinite precursors were synthesized according to know procedures by alcoholysis of methylphenyl- and methylpentafluorophenylchlorophosphine, respectively, in the presence of triethylamine. Compound **20** was

synthesized according to literature procedures.<sup>51-52</sup> All phosphine selenides **20-24** investigated were racemates. The phosphine selenides are not very stable; so all the reactions were carried out in inert atmosphere and the compounds stored under nitrogen.

#### 5.4.4 Synthesis of Phenylselenenylalkanes Derivatives

##### 5.4.4.1 General Method for the Synthesis of Selenides From Respective Alcohols<sup>81</sup>

The respective alcohol was dissolved in 10 ml dry pyridine in a round bottom flask fitted with an argon inlet and magnetic stirrer. Methanesulfonyl chloride was added at 0 °C under argon atmosphere on continuous stirring. The reaction mixture was allowed to warm to room temperature and stirred over night.

Crushed ice was then added into the reaction mixture and extracted twice with diethyl ether, 10 % HCl and saturated NaHCO<sub>3</sub> solution. The organic layer was washed with distilled water and dried over MgSO<sub>4</sub>. The solvent was evaporated in *vacuo* and the product was purified by column chromatography; CH<sub>2</sub>Cl<sub>2</sub>/petrol ether (7 : 1) were used as a eluent. The overall yield of protected alcohols (mesylates) were ca 90-95 %.

To a solution of diphenyldiselenide (PhSe)<sub>2</sub> in 20 ml of dry ethanol, sodiumborohydride (NaBH<sub>4</sub>), (300 mg, 7.9 mmol) was added over 15 min with continuous stirring under argon atmosphere. A strong effervesce (H<sub>2</sub> gas) occurs and the solution become colorless indicating the formation of C<sub>6</sub>H<sub>5</sub>Se<sup>-</sup>Na<sup>+</sup> salt. The protected alcohole (mesylates) were then added dropwise and the reaction mixture refluxed for two hours. The color of reaction mixture was become light yellow.

After cooling to room temperature, the solvent evaporated. The residue was dissolved in methylene chloride, washed one time with saturated ammonium chloride solution, two times with distilled water and dried over MgSO<sub>4</sub>. After filtration the solvent was evaporated and the product was purified by silica gel column chromatography, using *n*-pentane as eluent.

#### 5.4.4.2 General Method for the Synthesis of Bis-Selenides From Respective Ketones By Using $(\text{PhSe})_3\text{B}$ :<sup>81</sup>

To a solution of diphenyldiselenide  $(\text{PhSe})_2$  in 20 ml of dry ethanol, sodiumborohydride  $(\text{NaBH}_4)$ , (300 mg, 7.9 mmol) was added over 15 min with continuous stirring under argon atmosphere. A strong effervesce ( $\text{H}_2$  gas) occurs and the solution become colorless indicating the formation of  $\text{C}_6\text{H}_5\text{Se}^-\text{Na}^+$  salt. Carbon disulfide ( $\text{CS}_2$ ) was added and the reaction mixture was cooled down to  $0\text{ }^\circ\text{C}$ . At  $0\text{ }^\circ\text{C}$  borontribromide (1.0 ml) was added to the reaction mixture and stirred over night at room temperature.

The solvent was evaporated giving a white amorphous solid of  $(\text{PhSe})_3\text{B}$ : which was dissolved in dry methylene chloride. The ketones were added dropwise to the reaction mixture and stirred overnight, then refluxed for one hour. The color of the reaction mixture become light yellow.

After cooling to room temperature, the solvent was evaporated. The residue dissolved in methylene chloride, two times washed with distilled water and dried over  $\text{MgSO}_4$ . After filtration, the solvent was evaporated and the product was purified by silica gel column chromatography using petrol ether as eluent. Vinylselenide was also obtained as a by-product.

#### 5.4.4.3 General Method for the Synthesis of Selenides From Respective Halides<sup>81</sup>

To a solution of diphenyldiselenide  $(\text{PhSe})_2$  in 20 ml of dry ethanol, sodiumborohydride  $(\text{NaBH}_4)$ , (300 mg, 7.9 mmol) was added over 15 min with continuous stirring under argon atmosphere. A strong effervesce ( $\text{H}_2$  gas) occurs and the solution become colorless indicating the formation of  $\text{C}_6\text{H}_5\text{Se}^-\text{Na}^+$  salt. Alkyl halide was added dropwise and the reaction mixture refluxed for two hours. The color of the reaction mixture became light yellow.

After cooling to room temperature, the solvent evaporated. The residue was dissolved in methylene chloride, washed one time with saturated ammonium chloride solution, two times with distilled water and dried over  $\text{MgSO}_4$ . After filtration the solvent was eva-

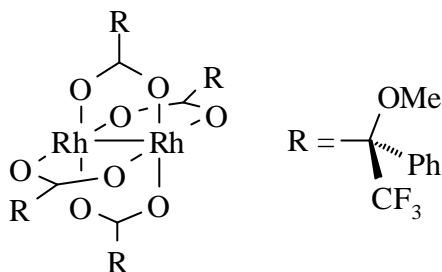
porated and the product was purified by silica gel column chromatography using petrol ether as eluent.

### 5.5 Method for the Synthesis of Selenochroman (39)

To a stirred mixture of freshly purified  $\text{AlBr}_3$  (975 mg, 3.6 mmol) and dry  $\text{CH}_2\text{Cl}_2$  (15.0 ml), a solution of 3-Phenylselenenyl-1-phenyl-1-propene (**38**) (1.0 g, 3.6 mmol) in dry  $\text{CH}_2\text{Cl}_2$  (26.0 ml) was added under argon atmosphere. After 2 hours at ambient temperature, the reaction mixture was poured into a 1N NaOH aqueous solution and extracted with  $\text{CH}_2\text{Cl}_2$ . The organic layer was washed with brine, dried over anhydrous  $\text{MgSO}_4$ , and concentrated. The crude product was then purified on silica gel. Elution with hexane afforded 500 mg of 3-phenylselenochroman (50 %) along with diphenyldiselenide.

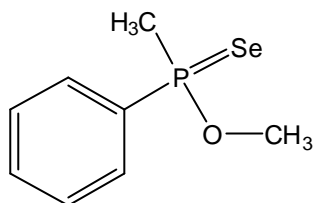
## 5.6 Collection of Spectroscopic Data

### 5.6.1 Tetrakis-[(R)-(+)-*a*-methoxy-*a*-trifluoromethylphenyl-acetate]-dirhodium(II)]



$\text{Rh}_2[(R)\text{-MTPA}]_4$ , **Rh-Rh**

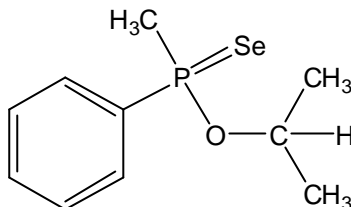
<b>Status</b>	:	Green powder	$\text{C}_{40}\text{H}_{32}\text{F}_{12}\text{O}_{12}\text{Rh}_2$	1138.48 $\text{g mol}^{-1}$
<b>M.P.</b>	:	203°C		
$[\alpha]_{\text{D}}^{20}$	:	+193.0 <sup>0</sup> (0.52 g/100 ml $\text{CHCl}_3$ )		
<b><sup>1</sup>H NMR</b>	:	400 MHz, $\text{CDCl}_3/\text{TMS}$ + 14 $\mu\text{L}$ of acetone- $\text{d}_6$ $\delta$ = 3.18 (s, $\text{OCH}_3$ ), 7.08 (m, arom. <i>m</i> -CH), 7.18 (m, arom. <i>p</i> -CH), 7.29 (m, <i>o</i> -CH)		
<b><sup>13</sup>C NMR</b>	:	100 MHz, $\text{CDCl}_3/\text{TMS}$ + 14 $\mu\text{L}$ of acetone- $\text{d}_6$ $d$ = 54.8 (s, $\text{OCH}_3$ ), 84.3 (q, $^2J(\text{FCC}) = 27.5$ Hz, C, quartet); 122.8 (q, $^1J(\text{FC}) = 287.9$ Hz, $\text{CF}_3$ ); 127.7 und 128.0 (s, <i>o</i> -/ <i>m</i> -C, Ph), 129.2 (s, <i>p</i> -C, Ph), 131.8 (s, <i>ipso</i> -C, Ph), 185.8 (s, C=O).		
<b>IR</b>	:	ATR $\tilde{\nu}$ = 3055 (w, Ph-H), 2956 (m, $\text{CH}_3$ ), 2864 (m, $\text{OCH}_3$ ), 1614 (s, Carboxylate), 1536 (w), 1494 (m, arom. C=C), 1451 (m, $\text{CH}_3$ ), 1392 (s, Carboxylate), 1322 (w), 1266 (m), 1159 (s, C- O-C), 1123 (m), 1083 (s), 1018 (s), 963 (m), 923 (m), 816 (s), 779 (m), 767 (s, monosubst. Aromat), 738 (m), 722 (m), 708 (s, monosubst. Aromat), 677 (s), 657 (s) $\text{cm}^{-1}$		
<b>FAB MS</b>	:	$m/z$ (rel. Int.) = 1291 (52, $\text{M}+\text{O}_2\text{NC}_6\text{H}_4\text{CH}_2\text{OH}^+$ ), 1259 (82), 1161 (49, $[\text{M}+\text{Na}]^+$ ), 1139 (48, $[\text{M}+\text{H}]^+$ ), 1138 (100, $\text{M}^+$ ), 1058 (96), 964 (32), 905 (58), 731 (13), 628 (20), 549 (30), 481 (31), 454 (40), 395 (27), 365 (45), 295 (55), 245 (36).		
<b>HR MS</b>		$\text{C}_{40}\text{H}_{32}\text{F}_{12}\text{O}_{12}\text{Rh}_2$ $\text{M}^+ = 1137.981222$		Calcd. = 1137.981201
<b>EA</b>		C = 42.20% Calcd. C = 42.26%	H = 1.83% Calcd. H = 2.90%	

5.6.2 *O*-Methyl methylphenylphosphinoselenoate (**20**)


---

<b>Status</b>	:	Yellow liquid	$C_8H_{11}OPSe$
<b>Yield</b>	:	35% (not optimized)	
<b><math>^1H</math> NMR</b>	:	400 MHz, $CDCl_3$ /TMS $\delta = 2.21$ (s, $CH_3$ , $^2J_{P,H} = 13.3$ Hz) $3.55$ (s, $OCH_3$ , $^3J_{P,H} = 14.7$ Hz) $7.94$ (m, <i>ortho</i> -H, $^3J_{P,H} = 14.0$ Hz) $7.51$ (m, <i>meta</i> -H), $7.55$ (m, <i>H</i> - <i>para</i> )	
<b><math>^{13}C</math> NMR</b>	:	100 MHz, $CDCl_3$ /TMS $\delta = 25.6$ ( $CH_3$ , $^1J_{P,C} = 73.0$ Hz) $52.1$ ( $OCH_3$ , $^2J_{P,C} = 5.8$ Hz) $131.6$ ( <i>ipso</i> -C, $^1J_{P,C} = 87.3$ Hz) $133.0$ ( <i>ortho</i> -C, $^2J_{P,C} = 11.7$ Hz) $128.3$ ( <i>meta</i> -C, $^3J_{P,C} = 12.9$ Hz) $132.2$ ( <i>para</i> -C, $^4J_{P,C} = 2.9$ Hz)	
<b><math>^{31}P</math> NMR</b>	:	162 MHz, $CDCl_3$ /TMS $\delta = 91.8$ ( $J_{Se,P} = 788.9$ Hz)	
<b><math>^{77}Se</math> NMR</b>	:	76 MHz, $CDCl_3$ /TMS $\delta = -279.0$ ( $J_{Se,P} = 789.3$ Hz)	
<b>IR</b>	:	ATR (neat) $\nu = 3053$ (w, Ph-H), 2938 (w, $CH_3$ ), 1435 (m, P-Ph), 1110 (s, C-O), 1023 (s, P-Ph), 884 (s), 735 (s, P=Se)	
<b>EIMS</b>	:	$m/z$ (rel. Int.) = 234 ( $M^+$ , 100), 219 (40), 204 (58), 154 (17), 139 (57), 123 (81), 109 (50), 91 (32), 77 (72)	

---

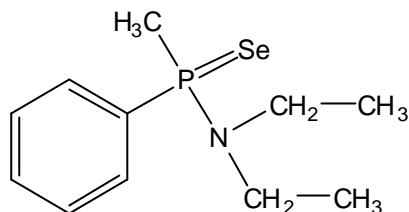
5.6.3 *O*-Isopropyl methylphenylphosphinoselenoate (**21**)


---

<b>Status</b>	:	Yellow liquid	$C_{10}H_{15}OPSe$
<b>Yield</b>	:	62% (not optimized)	
<b><math>^1H</math> NMR</b>	:	400 MHz, $CDCl_3/TMS$ $\delta = 2.17$ (s, $CH_3$ , $^2J_{P,H} = 13.3$ Hz) 1.36, 1.08 (d, $O-CH(CH_3)_2$ , $^3J_{P,H} = 6.3$ Hz) 4.74 (sep, $O-CH(CH_3)_2$ , $^2J_{P,H} = 13.3$ Hz) 7.90 (m, <i>ortho</i> -H, $^3J_{P,H} = 14.0$ Hz) 7.46 (m, <i>meta</i> -H), 7.54 (m, <i>para</i> -H)	
<b><math>^{13}C</math> NMR</b>	:	100 MHz, $CDCl_3/TMS$ $\delta = 27.3$ ( $CH_3$ , $^1J_{P,C} = 73.2$ Hz) 24.1, 23.5 ( $O-CH(CH_3)_2$ , $^3J_{P,C} = 4.0$ Hz) 71.5 ( $O-CH(CH_3)_2$ , $^2J_{P,C} = 5.2$ Hz) 135.5 ( <i>ipso</i> -C, $^1J_{P,C} = 88.9$ Hz) 130.9 ( <i>ortho</i> -C, $^2J_{P,C} = 11.7$ Hz) 128.2 ( <i>meta</i> -C, $^3J_{P,C} = 12.8$ Hz) 131.9 ( <i>para</i> -C, $^4J_{P,C} = 1-2$ Hz)	
<b><math>^{31}P</math> NMR</b>	:	162 MHz, $CDCl_3/TMS$ $\delta = 85.1$ ( $J_{Se,P} = 778.7$ Hz)	
<b><math>^{77}Se</math> NMR</b>	:	76 MHz, $CDCl_3/TMS$ $\delta = -270.0$ ( $J_{Se,P} = 779.1$ Hz)	
<b>IR</b>	:	ATR (neat) $\nu = 3054$ (w, Ph-H), 2975 (m, $CH_3$ ), 1436 (m, P-Ph), 1384 (m, $C(CH_3)_2$ ), 1372 (m, $C(CH_3)_2$ ), 1101 (s, P-Ph), 964 (m), 886 (s), 741 (s, P=Se)	
<b>EI MS</b>	:	$m/z$ (rel. Int.) = 262 ( $M^+$ , 79), 220 (90), 203 (63), 158 (47), 139 (100), 121 (34), 91 (47), 77 (79)	

---

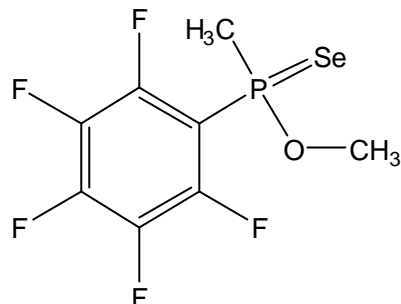


5.6.4 *N,N*-Diethyl methylphenylphosphinoselenoamidate (22)


---

<b>Status</b>	:	Yellow liquid	$C_{11}H_{18}NPSe$
<b>Yield</b>	:	52% (not optimized)	
<b><math>^1H</math> NMR</b>	:	400 MHz, $CDCl_3/TMS$ $\delta = 2.21$ (s, $CH_3$ , $^2J_{P,H} = 12.7$ Hz) 1.12 (t, $NCH_2-CH_3$ ) 3.01 (q, $NCH_2-CH_3$ , $^2J_{H,H} = 11.9$ Hz, $^3J_{H,H} = 7.1$ ) 7.97 (m, <i>ortho</i> -H, $^3J_{P,H} = 14.0$ Hz) 7.49 (m, <i>meta</i> -H), 7.52 (m, <i>para</i> -H)	
<b><math>^{13}C</math> NMR</b>	:	100 MHz, $CDCl_3/TMS$ $\delta = 24.4$ ( $CH_3$ , $^1J_{P,C} = 65.9$ Hz) 14.0 ( $NCH_2-CH_3$ , $^3J_{P,C} = 5.4$ Hz) 41.2 ( $NCH_2-CH_3$ , $^2J_{P,C} = 3.3$ Hz) 134.0 ( <i>ipso</i> -C, $^1J_{P,C} = 90.9$ Hz) 131.4 ( <i>ortho</i> -C, $^2J_{P,C} = 11.3$ Hz) 128.3 ( <i>meta</i> -C, $^3J_{P,C} = 12.7$ Hz) 131.6 ( <i>para</i> -C, $^4J_{P,C} = 2.9$ Hz)	
<b><math>^{31}P</math> NMR</b>	:	162 MHz, $CDCl_3/TMS$ $\delta = 60.9$ ( $J_{Se,P} = 728.3$ Hz)	
<b><math>^{77}Se</math> NMR</b>	:	76 MHz, $CDCl_3/TMS$ $-250.0$ ( $J_{Se,P} = 728.1$ Hz)	
<b>IR</b>	:	ATR (neat) $\nu = 3053$ (w, Ph-H), 2969 (m, $CH_3$ ), 1436 (m, P-Ph), 1378, (m), 1161 (s, P-Ph), 1101 (s, P-Ph), 1016 (s), 929 (s), 881 (s), 739 (s, P=Se)	
<b>EIMS</b>	:	$m/z$ (rel. Int.) = 275 ( $M^+$ , 46), 262 (46), 260 (25), 220 (68), 194 (86), 180 (21), 157 (16), 139 (70), 123 (84), 91 (24), 77 (28), 72 (100)	

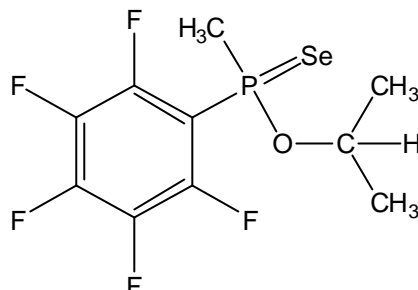
---

5.6.5 *O*-Methyl methylpentafluorophenylphosphinoselenoate (**23**)


---

<b>Status</b>	:	Yellow liquid	$C_8H_6OPSeF_5$
<b>Yield</b>	:	35% (not optimized)	
<b><math>^1H</math> NMR</b>	:	400 MHz, $CDCl_3$ /TMS $\delta = 2.42$ (s, $CH_3$ , $^2J_{P,H} = 14.4$ Hz, $^5J_{F,H} = 2.0$ Hz) $3.88$ (s, $OCH_3$ , $^3J_{P,H} = 15.9$ Hz, $^6J_{F,H} = 0.8$ Hz)	
<b><math>^{13}C</math> NMR</b>	:	100 MHz, $CDCl_3$ /TMS $\delta = 27.6$ ( $CH_3$ , $^1J_{P,C} = 77.4$ Hz, $^4J_{F,C} = 3.6$ Hz) $53.9$ ( $OCH_3$ , $^2J_{P,C} = 5.9$ Hz, $^5J_{F,C} = 5.9$ Hz) $112.5$ (dm, <i>ipso</i> -C), $145.8$ (dm, <i>ortho</i> -C) $137.9$ (dm, <i>meta</i> -C), $143.3$ (dm, <i>para</i> -C)	
<b><math>^{31}P</math> NMR</b>	:	162 MHz, $CDCl_3$ /TMS $\delta = 74.1$ ( $J_{Se,P} = 824.0$ Hz)	
<b><math>^{77}Se</math> NMR</b>	:	76 MHz, $CDCl_3$ /TMS $\delta = -145.0$ ( $J_{Se,P} = 821.0$ Hz)	
<b>IR</b>	:	ATR (neat) $\nu = 3010$ (w, Ph-F), $2914$ (w, $CH_3$ ), $1644$ (m), $1519$ (m), $1473$ (s, P-Ph), $1403$ (m, C-F), $1384$ (m, C-F), $1290$ (m, C-O), $1089$ (s, P-Ph), $1036$ (s), $976$ (s), $895$ (s, P- $CH_3$ ), $740$ (s, P=Se)	
<b>EIMS</b>	:	$m/z$ (rel. Int.) = $324$ ( $M^+$ , 100), $293$ (50), $244$ (17), $229$ (47), $213$ (88), $199$ (43), $81$ (35), $77$ (80)	

---

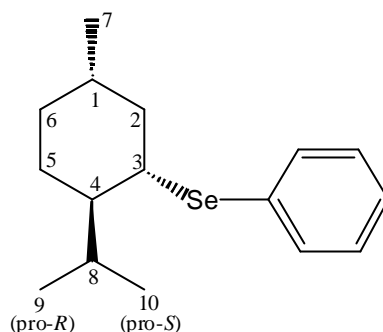
5.6.6 *O*-Isopropyl methylpentafluorophenylphosphinoselenoate (**24**)


---

<b>Status</b>	:	Yellow liquid	$C_{10}H_{10}OPSeF_5$
<b>Yield</b>	:	16% (not optimized)	
<b><math>^1H</math> NMR</b>	:	400 MHz, $CDCl_3/TMS$ $\delta = 2.42$ (s, $CH_3$ , $^2J_{P,H} = 14.4$ Hz, $^5J_{F,H} = 2.6$ Hz) 1.37, 1.40 (d, $O-CH(CH_3)_2$ , $^4J_{P,H} = 6.3$ Hz) 5.12 (sep, $O-CH(CH_3)_2$ , $^3J_{P,H} = 13.3$ Hz)	
<b><math>^{13}C</math> NMR</b>	:	100 MHz, $CDCl_3/TMS$ $\delta = 30.1$ ( $CH_3$ , $^1J_{P,C} = 73.6$ Hz, $^4J_{F,C} = 4.2$ Hz) 24.6, 23.1 ( $O-CH(CH_3)_2$ , $^3J_{P,C} = 2.7$ , 6.5, $^6J_{F,C} = 1.1$ Hz) 73.5 ( $O-CH(CH_3)_2$ , $^2J_{P,C} = 5.6$ Hz) 112.8 (dm, <i>ipso</i> -C), 145.9 (dm, <i>ortho</i> -C) 137.5 (dm, <i>meta</i> -C), 143.1 (dm, <i>para</i> -C)	
<b><math>^{31}P</math> NMR</b>	:	162 MHz, $CDCl_3/TMS$ $\delta = 68.6$ ( $J_{Se,P} = 808.0$ Hz)	
<b><math>^{77}Se</math> NMR</b>	:	76 MHz, $CDCl_3/TMS$ $\delta = -136.0$ ( $J_{Se,P} = 808.0$ Hz)	
<b>IR</b>	:	ATR (neat) $\nu = 2980$ (w, $CH_3$ ), 1644 (m), 1519 (s), 1474 (s, P-Ph), 1386 (m, $C(CH_3)_2$ ), 1375 (m, $C(CH_3)_2$ ), 1294 (m), 1093 (s, P-Ph), 980 (s, P-O), 895 (s), 730 (s, P=Se)	
<b>EI MS</b>	:	$m/z$ (rel. Int.) = 352 ( $M^+$ , 83), 310 (100), 292 (72), 229 (80), 215 (77), 163 (24), 143 (20), 81 (17)	

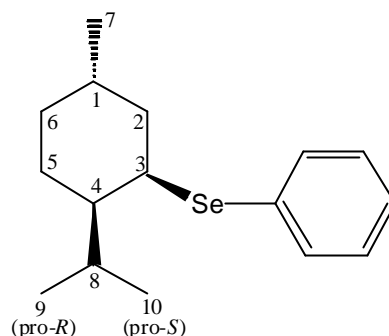
---

## 5.6.7 3-Phenylselenenylmenthan (25)



<b>Status</b>	:	Yellow oil	$C_{16}H_{24}Se$
<b>Reaction condition</b>	:	0.86 g (2.7 mmol) $(PhSe)_2$ 1.3 g (5.5 mmol) 1-methansulfonylneomenthan yield 55 %	
$[a]_D^{20}$	:	128.4	
$^1H$ NMR	:	400 MHz, $CDCl_3/TMS$ $\delta = 1.29$ (m, H-1ax), 2.07 (dm, H-2eq), 1.25 (m, H-2ax) 3.07 (td, H-3ax, $^2J_{H,Se} = 37.4$ Hz), 1.29 (tm, H-4eq) 1.70 (dm, H-5eq), 1.06 (td, H-5ax) 1.70 (dm, H-6eq), 0.87 (qm, H-6ax) 0.81 (d, $CH_3$ -7), 2.42 (septd, H-8) 0.77 (d, $CH_3$ -9), 0.92 (d, $CH_3$ -10) 7.55 (dm, <i>ortho</i> -H eq), 7.27 (tm, <i>meta</i> -H eq) 7.27 (tm, <i>para</i> -H eq)	
$^{13}C$ NMR	:	100 MHz, $CDCl_3/TMS$ $\delta = 34.3$ (C-1), 44.9 (C-2), 48.3 (C-3, $^1J_{C,Se} = 62.9$ Hz), 47.7 (C-4, $^2J_{C,Se} = 8.9$ Hz), 25.0 (C-5), 34.7 (C-6), 22.1 (C-7), 29.1 (C-8), 15.1 (C-9), 21.4 (C-10), 129.0 ( <i>ipso</i> -C eq), 135.5 ( <i>ortho</i> -C eq) 128.8 ( <i>meta</i> -C eq), 127.3 ( <i>para</i> -C eq)	
$^{77}Se$ NMR	:	76 MHz, $CDCl_3/TMS$ $\delta = 377.4$ ( $^1J_{Se,C} = 63.0$ Hz)	
<b>IR</b>	:	ATR (neat) $\nu = 3055$ (w, Ph-H), 2919 (m, $CH_3$ ), 2851 (w), 1577 (m), 1474 (m), 1435 (m), 1251 (m), 1125 (m), 1022 (m), 825 (m), 732 (s), 689 (s, C-Se)	
<b>EI MS</b>	:	$m/z$ (rel. Int.) = 296 ( $M^+$ , 51), 294 (27), 190 (72), 176 (43), 158 (34), 142 (72), 139 (73), 128 (41), 105 (34), 97 (49), 83 (100)	

## 5.6.8 3-Phenylselenenylneomenthan (26)

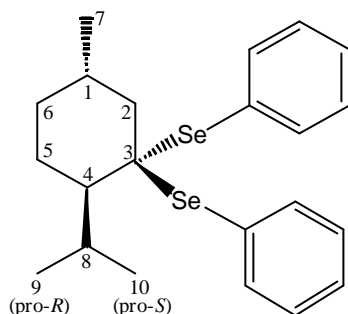



---

<b>Status</b>	:	Yellow oil	$C_{16}H_{24}Se$
<b>Reaction condition</b>	:	1.3 g (4.2 mmol) $(PhSe)_2$ 2.0 g (8.5 mmol) 1-methansulfonylmenthan yield 50 %	
<b><math>[\alpha]_D^{20}</math></b>	:	93.0	
<b><math>^1H</math> NMR</b>	:	400 MHz, $CDCl_3/TMS$ $\delta = 1.99$ (m, H-1eq), 1.99 (dm, H-2eq), 1.33 (ddd, H-2ax) 3.71 (m, H-3eq), 1.04 (ddt, H-4ax) 1.82 (dm, H-5eq), 1.15 (qm, H-5ax) 1.77 (dm, H-6eq), 0.91 (m, H-6ax) 0.87 (d, $CH_3$ -7), 1.69 (m, H-8) 0.89 (d, $CH_3$ -9), 0.93 (d, $CH_3$ -10) 7.55 (dm, <i>ortho</i> -H ax), 7.24 (tm, <i>meta</i> -H ax) 7.24 (tm, <i>para</i> -H ax)	
<b><math>^{13}C</math> NMR</b>	:	100 MHz, $CDCl_3/TMS$ $\delta = 27.7$ (C-1), 41.8 (C-2), 50.4 (C-3, $^1J_{C,Se} = 61.7$ Hz), 49.5 (C-4, $^2J_{C,Se} = 10.3$ Hz), 27.2 (C-5), 35.2 (C-6), 22.1 (C-7), 31.3 (C-8), 20.6 (C-9), 21.0 (C-10) 130.8 ( <i>ipso</i> -C ax), 134.1 ( <i>ortho</i> -C ax) 128.8 ( <i>meta</i> -C ax), 126.9 ( <i>para</i> -C ax)	
<b><math>^{77}Se</math> NMR</b>	:	76 MHz, $CDCl_3/TMS$ $\delta = 288.0$ ( $^1J_{Se,C} = 63.0$ Hz),	
<b>IR</b>	:	ATR (neat) $\nu = 3072$ (w, Ph-H), 2944 (m, $CH_3$ ), 2920 (w), 1579 (m), 1475 (m), 1436 (m), 1182 (m), 1022 (m), 858 (m), 733 (s), 691 (s, C-Se)	
<b>EIMS</b>	:	$m/z$ (rel. Int.) = 296 ( $M^+$ , 24), 190 (82), 176 (41), 142 (80), 139 (31), 128 (44), 105 (39), 97 (22), 83 (100)	

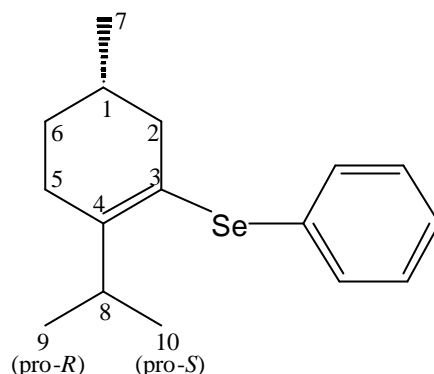
---

## 5.6.9 3,3- Bis-phenylselenenylmenthan (27)



<b>Status</b>	:	Yellow oil	$C_{22}H_{28}Se_2$
<b>Reaction condition</b>	:	1.0 g (3.2 mmol) (PhSe) <sub>2</sub> 0.54 g (3.5 mmol) menthone yield 20 %	
<b>[α]<sub>D</sub><sup>20</sup></b>	:	50.0	
<b><sup>1</sup>H NMR</b>	:	400 MHz, CDCl <sub>3</sub> /TMS $\delta$ = 2.01 (m, H-1ax), 1.79 (dt, H-2eq), 1.23 (dd, H-2ax) 1.38 (dd, H-4eq), 1.72 (dm, H-5eq), 1.49 (dddd, H-5ax) 1.73 (dm, H-6eq), 0.69 (qd, H-6ax), 0.61 (d, 3H, H-7) 3.02 (sept, H-8), 0.97 (d, CH <sub>3</sub> -9), 1.00 (d, CH <sub>3</sub> -10) 7.57 (dm, <i>ortho</i> -H eq), 7.82 (dm, <i>ortho</i> -H ax) 7.26 (tm, <i>meta</i> -H eq), 7.34 (tm, <i>meta</i> -H ax) 7.25 (tm, <i>para</i> -H eq), 7.33 (tm, <i>para</i> -H ax)	
<b><sup>13</sup>C NMR</b>	:	100 MHz, CDCl <sub>3</sub> /TMS $\delta$ = 29.9 (C-1), 48.0 (C-2), 66.8 (C-3, <sup>1</sup> J <sub>C,Se</sub> = 87.6 Hz) 51.7 (C-4), 23.1 (C-5), 34.8 (C-6) 21.1 (C-7), 28.9 (C-8), 24.2 (C-9) 19.0 (C-10) 129.5 ( <i>ipso</i> -C eq), 126.6 ( <i>ipso</i> -C ax) 138.1 ( <i>ortho</i> -C eq), 138.3 ( <i>ortho</i> -C ax) 128.5 ( <i>meta</i> -C eq), 128.5 ( <i>meta</i> -C ax) 128.6 ( <i>para</i> -C eq), 128.9 ( <i>para</i> -C ax)	
<b><sup>77</sup>Se NMR</b>	:	76 MHz, CDCl <sub>3</sub> /TMS $\delta$ = 495.0 (Se-eq), 400.0 (Se-ax)	
<b>IR</b>	:	ATR (neat) $\nu$ = 3055 (w, Ph-H), 2955 (m, CH <sub>3</sub> ), 2923 (w), 1576 (m), 1475 (m), 1436 (m), 1130 (m), 1021 (m), 733 (s), 688 (s, C-Se)	
<b>EIMS</b>	:	$m/z$ (rel. Int.) = 452 (M <sup>+</sup> , 3), 314 (97), 296 (64), 294 (98), 234 (42), 199 (87), 176 (58), 157 (100), 142 (85), 137 (85), 128 (58), 105 (68), 95 (85), 81 (85)	

## 5.6.10 3-Phenylselenenyl-3-menthene (28)

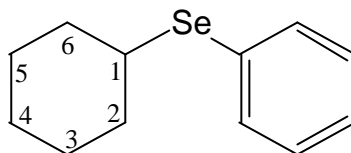



---

<b>Status</b>	:	Yellow oil	$C_{16}H_{22}Se$
<b>Reaction condition</b>	:	1.0 g (3.2 mmol) $(PhSe)_2$ 0.54 g (3.5 mmol) menthone yield 15 % (by product)	
<b><math>^1H</math>-NMR</b>	:	400 MHz, $CDCl_3/TMS$ $\delta = 1.68$ (m, H-1 ax) 2.34 (dm, H-2 eq), 1.94 (ddm, H-2 ax) 2.23 (dm, H-5 eq), 2.14 (tm, H-5 ax) 1.77 (dm, H-6 eq), 1.22 (m, H-6 ax) 0.88 (d, $CH_3$ -7), 3.40 (sept, H-8) 1.00 (d, $CH_3$ -9), 0.98 (d, $CH_3$ -10) 7.37 (dm, <i>ortho</i> -H), 7.24 (tm, <i>meta</i> -H) 7.21 (tm, <i>para</i> -H)	
<b><math>^{13}C</math>-NMR</b>	:	100 MHz, $CDCl_3/TMS$ $\delta = 30.6$ (C-1), 42.6 (C-2), 120.7 (C-3) 148.3 (C-4), 24.8 (C-5), 30.9 (C-6) 21.2 (C-7), 34.5 (C-8), 20.5 (C-9), 21.1 (C-10) 131.6 ( <i>ipso</i> -C, $^1J_{C,Se} = 87.6$ Hz), 131.2 ( <i>ortho</i> -C) 128.9 ( <i>meta</i> -C), 126.0 ( <i>para</i> -C)	
<b><math>^{77}Se</math> NMR</b>	:	76 MHz, $CDCl_3/TMS$ $\delta = 364.0$	
<b>IR</b>	:	ATR (neat) $\nu = 3055$ (w, Ph-H), 2919 (m, $CH_3$ ), 2851 (w), 1577 (m), 1435 (m), 1370 (m), 1251 (m), 1022 (m), 732 (s), 687 (s, C-Se)	
<b>EIMS</b>	:	$m/z$ (rel. Int.) = 294 ( $M^+$ , 100), 279 (12), 251 (8), 198 (15), 157 (11), 137 (43), 121 (77), 107 (21), 95 (58), 81 (66), 77 (33)	

---

## 5.6.11 Phenylselenenylcyclohexane (29)

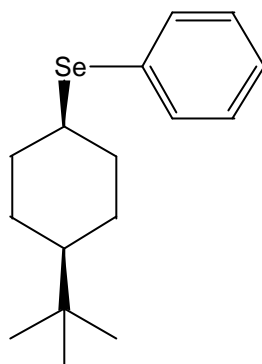



---

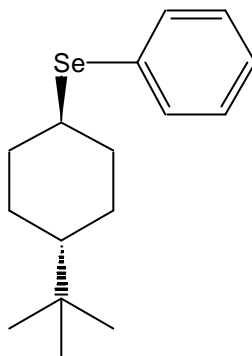
<b>Status</b>	:	Yellow oil	$C_{12}H_{16}Se$
<b>Reaction condition</b>	:	0.85 g (2.7 mmol) $(PhSe)_2$ 1.0 g (5.6 mmol) 1-methansulfonylcyclohexane yield 60 %	
<b><math>^1H</math> NMR</b>	:	400 MHz, $CDCl_3/TMS$ $\delta = 3.25$ (tt, H-1ax) 2.04 (dm, H-2/H-6eq), 1.51 (dq, H-2/H-6ax) 1.74 (dm, H-3/H-5eq), 1.33 (m, H-3/H-5ax) 1.60 (m, H-4eq), 1.25 (tt, H-4ax) 7.55 ( <i>ortho</i> -Heq) 7.27 ( <i>meta</i> -Heq) 7.25 ( <i>para</i> -Heq)	
<b><math>^{13}C</math> NMR</b>	:	100 MHz, $CDCl_3/TMS$ $\delta = 43.2$ (C-1, $^1J_{C,Se} = 60.8$ Hz), 34.2 (C-2/6, $^2J_{C,Se} = 9.5$ Hz), 26.9 (C-3/5), 25.7 (C-4) 129.1 ( <i>ipso</i> -C), 134.7 ( <i>ortho</i> -C, $^2J_{C,Se} = 9.5$ Hz) 128.8 ( <i>meta</i> -C), 127.2 ( <i>para</i> -C)	
<b><math>^{77}Se</math> NMR</b>	:	76 MHz, $CDCl_3/TMS$ $\delta = 400$ (brd. signal at room temp.) 400 (at 213 K)	
<b>IR</b>	:	ATR (neat) $\nu = 3070$ (w, Ph-H), 2925 (s), 2850 (m), 1578 (m), 1476 (m), 1436 (m), 1256 (m), 1181 (m), 1065 (m), 1022 (m), 992 (m), 734 (s), 689 (s, C-Se)	
<b>EIMS</b>	:	$m/z$ (rel. Int.) = 240 (38, $M^+$ ), 206 (21), 171 (14), 158 (100), 91 (12), 83 (24), 77 (18)	

---



5.6.12 *cis*-1-Phenylselenenyl-4-*tert*-butylcyclohexane (30)

<b>Status</b>	:	Yellow oil	$C_{16}H_{24}Se$
<b>Reaction condition</b>	:	0.47 g (1.5 mmol) $(PhSe)_2$ 0.70 g (3.0 mmol) <i>cis</i> -1-methansulfonyl-4- <i>tert</i> -butylcyclohexane yield 45 %	
<b><math>^1H</math>-NMR</b>	:	400 MHz, $CDCl_3/TMS$ $\delta = 3.76$ (br.s, H-1eq), 2.10 (br.d, H-2eq), 1.70 (tt, H-2ax) 1.65 (br.d, H-3eq), 1.50 (dq, H-3ax) 1.05 (tt, H-4eq), 1.65 (br.d, H-5eq) 1.50 (dq, H-5ax), 2.10 (br.d, H-6eq) 1.90 (dt, H, H-6ax), 0.87 (s, $^tBu-CH_3$ ) 7.53 ( <i>ortho</i> -Hax), 7.25 ( <i>meta</i> -Hax) 7.24 ( <i>para</i> -Hax)	
<b><math>^{13}C</math>-NMR</b>	:	100 MHz, $CDCl_3/TMS$ $\delta = 44.6$ (C-1, $^1J_{C,Se} = 58.1$ Hz), 32.6 (C-2), 23.1 (C-3) 48.3 (C-4), 23.1 (C-5), 32.6 (C-6), 32.6 ( $^tBu-C$ ), 27.5 ( $^tBu-CH_3$ ), 130.9 ( <i>ipso</i> -C ax, $^2J_{C,Se} = 9.0$ Hz) 133.8 ( <i>ortho</i> -C ax, $^2J_{C,Se} = 9.0$ Hz) 128.9 ( <i>meta</i> -C ax), 126.9 ( <i>para</i> -C ax)	
<b><math>^{77}Se</math> NMR</b>	:	76 MHz, $CDCl_3/TMS$ $\delta = 338.0$ (at room temp.) 325.0 (at 213 K)	
<b>IR</b>	:	ATR (neat) $\nu = 3071$ (w, Ph-H), 2959 (m, $CH_3$ ), 2937 (m), 1577 (m), 1474 (m), 1436 (m), 1364 (m), 1252 (m), 1068 (m), 1019 (m), 733 (s), 690 (s, C-Se)	
<b>EIMS</b>	:	$m/z$ (rel. Int.) = 296 ( $M^+$ , 100), 281 (25), 160 (47), 158 (99), 139 (41), 123 (45), 97 (47), 81 (81), 78 (38)	

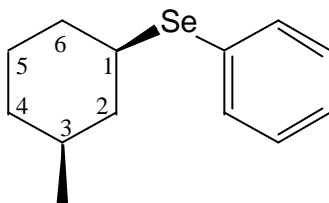
5.6.13 *trans*-1-Phenylselenenyl-4-*tert*-butylcyclohexane (31)


---

<b>Status</b>	:	Yellow oil	$C_{16}H_{24}Se$
<b>Reaction condition</b>	:	0.38 g (1.2 mmol) $(PhSe)_2$ 0.56 g (2.4 mmol) <i>trans</i> -1-methansulfonyl-4- <i>tert</i> -butylcyclohexane yield 25 %	
<b><math>^1H</math> NMR</b>	:	400 MHz, $CDCl_3/TMS$ $\delta = 3.09$ (tt, H-1ax), 2.13 (dm, H-2eq), 1.45 (qm, H-2ax) 1.79 (dm, H-3eq), 1.02 (m, H-3ax), 1.01 (m, H-4ax) 1.79 (dm, H-5eq), 1.02 (m, H-5ax), 2.13 (dm, H-6eq) 1.45 (qm, H-6ax), 0.81 (s, $^tBu-CH_3$ ) 7.54 ( <i>ortho</i> -H eq), 7.25 ( <i>meta</i> -H eq) 7.24 ( <i>para</i> -H eq)	
<b><math>^{13}C</math> NMR</b>	:	100 MHz, $CDCl_3/TMS$ $\delta = 42.9$ (C-1, $^1J_{C,Se} = 61.5$ Hz), 34.9 (C-2/6, $^2J_{C,Se} = 9.9$ Hz), 28.6 (C-3/5), 47.3 (C-4) 32.5 ( $^tBu-C$ ), 27.5 ( $^tBu-CH_3$ ) 129.1 ( <i>ipso</i> -C eq), 134.8 ( <i>ortho</i> -C eq, $^2J_{C,Se} = 9.4$ Hz) 128.8 ( <i>meta</i> -C eq), 127.2 ( <i>para</i> -C eq)	
<b><math>^{77}Se</math> NMR</b>	:	76 MHz, $CDCl_3/TMS$ $\delta = 406.0$ (at room temp.) 392.0 (at 213 K)	
<b>IR</b>	:	ATR (neat) $\nu = 3074$ (w, Ph-H), 2964 (m, $CH_3$ ), 2937 (m), 1578 (m), 1476 (m), 1364 (m), 1158 (m), 1022 (m), 1001 (m), 736 (s), 691 (s, C-Se)	
<b>EIMS</b>	:	$m/z$ (rel. Int.) = 296 ( $M^+$ , 82), 281 (9), 170 (23), 158 (85), 139 (32), 123 (49), 97 (50), 83 (100), 77 (41)	

---

## 5.6.14 1-Phenylselenenyl-3-methylcyclohexane (32)

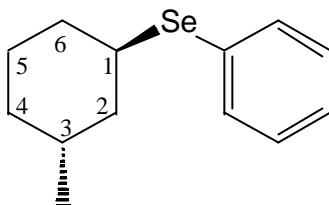



---

<b>Status</b>	:	Yellow oil	$C_{13}H_{18}Se$
<b>Reaction condition</b>	:	0.85 g (2.7 mmol) $(PhSe)_2$ 1.0 g (5.2 mmol) <i>cis</i> -1-methansulfonyl-3-methylcyclohexane yield 55 %	
<b><math>^1H</math> NMR</b>	:	400 MHz, $CDCl_3/TMS$ $\delta = 3.17$ (tt, H-1ax), 2.05 (dm, H-2eq), 1.14 (tm, H-2ax) 0.86 (m, H-3eq), 0.87 (d, $CH_3$ ) 2.03 (dm, H-4eq), 1.34 (m, H-4ax) 1.76 (tm, H-5eq), 1.29 (m, H-5ax) 1.88 (m, H-6eq), 1.67 (m, H-6ax) 7.55 ( <i>ortho</i> -Heq), 7.25 ( <i>meta</i> -Heq) 7.27 ( <i>para</i> -Heq)	
<b><math>^{13}C</math> NMR</b>	:	100 MHz, $CDCl_3/TMS$ $\delta = 42.5$ (C-1), 43.0 (C-2, $^2J_{C,Se} = 9.0$ Hz), 34.1 (C-3) 34.0 (C-4), 27.3 (C-5), 32.2 (C-6), 22.5 ( $CH_3$ ) 129.1 ( <i>ipso</i> -C), 134.8 ( <i>ortho</i> -C, $^2J_{C,Se} = 9.2$ Hz) 128.8 ( <i>meta</i> -C), 127.2 ( <i>para</i> -C)	
<b><math>^{77}Se</math> NMR</b>	:	76 MHz, $CDCl_3/TMS$ $\delta = 411.0$ (at room temp.) 399.0 (at 213 K)	
<b>IR</b>	:	ATR (neat) $\nu = 3070$ (w, Ph-H), 2922 (s), 2842 (m), 1579 (m), 1476 (m), 1436 (m), 1255 (m), 1182 (m), 1064 (m), 1022 (m), 853 (m), 734 (s), 690 (s, C-Se)	
<b>EIMS</b>	:	$m/z$ (rel. Int.) = 254 (81, $M^+$ ), 160 (46), 158 (99), 97 (100), 81 (29), 78 (37)	

---

## 5.6.15 1-Phenylselenenyl-3-methylcyclohexane (33)

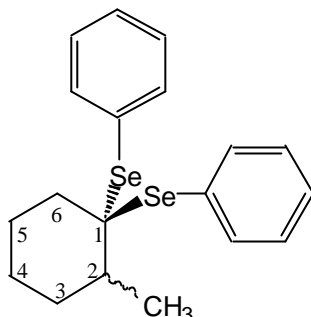



---

<b>Status</b>	:	Yellow oil	$C_{13}H_{18}Se$
<b>Reaction condition</b>	:	0.85 g (2.7 mmol) $(PhSe)_2$ 1.0 g (5.2 mmol) <i>trans</i> 1-methansulfonyl-3-methylcyclohexane yield 55 %	
<b><math>^1H</math> NMR</b>	:	400 MHz, $CDCl_3/TMS$ $\delta = 3.70$ (p, H-1 eq) 1.93 (dm, H-2 eq), 1.49 (dm, H-2 ax) 1.89 (tt, H-3 ax), 0.90 (d, $CH_3$ ) 1.67 (m, H-4 eq), 1.01 (dm, H-4 ax) 1.71 (m, H-5 eq), 1.56 (m, H-5 ax) 1.84 (m, H-6 eq), 1.75 (m, H-6 ax) 7.53 ( <i>ortho</i> -H ax) 7.25 ( <i>meta</i> -H ax) 7.27 ( <i>para</i> -H ax)	
<b><math>^{13}C</math> NMR</b>	:	100 MHz, $CDCl_3/TMS$ $\delta = 43.5$ (C-1, $^1J_{C,Se} = 59.8$ Hz), 40.5 (C-2), 28.5 (C-3) 34.3 (C-4), 22.2 (C-5), 32.2 (C-6), 21.6 ( $CH_3$ ) 130.6 ( <i>ipso</i> -C), 133.9 ( <i>ortho</i> -C, $^2J_{C,Se} = 9.5$ Hz) 128.9 ( <i>meta</i> -C), 127.0 ( <i>para</i> -C)	
<b><math>^{77}Se</math> NMR</b>	:	76 MHz, $CDCl_3/TMS$ $\delta = 360.0$ (at room temp.) 333 (at 213 K)	
<b>IR</b>	:	ATR (neat) $\nu = 3070$ (w, Ph-H), 2922 (s), 2842 (m), 1579 (m), 1476 (m), 1436 (m), 1255 (m), 1182 (m), 1064 (m), 1022 (m), 853 (m), 734 (s), 690 (s, C-Se)	
<b>EIMS</b>	:	$m/z$ (rel. Int.) = 254 (81, $M^+$ ), 160 (46), 158 (99), 97 (100), 81 (29), 78 (37)	

---

## 5.6.16 1,1-Bis-phenylselenenyl-2-methylcyclohexane (34)

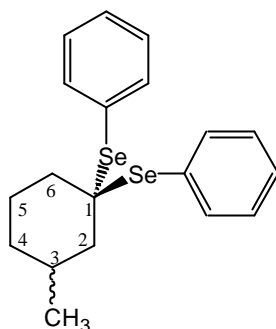



---

<b>Status</b>	:	Yellow oil	$C_{19}H_{22}Se_2$
<b>Reaction condition</b>	:	1.0 g (3.2 mmol) $(PhSe)_2$ 0.39 g (3.5 mmol) 2-methylcyclohexane yield 35 %	
<b><math>^1H</math> NMR</b>	:	400 MHz, $CDCl_3/TMS$ $\delta = 1.70$ (tt, H-2ax) 1.52 (dm, H-3eq), 1.75 (ddm, H-3ax) 1.72 (m, H-4eq), 1.21 (dm, H-4ax) 1.65 (m, H-5eq), 1.02 (ttm, H-5ax) 1.87 (dm, H-6eq), 1.57 (dm, H-6ax), 1.34 (d, $CH_3$ ) 7.86 (1H, <i>ortho</i> -Hax), 7.60 (1H, <i>ortho</i> -Heq) 7.37 (1H, <i>meta</i> -Hax), 7.27 (1H, <i>meta</i> -Heq) 7.40 (1H, <i>para</i> -Hax), 7.33 (1H, <i>para</i> -Heq)	
<b><math>^{13}C</math> NMR</b>	:	100 MHz, $CDCl_3/TMS$ $\delta = 65.6$ (C-1, $^1J_{C,Se} = 66.5$ Hz), 41.4 (C-2, $^2J_{C,Se} = 14.9$ Hz) 31.3 (C-3), 23.8 (C-4), 25.9 (C-5), 38.7 (C-6), 20.2 ( $CH_3$ ), 126.2 ( <i>ipso</i> -C ax), 129.4 ( <i>ipso</i> -C eq) 138.3 ( <i>ortho</i> -C ax, $^2J_{C,Se} = 9.9$ Hz), 138.0 ( <i>ortho</i> -C eq, $^2J_{C,Se} = 8.2$ Hz) 128.6 ( <i>meta</i> -C ax), 128.6 ( <i>meta</i> -C eq) 128.8 ( <i>para</i> -C ax), 128.7 ( <i>para</i> -C eq)	
<b><math>^{77}Se</math> NMR</b>	:	76 MHz, $CDCl_3/TMS$ $\delta = 500.0$ (Se eq), 379.0 (Se ax) (at room temp.) 486.0 (Se eq), 366.0 (Se ax) (at 243 K)	
<b>IR</b>	:	ATR (neat) $\nu = 3056$ (w, Ph-H), 2919 (m), 2851 (w), 1577 (w), 1474 (m), 1435 (s), 1065 (m), 1022 (m), 731 (s), 687 (s, C-Se)	
<b>EIMS</b>	:	$m/z$ (rel. Int.) = 410 (9, $M^+$ ), 314 (4), 253 (78), 239 (15), 158 (24), 95 (100), 81 (24), 78 (26)	

---

## 5.6.17 1,1-Bis-phenylselenenyl-3-methylcyclohexane (35)

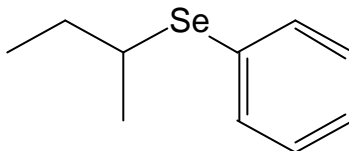



---

<b>Status</b>	:	Yellow oil	$C_{19}H_{22}Se_2$
<b>Reaction condition</b>	:	1.0 g (3.2 mmol) (PhSe) <sub>2</sub> 0.39 g (3.5 mmol) 3-methylcyclohexane yield 46 %	
<b><sup>1</sup>H NMR</b>	:	400 MHz, CDCl <sub>3</sub> /TMS $\delta$ = 2.06 (m, H-2eq), 1.40 (dd, H-2ax) 1.98 (m, H-3ax), 1.69 (m, H-4eq), 0.65 (dq, H-4ax) 1.46 (dm, H-5eq), 1.90 (ttt, H-5ax) 2.02 (dm, H-6eq), 1.65 (m, H-6ax), 0.78 (d, CH <sub>3</sub> ) 7.80 ( <i>ortho</i> -Hax), 7.61 ( <i>ortho</i> -Heq) 7.33 ( <i>meta</i> -Hax), 7.28 ( <i>meta</i> -Heq) 7.40 ( <i>para</i> -Hax), 7.36 ( <i>para</i> -Heq)	
<b><sup>13</sup>C NMR</b>	:	100 MHz, CDCl <sub>3</sub> /TMS $\delta$ = 56.8 (C-1), 47.1 (C-2), 29.7 (C-3), 33.7 (C-4) 23.7 (C-5), 37.9 (C-6, <sup>2</sup> J <sub>C,Se</sub> = 11.5 Hz), 21.9 (CH <sub>3</sub> ) 127.5 ( <i>ipso</i> -C ax), 129.0 ( <i>ipso</i> -C eq) 137.8 ( <i>ortho</i> -C ax, <sup>2</sup> J <sub>C,Se</sub> = 9.4 Hz) 138.2 ( <i>ortho</i> -C eq, <sup>2</sup> J <sub>C,Se</sub> = 8.4 Hz) 128.7 ( <i>meta</i> -C ax), 128.6 ( <i>meta</i> -C eq) 128.9 ( <i>para</i> -C.ax), 128.8 ( <i>para</i> -C eq)	
<b><sup>77</sup>Se NMR</b>	:	76 MHz, CDCl <sub>3</sub> /TMS $\delta$ = 568.0 (Se eq), 431.0 (Se ax) (at room temp.) 558.0 (Se eq), 422.0 (Se ax) (at 243 K)	
<b>IR</b>	:	ATR (neat) $\nu$ = 3050 (w, Ph-H), 2924 (w), 2912 (m), 1575 (w), 1474 (m), 1434 (m), 1252 (m), 1130 (m), 1021 (m), 737 (s), 689 (s, C-Se)	
<b>EIMS</b>	:	$m/z$ (rel. Int.) = 410 (7, M <sup>+</sup> ), 323 (9), 253 (83), 191 (8), 157 (24), 121 (10), 95 (100), 77 (23)	

---

## 5.6.18 2-Phenylselenenylbutane (36)

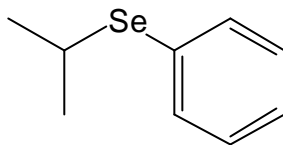



---

<b>Status</b>	:	Yellow oil	$C_{10}H_{14}Se$
<b>Reaction condition</b>	:	1.7 g (5.5 mmol) $(PhSe)_2$ 2.0 g (10.9 mmol) 2-iodobutane yield 95 %	
<b><math>^1H</math> NMR</b>	:	400 MHz, $CDCl_3/TMS$ $\delta = 3.24$ (tq, H-2), 1.70 (m, H-3), 1.61 (m, H-3) 1.40 (d, $J = 6.9$ Hz), 1.00 (t, $J = 7.4$ Hz) 7.55 (dm, H-ortho), 7.26 (m, H-meta/para)	
<b><math>^{13}C</math> NMR</b>	:	100 MHz, $CDCl_3/TMS$ $\delta = 21.6$ (C-1), 41.5 (C-2), 30.5 (C-3), 12.3 (C-4) 129.5 ( <i>ipso</i> -C), 134.9 ( <i>ortho</i> -C) 128.8 ( <i>meta</i> -C), 127.3 ( <i>para</i> -C)	
<b><math>^{77}Se</math> NMR</b>	:	76.3 MHz, $CDCl_3/TMS$ $\delta = 398.0$ (at room temperature) 385.0 (at 213 K)	
<b>IR</b>	:	ATR (neat) $\nu = 3071$ (w, Ph-H), 2963 (s), 2873 (m), 1579 (m), 1476 (s), 1437 (m), 1377 (m), 1201 (m), 1022 (m), 738 (s), 692 (s, C-Se)	
<b>EIMS</b>	:	$m/z$ (rel. Int.) = 214 (70, $M^+$ ), 158 (100), 157 (54), 78 (64), 77 (51)	

---

## 5.6.19 2-Phenylselenenylpropane (37)



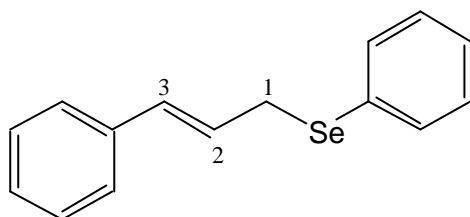

---

<b>Status</b>	:	Yellow oil	$C_9H_{12}Se$
<b>Reaction condition</b>	:	0.78 g (2.5 mmol) $(PhSe)_2$ 0.62 g (5.1 mmol) 2-bromopropane yield 90 %	
<b><math>^1H</math> NMR</b>	:	400 MHz, $CDCl_3/TMS$ $\delta = 3.45$ (sept, H-2), 1.43 (d, $J = 6.8$ Hz) 7.55 (dm, H-ortho), 7.28-7.25 (m, H-meta/para)	
<b><math>^{13}C</math> NMR</b>	:	100 MHz, $CDCl_3/TMS$ $\delta = 24.2$ (C-1, $^1J_{C,Se} = 13.0$ Hz), 33.8 (C-2) 129.6 (ipso-C), 134.8 (ortho-C, $^2J_{C,Se} = 9.2$ Hz) 128.8 (meta-C), 127.3 (para-C)	
<b><math>^{77}Se</math> NMR</b>	:	76.3 MHz, $CDCl_3/TMS$ $\delta = 428.0$	
<b>IR</b>	:	ATR (neat) $\nu = 2988$ (w, Ph-H), 2951 (m), 2895 (m), 1507 (m), 1262 (s), 1216 (m), 1154 (m), 10696 (s), 1023 (s), 800 (s), 738 (m), 691 (s, C-Se)	
<b>EIMS</b>	:	$m/z$ (rel. Int.) = 200 (91, $M^+$ ), 158 (100), 85 (23), 78 (86), 77 (45)	

---



## 5.6.20 3-Phenylselenenyl-1-phenyl-1-propene (38)

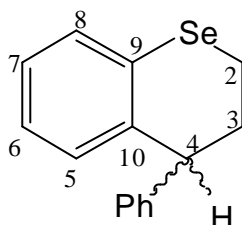



---

<b>Status</b>	:	Yellow oil	$C_{15}H_{14}Se$
<b>Reaction condition</b>	:	2.5 g (8.0 mmol) $(PhSe)_2$ 2.5 g (16.0 mmol) cinamoyl chloride yield 65 %	
<b><math>^1H</math> NMR</b>	:	400 MHz, $CDCl_3/TMS$ $\delta = 3.69$ (d, $^2J_{SeH} = 12.5$ Hz, H-1) 6.32 (dt, H-2), 6.25 (d, 1H, H-3) 7.55 ( <i>ortho</i> -H), 7.20 - 7.32 (m, aromatic H)	
<b><math>^{13}C</math> NMR</b>	:	100 MHz, $CDCl_3/TMS$ $\delta = 30.7$ (C-1), 125.8 (C-2), 132.0 (C-3) 136.7 ( <i>ipso</i> -C, Se-Ph), 129.7 ( <i>ipso</i> C-Ph) 133.9 ( <i>ortho</i> -C Se-Ph) 128.9, 128.5, 127.4, 127.3, 126.2 (aromatic CH)	
<b><math>^{77}Se</math> NMR</b>	:	76 MHz, $CDCl_3/TMS$ $\delta = 342.0$ ( $^2J_{Se,H} = 12.5$ Hz)	
<b>IR</b>	:	ATR (neat) $\nu = 3057$ (w, Ph-H), 3025 (m), 1576 (m), 1476 (m), 1435 (m), 725 (m), 687 (s, C-Se)	
<b>EIMS</b>	:	$m/z$ (rel. Int.) = 274 ( $M^+$ , 19), 189 (9), 157 (14), 131 (18), 117 (100), 91 (26)	

---

## 5.6.21 3-Phenylselenenochroman (39)




---

<b>Status</b>	:	Yellow oil	$C_{15}H_{14}Se$
<b>Reaction condition</b>	:	0.97 g (3.6 mmol) $AlBr_3$ 1.0 g (3.6 mmol) 3-Phenylselenenyl-1-phenyl-1-propene yield 50 %	
<b><math>^1H</math> NMR</b>	:	400 MHz, $CDCl_3/TMS$ $\delta = 2.89-2.85$ (m, H-2), $2.45-2.29$ (m, H-3) 4.21 (dd, $J_{eq,ax} = 5.6$ , $J_{eq,eq} = 3.8$ Hz, H-2) 6.89 (dd, H-5), 7.10 (m, H-6), 6.97 (m, H-7) 7.32 (dd, H-8), 7.07 (dd, H-ortho-Ph) 7.26 (m, H-meta-Ph), 7.20 (t, H-para-Ph)	
<b><math>^{13}C</math> NMR</b>	:	100 MHz, $CDCl_3/TMS$ $\delta = 16.6$ (C-2), 30.6 (C-3), 45.7 (C-4), 131.3 (C-5) 127.2 (C-6), 124.9 (C-7), 128.9 (C-8), 128.4 (C-9) 138.2 (C-10), 143.7 ( <i>ipso</i> -C Ph), 128.3 ( <i>ortho</i> -C Ph), 128.4 ( <i>meta</i> -C, Ph), 126.3 ( <i>para</i> -C Ph)	
<b><math>^{77}Se</math> NMR</b>	:	76 MHz, $CDCl_3/TMS$ $\delta = 209.0$	
<b>IR</b>	:	ATR (neat) $\nu = 3059$ (w, Ph-H), 3025 (m), 2938 (m), 2356 (s), 2324 (s), 2163 (s), 1981 (m), 1494 (s), 1474 (m), 1434 (m), 895 (s), 759 (s), 743 (s), 701 (s, C-Se)	
<b>EIMS</b>	:	$m/z$ (rel. Int.) = 274 ( $M^+$ , 19), 189 (9), 157 (14), 131 (18), 117 (100), 91 (26)	

---

**6 REFERENCES**

- 1 C. J. Löwig. *Pogg. Ann.* **1836**, 37, 552.
- 2 J. E. Oldfield. *J. Nutr.* **1987**, 117, 2002.
- 3 D. L. Klayman, W. H. H. Günther, Eds., *Organic Selenium Compounds: Their Chemistry and Biology*, Wiley, New York, **1973**.
- 4 J. T. Rotruck, A. L. Pope, H. E. Ganther, A. B. Swanson, D. G. Hafeman, W. G. Hoekstra, *Science* **1973**, 179, 588.
- 5 G.-Q.-Yang, *Selenium in Biology and Medicine*, Eds. G. F. Combs, Jr., J. E. Spallholz, O. A. Levander, J. E. Oldfield, Vol. A, p. 9, Van Nostrand Reinhold, New York, **1987**.
- 6 A. Passwater, *Selenium as Food and Medicine*, Keats Publishers, New Canaan, CN, **1980**.
- 7 S. S. Dharmatti, H. E. Weaver, *Phy. Rev.* **1952**, 86, 259.
- 8 H. E. Walchli, *Phy. Rev.* **1953**, 90, 331.
- 9 T. Birchall, R. J. Gillespie, S. L. Verkis, *Can. J. Chem.* **1965**, 43, 1672.
- 10 M. Lardon, *J. Am. Chem. Soc.* **1970**, 92, 5063.
- 11 A. Horeau, J. P. Guette, *Tetrahedron* **1974**, 30, 1923.
- 12 J. A. Dale, H. S. Mosher, *J. Am. Chem. Soc.* **1973**, 95, 512.
- 13 P. L. Rinaldi, *The Determination of Absolute Configuration using Nuclear Magnetic Resonance Techniques. Progr. NMR Spectroscopy*, **1982**, 15, 291.
- 14 K. Mislow, M. Raban, *Stereoisomeric relations of group in molecules. Top. Stereochem.* **1967**, 1, 1.
- 15 W. H. Pirkle, *J. Am. Chem. Soc.* **1966**, 88, 1837.
- 16 W. H. Pirkle, D. J. Hoover, *NMR Chiral Solvating Agents* in N. L. Allinger, E. L. Eliel (Hrsg.): *Top. Stereochem.* **1982**, 13, 263.
- 17 S. G. Davies, J. Dupont, R. J. C. Easton, *Tetrahedron: Asymm.* **1990**, 1, 279.

- 18 A. Guerra, L. Lunazzi, *J. Org. Chem.* **1995**, *60*, 7959.
- 19 J. Drabowicz, B. Budzinski, M. Mikolajczyk, *Tetrahedron: Asymm.* **1992**, *3*, 1231.
- 20 M. J. P. Harger, R. Sreedharan-Menon, *J. Chem. Soc., Chem. Commun.* **1994**, *14*, 1619.
- 21 R. R. Fraser, *Nuclear Magnetic Resonance analysis using Chiral Shift Reagents* in J. D. Morrison (Hrsg.): *Asymmetric Synthesis*, Academic Press, New York, **1983**, *1*, 173.
- 22 G. M. Whitesides, D. W. Lewis, *J. Am. Chem. Soc.* **1970**, *92*, 6979.
- 23 R. Hazama, K. Umakoshi, C. Kabuto, K. Kabuto, Y. Sasaki, *Chem. Commun.* **1996**, *1*, 15.
- 24 K. Kabuto, Y. Sasaki, *Tetrahedron Lett.* **1990**, *31*, 1031.
- 25 K. Kabuto, K. Sasaki, Y. Sasaki, *Tetrahedron: Asymm.* **1992**, *3*, 1357.
- 26 J. Kido, Y. Okamoto, H. G. Brittain, *J. Org. Chem.* **1991**, *56*, 1412.
- 27 R. Hulst, N. K. Vries, B. L. Feringa, *J. Org. Chem.* **1994**, *59*, 7453.
- 28 T. J. Wenzel, R. E. Sleves, *Anal. Chem.* **81**, *53*, 393.
- 29 M. Audit, P. Demerseman, N. Goasdoue, N. Platzter, *Org. Magn. Res.* **83**, *21*, 689.
- 30 M. Gerards, G. Snatzke, *Tetrahedron: Asymm.* **1990**, *1*, 221.
- 31 J. Frelek, A. Perkowska, G. Snatzke, M. Tima, U. Wagne, H. P. Wolff, *Spectrosc. Int. J.* **1983**, *2*, 274.
- 32 B. Kojic-Prodic, R. Marcec, B. Nigovic, Z. Raza, V. Sunjic, *Tetrahedron: Asymm.* **1992**, *3*, 1.
- 33 K. Wypchlo, H. Duddeck, *Tetrahedron: Asymm.* **1994**, *5*, 27.
- 34 K. Wypchlo, H. Duddeck, *Chirality* **1997**, *9*, 601.
- 35 S. Hameed, R. Ahmad, H. Duddeck, *Magn. Reson. Chem.* **1998**, *36*, 47.

- 36 S. Hameed, R. Ahmad, H. Duddeck, *Heteroatom Chem.* **1998**, *9*, 471.
- 37 C. Meyer, H. Duddeck, *Magn. Reson. Chem.* **2000**, *38*, 29.
- 38 S. Rockitt, H. Duddeck, A. Drabczynska, K. Kiec.Kononowicz, *Eur. J. Org. Chem.* **2000**, 3489.
- 39 S. Rockitt, H. Duddeck, J. Omelanczuk, *Chirality* **2001**, *13*, 214.
- 40 S. Malik, H. Duddeck, J. Omelanczuk, M. I. Choudhary, *Chirality* **2002**, *14*, 407.
- 41 (a) H. Duddeck, S. Malik, T. Gáti, G. Tóth, M. I. Choudhary, *Magn. Reson. Chem.* **2002**, *40*, 153; (b) S. Malik, S. Moeller, H. Duddeck, M. I. Choudhary, *Magn. Reson. Chem.* **2002**, *40*, 659; (c) S. Malik, S. Moeller, H. Duddeck, M. I. Choudhary, Manuscript submitted to *Organometallics*.
- 42 (a) G. R. Sullivan, *Chiral lanthanide shift reagents. Top Stereochem.* **1978**, *10*, 287; (b). P. L. Rinaldi, *The determination of absolute configuration using nuclear magnetic resonance techniques. Progr. NMR Spectrosc.* **1983**, *15*, 291;(c) D. Parker, *Chem. Rev.* **1991**, *91*, 1441; (d) R. Rothild, *Enantiomers* **2000**, *5*, 457.
- 43 R. Hulst, R. M. Kellog, B. L. Feringa, *Rev. Trav. Chim. Pay-Bas.* **1995**, *144*, 115.
- 44 J. Omelanczuk, M. Mikolajczyk, *Tetrahedron: Asymm.* **1996**, *7*, 2687 and reference cited therein.
- 45 For a compilation of various investigation see: *Selenium-77 Nuclear Magnetic Resonance Spectroscopy*, H. Duddeck, *Progr. NMR Spectroscopy* **1995**, *27*, 1
- 46 P. Michelsen, U. Annby, S. Gronowitz, *Chem. Scr.* **1984**, *24*, 251
- 47 L. A. Silks III, R.B. Dunlap, J. D. Odom, *J. Am. Chem. Soc.* **1990**, *112*, 4979
- 48 L. A. Silks III, J. Peng, J. D. Odom, R. B. Dunlap, *J. Chem. Soc. Perkin Trans. 2*, **1991**, 2495.
- 49 L. A. Silks III, J. Peng, J. D. Odom, R. B. Dunlap, *J. Org. Chem.* **1991**, *56*, 6733.

- 50 G. R. Weisman, *Asymmetric Synthesis*, Ed. J. D. Morrison, Vol. 1, p. 153, Academic Press, New York, London, **1983**.
- 51 B. A. Arbuzov, A. S. Ionkin, Yu-Ya. Efremov, O. A. Erastov, V. M. Nekhoroshkov, *Izv. Akad. Nauk. SSSR, Ser. Khim.* **1987**, 455; engl. transl. p. 413. Chem. Abstr. *108*:37954p.
- 52 A. S. Ionkin, Yu-Ya. Efremov, V. M. Nekhoroshkov, O. A. Erastov, B. A. Arbuzov. *Izv. Akad. Nauk. SSSR, Ser. Khim.* **1987**, 2551; engl. transl. p. 2369. Chem. Abstr. *110*:23964w.
- 53 J. M. Briggs, E. W. Randall, *J. Chem. Soc. Perkin Trans. 2*, **1973**, 1789.
- 54 See for example: G. Hägele, M. Weidenbruch, *Chem. Ber.* **1973**, *106*, 460.
- 55 (a) Y. Senda, S. Imaizumi, *Tetrahedron* **1975**, *31*: 2905; (b) J. Firl, G. Kresze, T. Bosch, V. Arndt, *Liebigs Ann. Chem.* **1978**, 87; and references cited therein.
- 56 S. H. Grover, J. B. Stothers, *Can. J. Chem.* **1974**, *52*, 870.
- 57 J. M. Buriak, J.A. Osborn, *J. Chem. Soc., Chem. Commun.* **1995**, 689.
- 58 (a) G. Uray, In Houben-Weyl: *Methods in Organic Chemistry*, (eds.) Georg Thieme: Stuttgart, **1996**, 253. (b) J. M. Seco, E. Quinoa, R. Riguera, *Tetrahedron: Asymm.* **2001**, *12*, 2915.
- 59 (a) H. Duddeck, P. Wagner, S. Gegner, *Tetrahedron Lett.* **1985**, 1205; (b) H. Duddeck, P. Wagner, A. Biallaß, *Magn. Reson. Chem.* **1991**, *29*, 248; (c) H. Duddeck, P. Wagner, B. Rys, *Magn. Reson. Chem.* **1993**, *31*, 736.
- 60 J. A. Hirsch, *Top. Stereochem.* N. L. Allinger, E. L. Eliel, eds., **1967**, *1*: 199.
- 61 (a) F. A. Cotton, R. A. Walton, *Multiple Bonds between Metal Atoms*, 2<sup>nd</sup> ed.; Clarendon, Oxford, **1993**; (b) E. B. Boyar, S. D. Robinson, *Coord. Chem. Rev.* **1983**, *50*, 109.
- 62 (a) C. Mertis, M. Kravaritoy, M. Chorianopoulou, S. Koinis, N. Psaroudakis, *Top. Mol. Organ. Eng.* **1994**, *11*, 321.
- 63 For example: (a) G. Snatzke, U. Wagner, H. P. Wolff, *Tetrahedron* **1981**, *37*, 349; (b) M. Gerards, G. Snatzke, *Tetrahedron: Asymm.* **1990**, *1*, 221; (c) F. A.

- Cotton, L. R. Falvello, M. Gerards, G. Snatzke, *J. Am. Chem. Soc.* **1990**, *112*, 8979.
- 64 For recent publications see: (a) F. A. Cotton, E. V. Dikarev, S. E. Stiriba, *Inorg. Chem.* **1999**, *38*, 4877; (b) F. A. Cotton, E. V. Dikarev, M. A. Petrukhina, S. E. Stiriba, *Inorg. Chem.* **2000**, *39*, 1748.
- 65 S. Rockitt, R. Wartchow, H. Duddeck, A. Drabczynka, K. Kiec-Kononowicz, *Z. Naturforsch.* **2001**, *56b*, 319.
- 66 K. A. Connors, *Binding Constant, The Measurement of Molecular Complex Stability*; Wiley-Interscience: New York, **1987**, pp 24.
- 67 M. T. Blanda, J. H. Horner, M. Newcomb, *J. Org. Chem.* **1989**, *54*, 4626.
- 68 Phosphines are even stronger ligands so that individual adducts can be observed by NMR spectroscopy at room temperature. They prefer  $L \rightarrow [Rh-Rh]$  (1:1-adduct) if both components are equimolar with even greater selectivity than selenides. In a molar excess of  $L$ , however,  $L \rightarrow [Rh-Rh] \leftarrow L$  (2:1-adducts) are formed: *Stable Rh<sub>2</sub>(MTPA)<sub>4</sub>-Phosphine Adducts – The First Example of P-Chirality Recognition by <sup>103</sup>Rh NMR Signals*. (a) D. Magiera, W. Baumann, I. S. Podkorytov, J. Omelanczuk, H. Duddeck, *Eur. J. Inorg. Chem.* in print; (b) *NMR Study of Phosphine-Rh<sub>2</sub>(MTPA)<sub>4</sub>-Adducts – Characterisation and Chiral Discrimination*. D. Magiera, J. Omelanczuk, K. M. Pietrusiewicz, H. Duddeck, In preparation.
- 69 J. Sandström, *Dynamic NMR Spectroscopy*, Academic Press, **1982**, p 1.
- 70 (a) B. S. Lukjanow, M. I. Knjazschanski, J. W. Rewinski, L. E. Niworozschkin, W. I. Minkin, *Tetrahedron Lett.* **1987**, *26*, 2365; (b) M. Hori, T. Kataoka, H. Shimizu, K. Tsutsumi, S. Imaoka, *Heterocycles* **1987**, *26*, 2365; (c) M. Hori, T. Kataoka, H. Shimizu, K. Tsutsumi, *Tetrahedron Lett.* **1989**, *30*, 981; (d) T. Kataoka, K. Tsutsumi, K. Kano, K. Mori, M. Miyake, M. Yokota, H. Shimizu, M. Hori, *J. Chem. Soc. Perkin Trans. 1*, **1990**, 3017; (e) T. Kataoka, T. Iwama, S. Tsujiyama, *Chem. Commun.* **1998**, 197.
- 71 For a general review of *selenocyclic and tellurocyclic compounds*, see: L. E. Christiaens, *Comprehensive Heterocyclic Chemistry II*, vol. 5, ed. by A. R. Katritzky, C. W. Rees, E. F. V. Scriven, Pergamon, Oxford, **1996**, pp. 619.

- 72 A. H. Ingall, *Comprehensive Heterocyclic Chemistry II*, Vol. 5, ed. by A. R. Katritzky, C. W. Rees, E. F. V. Scriven, Pergamon, Oxford, **1996**, pp. 501.
- 73 (a) R. Weber, L. Christiaens, P. Thibaut, M. Renson, *Tetrahedron* **1974**, *30*, 3865; (b) A. Luxen, L. Christiaens, M. Renson, *J. Org. Chem.* **1980**, *45*, 3535; (c) D. H. Wadsworth, M. R. Detty, *J. Org. Chem.* **1980**, *45*, 4611; (d) M. Loth-Compere, A. Luxen, P. Thibaut, L. Christiaens, M. Guillaume, M. Renson, *J. Heterocycl. Chem.* **1981**, *18*, 343; (e) M. R. Detty, B. J. Murray, *J. Am. Chem. Soc.* **1983**, *105*, 883; (f) C. Lemaire, A. Luxen, L. Christiaens, M. Guillaume, *J. Heterocycl. Chem.* **1983**, *20*, 811; (g) A. J. Luxen, L. E. E. Christiaens, M. J. Renson, *J. Organomet. Chem.* **1985**, *287*, 81; (h) R. Okazaki, A. Ishii, N. Inamoto, *J. Chem. Soc., Chem Commun.* **1986**, 71; (i) A. Ishii, R. Okazaki, N. Inamoto, *Bull. Chem. Soc. Jpn.* **1986**, *59*, 2529; (j) M. Hori, T. Kataoka, H. Shimizu, K. Hu Y.-Z. Tsutsumi, M. Nishigiri, *J. Chem. Soc. Perkin Trans. 1*, **1990**, 39; (k) E. A. Jakobs, L. E. E. Christiaens, M. J. Renson, *Heterocycles* **1992**, *34*, 1119; (l) H. Sashida, K. Ito, T. Tsuchiya, *Chem. Pharm. Bull.* **1995**, *43*, 19.
- 74 (a) P. A. Grieco, S. Gilman, M. Nishizawa, *J. Org. Chem.* **1976**, *41*, 1485; (b) P. A. Grieco, J. Y. Jaw, D. A. Claremon, K. C. Nicolaou, *J. Org. Chem.* **1981**, *46*, 1215; (c) T. G. Back, D. J. McPhee, *J. Org. Chem.* **1984**, *49*, 3842; (d) K. C. Nicolaou, N. A. Petasis, D. A. Claremon, *Tetrahedron* **1985**, *41*, 4835; (e) F. A. Davis, R. T. Reddy, *J. Org. Chem.* **1992**, *57*, 2599.
- 75 Lewis acid promoted [3,3]-sigmatropic rearrangement mechanism cannot be excluded. However, our results exhibit some differences from the previously reported seleno-Claisen rearrangement. Vallee *et al.* described that a five-membered ring product was mainly obtained in the thermal seleno-Claisen rearrangement of allyl phenyl selenide.
- 76 W. C. Still, M. Khan, A. Mitra, *J. Org. Chem.* **1978**, *43*, 2923.
- 77 *Anfärbereagenzien für Dünnschicht- und Papierchromatographie*, E. Merck, Darmstadt, **1970**.
- 78 H. Günther, *NMR-Spektroskopie*, 2. Aufl., Thieme, Stuttgart, **1983**, 52.



- 79 (a) G. H. P. Roos, M. A. McKervey, *Synth. Commun.* **1992**, 22, 1751; (b) C. R. Wilson, H. Taube, *Inorg. Chem.* **1975**, 14, 405.
- 80 K. Wypchlo, *DirhodiumKomplexe als Hilfsreagenzien in der <sup>1</sup>H-NMR-Spektroskopie - Chirale Erkennung von Olefinen und Epoxiden*. Dissertation, Universität, Hannover, **1994**.
- 81 P. Wagner, *Untersuchung zum Zusammenhang zwischen Struktur und <sup>77</sup>Se-NMR-Parametern selenhaltiger organischer Verbindungen*. Dissertation, Ruhr-Universität Bochum, **1990**.



## CURRICULUM VITAE

### Personal Information

Name	Muhammad Shahid Malik
Date of Birth	05. February 1970
Place of Birth	Lahore, Pakistan
Family Status	Single
Nationality	Canadian

### Education

September, 2000	Diploma in German Language
January, 2000	Diploma in LC-MS
1995-1998	Master of Philosophy (MPhil.)
1992-1995	Master of Science (MSc.)
1988-1992	Bachelor of Science (BSc.)
1985-1988	High School (FSc.)
1975-1985	School (Metric)

### Scholarships Awarded

June 2000-to present	Deutscher Akademischer Austauschdienst (DAAD)
June 1999-May 2000	Commission on Science and Technology for Sustainable Development in the South (COMSATS)
June 1996-May 1999	University Grants Commission (UGC)

### Travelling Grants Awarded

July, 2002	Deutscher Akademischer Austauschdienst (DAAD) travel grant for 52. Nobel prize winner meeting in Lindau.
June-July, 2001	Deutsche Forschungsgemeinschaft (DFG) Grant for travelling to Budapest

### Research Experiences

October 1997-September 1999	Senior Research Fellow
September 1996-september 1997	Junior Research Fellow

**Research Publications**

Phenylselenenylmenthane derivatives and their enantiomeric discrimination by  $^1\text{H}$  and  $^{13}\text{C}$  NMR spectroscopy in the presence of a chiral dirhodium complex,

SHAHID MALIK, STEFAN MOELLER, HELMUT DUDDECK AND MUHAMMAD I. CHOUDHARY,

*Magn. Reson. Chem.*, 40, 659, **2002**.

Structure of a calotropagenin-derived artifact from *Calotropis Procera*,

ATEF G. HANNA, NAGWA M. M. SHALABY, NAGY A. M. MORSEY, ANDRÁS SIMON, GÁRBOR TÓTH, SHAHID MALIK AND HELMUT DUDDECK,

*Magn. Reson. Chem.* 40, 599, **2002**.

First direct discrimination of chiral phosphine selenide (P=Se) derivatives by multinuclear magnetic resonance spectroscopy in the presence of a chiral dirhodium complex,

SHAHID MALIK, HELMUT DUDDECK, JAN OMELANCZUK AND MUHAMMAD I. CHOUDHARY,

*Chirality*, 14, 407, **2002**.

Complexation of selenium to (*R*)- $\text{Rh}_2(\text{MTPA})_4$  thermodynamics and stoichiometry,

HELMUT DUDDECK, SHAHID MALIK, TAMÁS GÁTI, GÁBOR TÓTH AND MUHAMMAD I. CHOUDHARY,

*Magn. Reson. Chem.* 40, 153, **2002**.

Triterpenes from *Mimusops elengi*,

NUSRAT JAHAN, ABDUL MALIK, GHULAM MUSTAFA, ZAHEER AHMED, SAEED AHMED, ERUM ANIS, SHAHID MALIK, SHAHIDA SUJAAT, NIGHAT AFZA AND ATTA-UR-RAHMAN,

*Natural Product Letters*, 15(3), 177, **2001**.

New Antioxidant and Antimicrobial Ellagic Acid Derivatives from *Pteleopsis hylodendron*,

ATTA-UR-RAHMAN, F. N. NGOUNOU, M. IQBAL CHOUDHARY, SHAHID MALIK, TALAT MAKHMOOR, M. NUR-E-ALAM, SEEMA ZAREEN, D. LONSTI, J. F. AYAFOR AND B. L. SONDEGAM,

*Planta Medica*, 67(4), 335, **2001**.

New Isoflavones from *Ceiba pentandra*,

F. N. NGOUNOU, A. L. MELI, D. LONSTI, B. L. SONDEGAM, ATTA-UR-RAHMAN, M. IQBAL CHOUDHARY, SHAHID MALIK, FARZANA AKHTAR,

*Phytochemistry*, 54, 107, **2000**.

Two saponins from *Pteleopsis hylodendron*,

F. N. NGOUNOU, ATTA-UR-RAHMAN, M. IQBAL CHOUDHARY, SHAHID MALIK, SEEMA ZAREEN, RIAZ ALI, D. LONSTI, B. L. SONDEGAM,

*Phytochemistry*, 52, 917, **1999**.

Spatozoate and varnasterol from the brown alga *Spatoglossum variabile*,

ATTA-UR-RAHMAN, M. IQBAL CHOUDHARY, SAFDAR HAYAT, A. MAJEED KHAN, AFTAB AHMAD, SHAHID MALIK

*Phytochemistry*, 52, 495, **1999**.

Chemical Constituents from Marine Organisms,

ATTA-UR-RAHMAN, M. SHABIR, A. MAJEED KHAN, SAFDAR HAYAT, AMBER NASREEN, SHAHID MALIK AND M. IQBAL CHOUDHARY,

*Natural Product Letters*, 13(4), 255, **1999**.

### **Poster Presentation**

Poster presented on 14<sup>th</sup> International Symposium on Chirality, Hamburg, Germany, September 8-12, **2002**.

Poster presented on 4<sup>th</sup> Central European NMR Symposium and 4<sup>th</sup> Central European Bruker NMR Users, Budapest, Hungary, September 2-3, **2002**.

Poster presented on 2nd German-Polish workshop on Chemistry of Natural Products Synthesis, Chirality and Diversity, Organized by Institute for Organic Chemistry, University of Hannover, Hannover, Germany, June 13-16, **2002**.

Poster presented on 17<sup>th</sup> NMR Valtice, Organized by Central European NMR Discussion, Valtice, Czech Republic, April 8-10, **2002**.

Poster presented on 8<sup>th</sup> International Symposium on Natural Product Chemistry Organized by H.E.J. Research Institute of Chemistry, Karachi, Pakistan, January 18-22, **2000**.

Poster presented on 6<sup>th</sup> International Symposium on Protein Structure-Function Relationship Organized by H.E.J. Research Institute of Chemistry, Karachi, Pakistan, **1999**.

Poster presented on 7<sup>th</sup> International Symposium on Natural Product Chemistry Organized by H.E.J. Research Institute of Chemistry, Karachi, Pakistan, December 28<sup>th</sup>-January 1<sup>st</sup>, **1997-1998**.

Poster presented on 6<sup>th</sup> International Symposium on Natural Product Chemistry Organized by H.E.J. Research Institute of Chemistry, Karachi, Pakistan, January 4-8, **1996**.

Poster presented on 7<sup>th</sup> National Chemistry Conference held in Quetta, Pakistan, June 2-4, **1996**.

### **Publications Submitted**

Phenylselenenylalkanes, Their Adducts with the Dirhodium Complex  $\text{Rh}_2(\text{MTPA})_4$  and Ligand Exchange Mechanisms in Solution as Studied by  $^1\text{H}$ ,  $^{13}\text{C}$  and  $^{77}\text{Se}$  NMR Spectroscopy

S. MALIK, S. MOELLER, G. TÓTH, T. GÁTI, M. I. CHOUDHARY AND H. DUDDECK

submitted to *Organometallics* **2002**.

Dirhodium Tetraacylate Complex and Monovalent Ligands. Adduct Formation in Solution as Monitored by NMR Spectroscopy

ZBIGNIEW ROZWADOWSKI, SHAHID MALIK, GÁBOR TÓTH, TAMÁS GÁTI AND HELMUT DUDDECK,

accepted *J. Chem. Soc., Dalton Trans.* **2002**

Purine Derivative from the Marine Sponge *Psammaphysilla Purpurea*,

T. NARENDER, T. V. GOUD, R. WARTCHOW, S. MALIK, H. DUDDECK AND Y. VENKATESWARLU,

Submitted to *Biochemical Systematics and Ecology*, **2002**

### **Manuscripts under preparation**

New Diterpenoids from *Givotia madagascariensis*

M. ANDZIANARIJAONA, S. MALIK, H. S. KREBS, AND H. DUDDECK,

Manuscript under preparation.

Three New Triterpenoids from *Kresa sesiflora*

M. ANDZIANARIJAONA, S. MALIK, H. S. KREBS, AND H. DUDDECK,

Manuscript under preparation

## **Workshop Participation**

2<sup>nd</sup> German-Polish Workshop, Chemistry of Natural Products - Synthesis, Chirality, Diversity; Hannover, Leibnizhaus, June 13-15, **2002**.

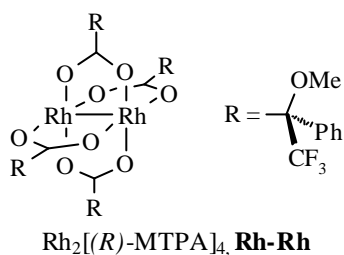
Workshop on the Technology for Product Development from Medicinal Plants held at H.E.J. Research Institute of Chemistry, January 21-27, **2000**.

Workshop on the Use of Bioassay Techniques for New Drug Development held at H.E.J. Research Institute of Chemistry, July 8, **1997**.

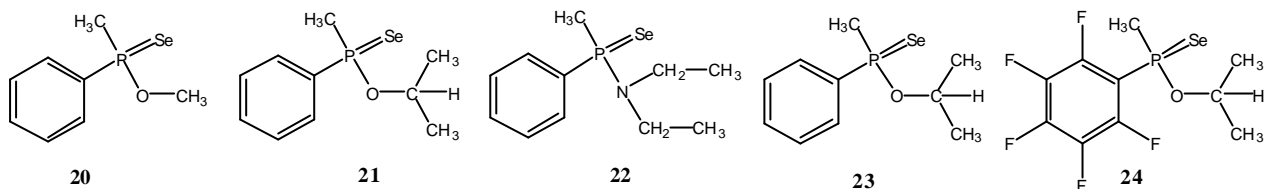
ANRAP Workshop on Photochemical Techniques held at H.E.J. Research Institute of Chemistry, November 16-20, **1996**.

### Reference:

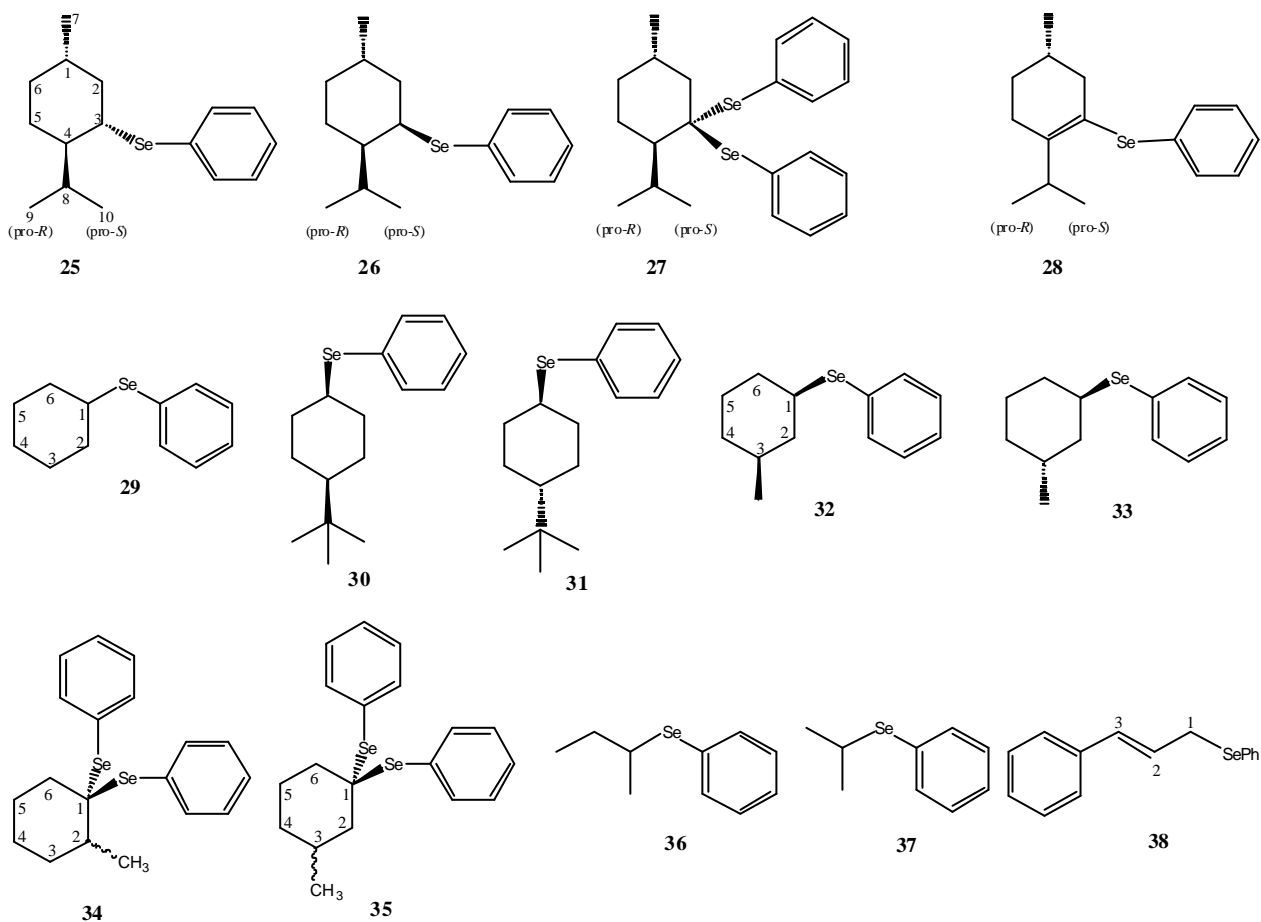
Prof. Dr. Helmut Duddeck  
Institute for Organic Chemistry  
University Hannover  
Schneiderberg 1B, 30167, Hannover  
Germany  
[duddeck@mbox.oci.uni-hannover.de](mailto:duddeck@mbox.oci.uni-hannover.de)  
Ph: +49-511-762-4615  
Fax: +49-511-762-4616



### Structures of Phosphine Selenide Derivatives



### Structures of Phenylselenenylalkane and alkene Derivatives



### Structure of Selenochroman

